FINAL REPORT for the project

Microplastic concentration in sediments and waters of Matagorda and San Antonio Bays: Initial assessment and mitigation plans

Award # UTA21-000049 - MBMT Contract #010

PIs: Cornel Olariu and Zhanfei Liu, The University of Texas at Austin

PhD students: Will Bailey, Xiangtao Jiang

Postdoctoral scholar: Kaijun Lu

Research Associate: Jianhong Xue

Undergraduate students: Danielle Portice, Cole Carraba, Ella Clark, Lilian Alameda, Josh Miller, Caroline Mallinson, Avery Bryan, and Enrico de Cesare Leite

1. SUMMARY RESULTS

The research project focused on understanding the quantity and transport of microplastics in the sediment and water of the Matagorda and San Antonio Bays. The project scope was to map the concentration of microplastic particles in the water and surface sediments (top 10 cm) of the Matagorda and San Antonio Bays, focusing on (1) identifying the areas with high concentrations of microplastics ("hot spots") in Matagorda and San Antonio bays, (2) tracking the most likely sources for microplastics in the Matagorda Bay (recent or past), and (3) understanding the microplastics transport pathways in the estuaries from primary sources (entering the bay), and secondary sources (within the bay) such as erosion/resuspension and re-sedimentation.
The project had research, educational, and environmental components that are separately summarized below.

For research, sampling methodology and analyses have been developed together with the creation of maps and the interpretation of the results. During the project, multiple analytical methods have been tried out for identifying microplastics. Some methods such as density separation, microscopic identification, and Fourier transformed infrared (FTIR) are widely used, but during the project novel methods have also been tested, such as CT (computer tomography) scan of the sediments containing plastic materials and pyrolysis coupled with gas chromatography mass spectrometry (Py-GC/MS).

During the project's field work, hundreds of samples have been collected and analyzed. Microplastics (MP) were found in all sediment and water samples. The number of microplastics in sediments range from 1 and 30 per 100 g wet sediments from the bay bottom and between 1 and 10 in sediment cores. Despite the widespread presence, the microplastics concentrations found in Matagorda and San Antonio bays are less than in other coastal environments reported in studies. The spatial variability identifies higher MP concentration in the sediments in the proximity of Lavaca Bay and Colorado Delta, suggesting these areas as likely MP sources in the bays. However, no extremely high values (hot spots) have been identified within the bays.

In addition to microplastics, analyses for the sediment grain size and total organic carbon (TOC) were made on the collected samples. The data analysis of the microplastics concentration versus possible controlling elements (water depth, distance to the shoreline, sediment grainsize, TOC content) was made. No correlation was found between the number of microplastics and location in the lake (distance from shore, water depth) or sediment type (grain size, total organic matter concentration). However, it was observed that microplastics were larger than the grain size of the sediments hosting them, indicating higher mobility for the microplastic fragments. The samples from the sediment cores (below the bay bottom) show microplastics present in sediments tens of cm, and down to over 1m deep, but in lower concentration (1 to 10 particles per 100g wet sediment). No specific trend of less or more particles varying with depth were found.

MP was also found in water samples with a concentration between 1 and 40 particles/ m^3 of water. The presence of the MP in the water column supports the idea of high mobility of the MP, concurring with the sediment analysis results.
The overall research results indicate that Matagorda and San Antonio bays are not "ultimate sinks" for the microplastics but are temporary staging areas for the microplastics, which eventually are transported into the Gulf of Mexico.
Observation of the water circulation between bays and the Gulf of Mexico through the Ship Channel and Pass Cavallo, and also the coastal flood water during storms and hurricanes, supports the idea that sediment in the bays, which are mostly around 3 m (10 ft) deep, are resuspended and transported into the Gulf of Mexico, together with the microplastics.

Education was a significant component of the project with one post-doctoral scholar, two graduate students and eight undergraduate students directly involved in the data collection, analysis, and interpretation of the results. The educational impact was larger through student presentations at the university's Jackson School of Geosciences Student Symposium, Undergraduate Research Symposium at UTMSI, and state conferences on microplastics (Texas Plastic Pollution Symposium) and national research conferences (American Geophysical Union, Geological Society of America). The presentations raise awareness about microplastics pollution, the research method, and the findings of this study. The working on the project instructed students on research methods and taught them about the sedimentary processes in Matagorda and San Antonio bays, emphasizing the coastal areas as sensitive environments to anthropogenic pressure. Some undergraduate students involved in the project went further to work for environmental companies or to pursue graduate education. The topic of microplastics also attracted students toward other research projects focused on microplastics looking at tire abrasion microplastics on Texas roads, and microplastics in the sediments of Lake Austin and Lady Bird Lake. After publication of an article with the research results from Matagorda and San Antonio bays (Bailey et al., 2024), news sites (*Inside Climate News* and *Chron*) reported the findings, "educating" the wider public.

Environmental implications of the results are linked to the microplastic mapping research and findings have positive and negative implications related to microplastics in coastal environments. Some implications might be specific to the Matagorda Bay system, and others can be generalized to the northern Gulf of Mexico area. The observations of widespread microplastic presence in bay sediments, but at low concentrations can be seen as good and bad at the same time.
The key finding that microplastics are present in bay sediments at all locations sampled and even deeper (over 1 m (3 ft) in cores) in the sediment is worrisome. However, "the positive" observation is that the number of microplastics particles (larger than 40 microns) is relatively low, between 1 and 30 per 100 g wet sediment, significantly less than reported in other studies on sediments from Narragansett Bay in Rhode Island or Tokyo Bay in Japan which are surrounded by large urban areas.

The lack of identification of specific "hot" spots with high microplastics concentration is good, since we couldn't identify a highly polluted microplastics area that might affect the ecosystem. Meanwhile, if the microplastics are dispersed throughout the bays, it means that once released in the system, it is difficult to clean them up since they exist everywhere but in small quantities.
The high mobility (easy to resuspend and transport by water currents) of the microplastics relative to the sediment is good news for the long-term ecology of the coastal bays because it is preferentially "washed out" of the bays. However, because microplastics are in suspension for longer, there might be times when they reach a higher concentration in the sediment-water interface where filter-feeding organisms might take up the microplastics.

As a **wider impact**, the research project was influential in expanding microplastic research at the University of Texas. William Bailey, one of the graduate students working on the Matagorda Microplastics project was awarded a fellowship from the French government and visited University of Perpignan in southern France, where he initiated a collaboration with scientists there to work on microplastics from the Mediterranean lagoons. Because of our improved knowledge on the microplastics sampling and analysis, our university initiated a collaboration with the city of Austin to estimate microplastics in Austin Lake and Lady Bird Lake. Graduate student Xiangtao Jiang obtained his PhD and went on to work for one of the material testing centers of Apple because of his extensive experience with plastics. Postdoc fellow Dr. Kaijun Lu took on a position of Assistant Professor at Coastal Carolina University.

2. THE MATAGORDA AND SAN ANTONIO BAYS OVERVIEW

Matagorda Bay formed behind the coastal barrier of the Matagorda Peninsula and the flooded valleys (Lavaca, Tres Palacios) or deltas (Colorado) of the Texas coastal rivers (Figure 1). The San Antonio Bay has Guadalupe and San Antonio rivers forming a delta to the north, and is separated from the Gulf of Mexico (GOM) by the Matagorda Island (Figure 1). The Matagorda Bay has an area of 244,490 acres (about 990 km^2) and a maximum water depth of over 4 m (12 ft), but most of the bay is less than 3 m (10 ft) deep. The shape/morphology of the bay is typical for northern Gulf of Mexico coastal bays with multiple elongated flooded river valleys landward, to the north, and a relatively smooth southern side where the lagoon is separated from the Gulf of Mexico by a few hundred meters wide sand spit/barriers (Figure 1). The barriers are cut by tidal channels/ passes (Fig. 1) that are active temporarily during storms/ hurricanes or are permanently kept open by tidal currents or anthropogenic intervention (dredging).

There are some particularities to Matagorda Bay by comparison with other Texas bays. The Colorado River, one of the large rivers (catchment of 42,300 sq mi/ 109,500 km^2), drains into the northern Gulf of Mexico, which is discharging water and sediments partially into the Matagorda Bay (Fig. 1) and separating the bay in two distinct water bodies (i.e. Matagorda and East Matagorda bays). Another particularity is that the Matagorda Bay is loosely connected to the west with the San Antonio Bay. In other words, Matagorda is part of a "string" of bays which we will

refer to as the Matagorda Bay System, with each bay having distinct sediment, water and possible microplastics circulation. The creeks and rivers that discharge into the bays from the north have smaller catchment sizes, water, and sediment discharge (Figure 1).

A comprehensive study characterizing the bottom sediments of the Matagorda Bay (McGowen et al., 1979) shows grainsize variability from sands to clays (Figure 2). On the grainsize distribution map the mud fraction distribution likely points to lower energy and consequently the location for potential long-term microplastics accumulation areas. The same report also has maps of total organic carbon (TOC) in sediments. The detailed report of McGowen et al. (1979) allows us to compare the sediment type changes (if any) over decades of bay evolution.

The bathymetry distribution in the Matagorda Bay (see the blue contour lines on figure 2) shows a depth of over 12 ft (over 3.6m) in the central area of the bay, with most of the bay between 6ft (1.8m) and 12ft (3.6m). The San Antonio Bay is shallower with a maximum water depth of around 7 ft (2.1m). The relatively shallow water in the bays allows the waves and currents to continuously resuspend and transport the sediments.

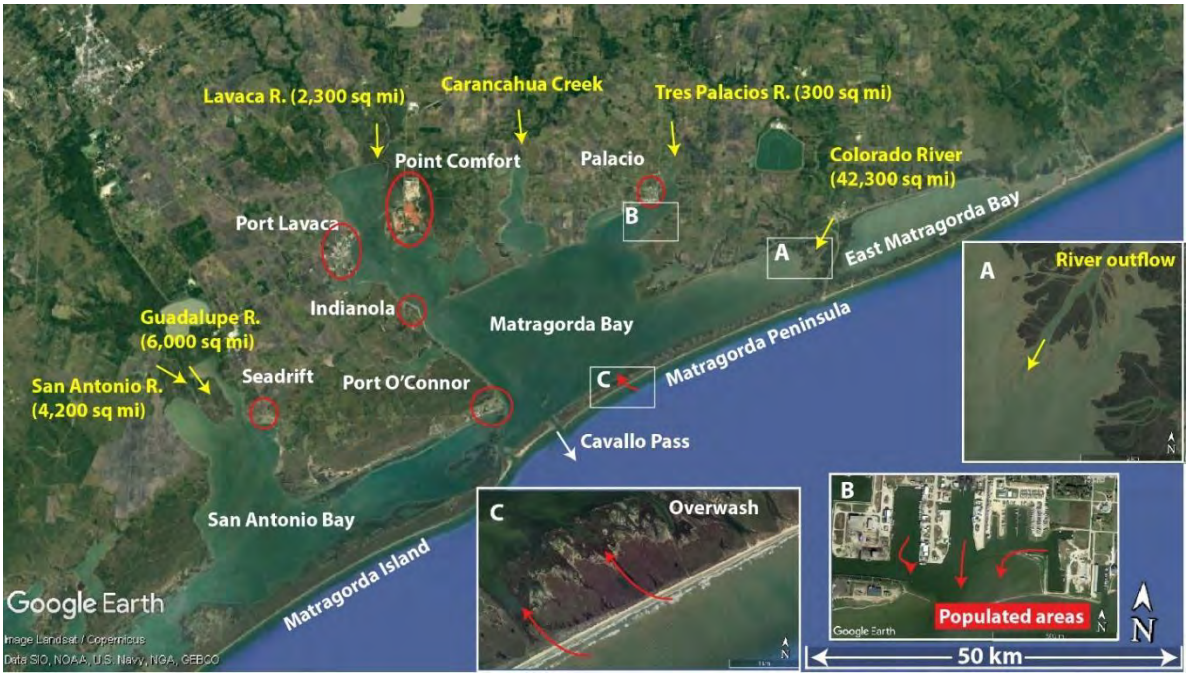

Figure 1. Google Earth satellite image of the Matagorda and San Antonio bays with the identification of the main morphological elements rivers, barriers/islands, pass/outflow). The three principal sources of microplastics into sediments are hypothesized (in the project the proposal) and identified on the map. In insets (A) river inflows (Colorado, Guadalupe, Lavaca, Tres Palacios, note variable catchment size with yellow), (B) populated areas along bay shores, and (C) Gulf of Mexico storm barrier overwash.

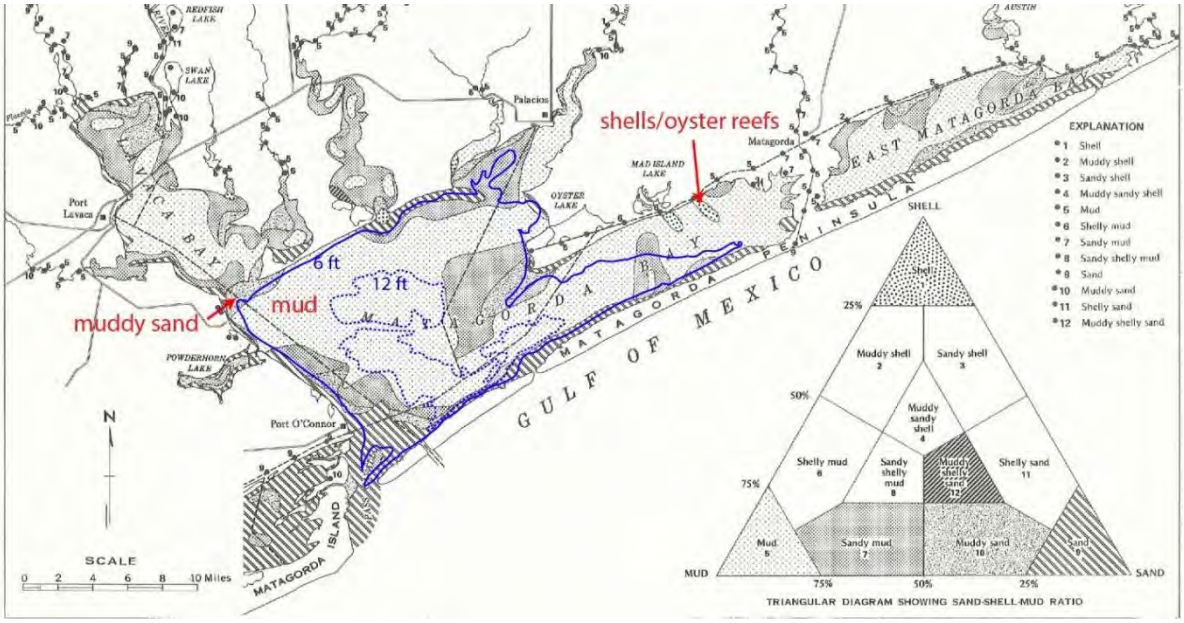

Figure 2. Matagorda Bay sediment grainsize distribution (form McGowen et al., 1979). With blue are 6 and 12 ft water depth isobaths lines, from navigation charts. Note that mud and sandy mud dominate the bay floor in the deepest part of the bay. Also note that Lavaca Bay and Carancahua Bay (next to the east) are separated at the mouth by sand or sandy mud.

3. MICROPLASTICS SAMPLING AND ANALYSIS METHODS

3.1 Sampling Overview: Multiple sampling trips were conducted to collect samples from the Matagorda Bay System starting with the summer 2021. For field collection, we used the *Mowdy* boat from University of Texas, Marine Science Institute in Port Aransas. Multiple instruments were used for sampling for water parameters, and superficial sediments from the bay bottom and from deeper sediments were also collected (Figure 3). Sonar data was recorded along the boat routes between the sampling locations, and exact sampling locations were saved as waypoints. Physical-chemical properties of the water (temperature, PH, salinity, dissolved oxygen) were measured at each sample location using a CTD sonde. A Secchi disk was used to measure water turbidity to test the possibility of correlating the ancillary turbidity measurements with satellite imagery and calibrate satellite images reflectance during the September 2021 trip.

Field sampling procedures were designed to minimize the potential risk of plastic contamination (e.g. utilizing metal tube sleeves for coring). The coring devices of a 3-inch diameter and 2 ft or 5 ft long (Figure 4) were tested in lakes around Austin before deploying them in Matagorda Bay. Ponar grab sampler was used for collecting bay bottom sediments. Sediment samples were stored in plastic bags lined with aluminum foil, and core sleeves were capped with aluminum caps to avoid contamination (Figure 5). The samples were indexed and stored in a cold room at Pickle Campus of the University of Texas at Austin.

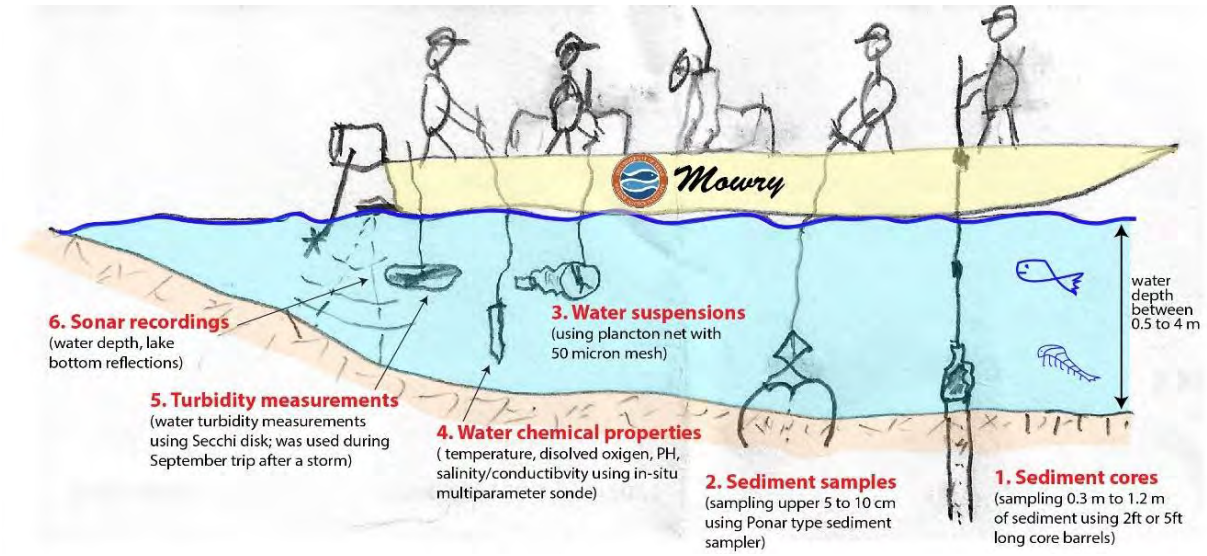

Figure 3. Sketch depicting the different types of data collected at sampling stations at the San Antonio and Matagorda bays of Texas. At each station, a sediment grab sample or a sediment core was collected.

Over the course of several sampling events, we collected sediment samples at 89 locations with broad spatial coverage of both San Antonio and Matagorda bays (Figure 6). Of the 89, 54 were grab samples from the top 10 to 20 cm of surface sediments, and 35 location's cores (at least one foot/ 30 cm long) have been collected. Additionally, 14 water samples were collected using 150 µm mesh plankton nets.

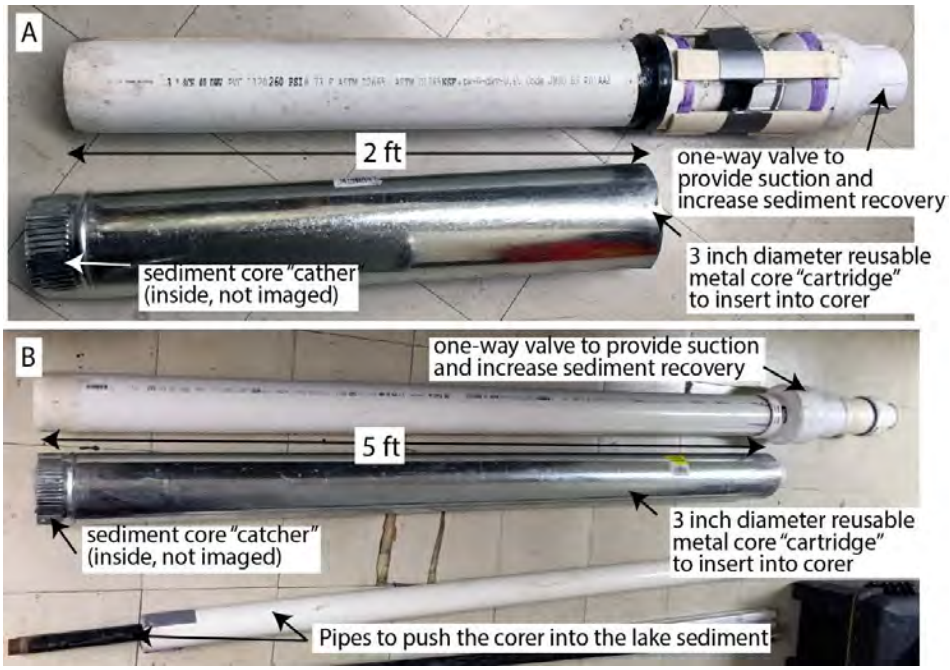

Figure 4. Push core devices for microplastics. A – Two feet long corer. B – Five feet corer. Note that both are designed to utilize reusable metal "cartridges" or "sleeves" to minimize contamination. The metal sleeves can be reused once the collected sediment has been analyzed.

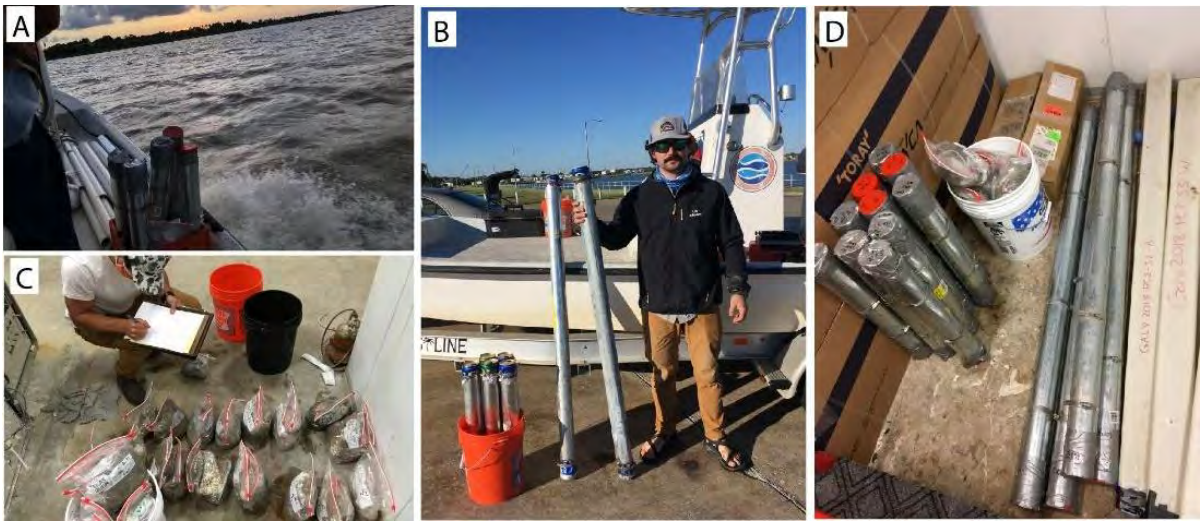

Figure 5. Sediment samples for microplastic analyses. A- cores on the boat during sampling. B- 2&5 ft cores to be transported to UT lab. C- Indexing of grab samples before storage. D- Samples/ cores stored in cold room.

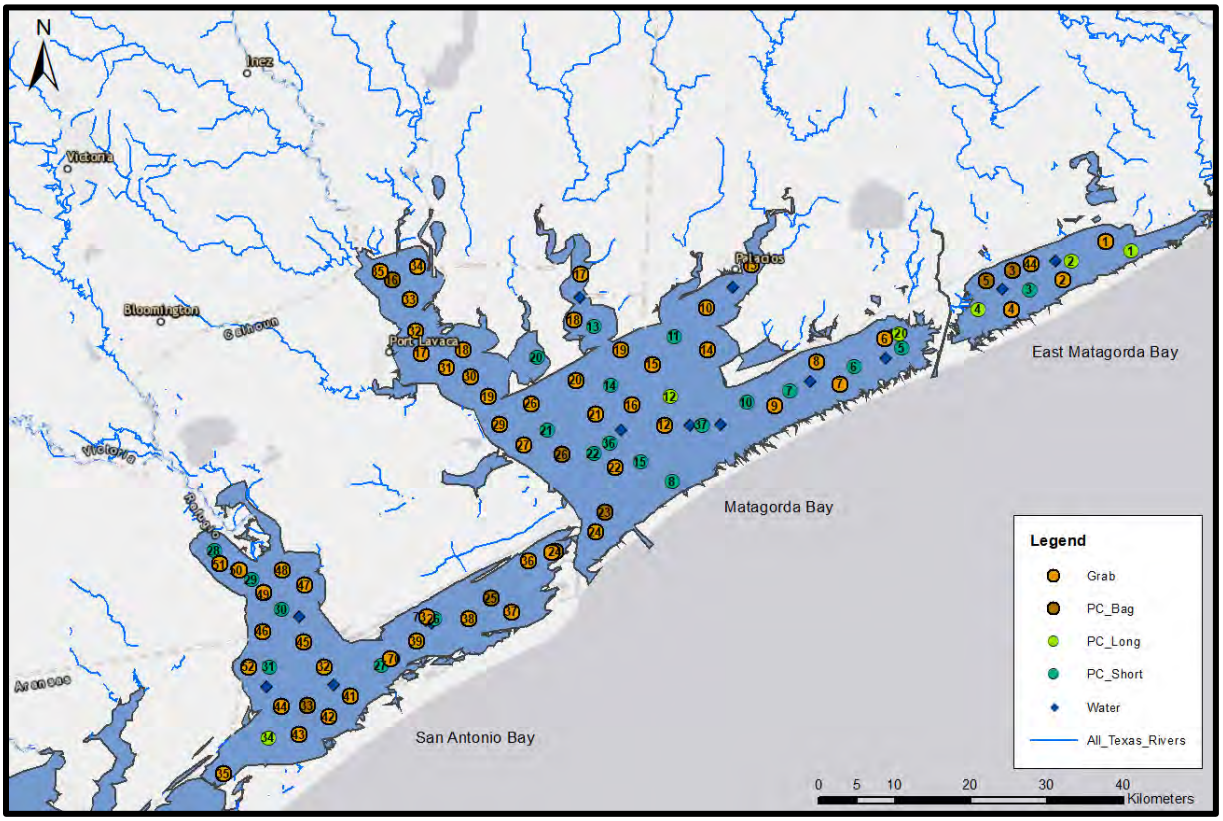

Figure 6. Location map of sampling campaign on San Antonio and Matagorda bays. PC long and short correspond to 5 ft and 2 ft push core locations, PC bag indicates the proposed core location where only a grab sample was recovered. Water sites indicate locations where phytoplankton net samples were collected. Salinity, temperature, PH and Dissolved Oxygen data were recorded at most sites.

3.2 Sediment laboratory analyses were conducted on selected samples to evaluate different elutriation methods for separating microplastics from sediments. Initial methods used a range of sediment amounts (i.e., between 100g to 400g), different salts (e.g. NaCl, $ZnCl_2$), and separation methods such as normal beaker, funnels, or "sliced" glass beaker described by scientists at Japan Agency for Marine-Earth Science and Technology (JAMSTEC). We evaluated two density-separation approaches. A funnel-based setup exhibited abrupt discharge of sediment and heavy liquid ($ZnCl_2$), preventing reproducible recovery of the buoyant fraction despite repeated trials. A sliced-beaker ("JAMSS") design efficiently separated floating particles but was prone to leakage, which, coupled with the corrosive nature of $ZnCl_2$, posed unacceptable safety risks. Based on these findings, we adopted an alternative heavy-liquid protocol with a sealed apparatus. Based on preliminary experiments, we identified the best approach to extract MPs from an organic matrix and clay particles. Based on these considerations, we determined using a lithium metatungstate (LMT) solution for density separation is the most reliable metric for ensuring maximum extraction of plastics from the sediments. The efficiency of the LMT solution lies in the specific gravity of about 2.9 g/cm^3 that is adequate for the preparation of high-density liquid (c.a. 1.5 g/cm^3) necessary to separate microplastics.

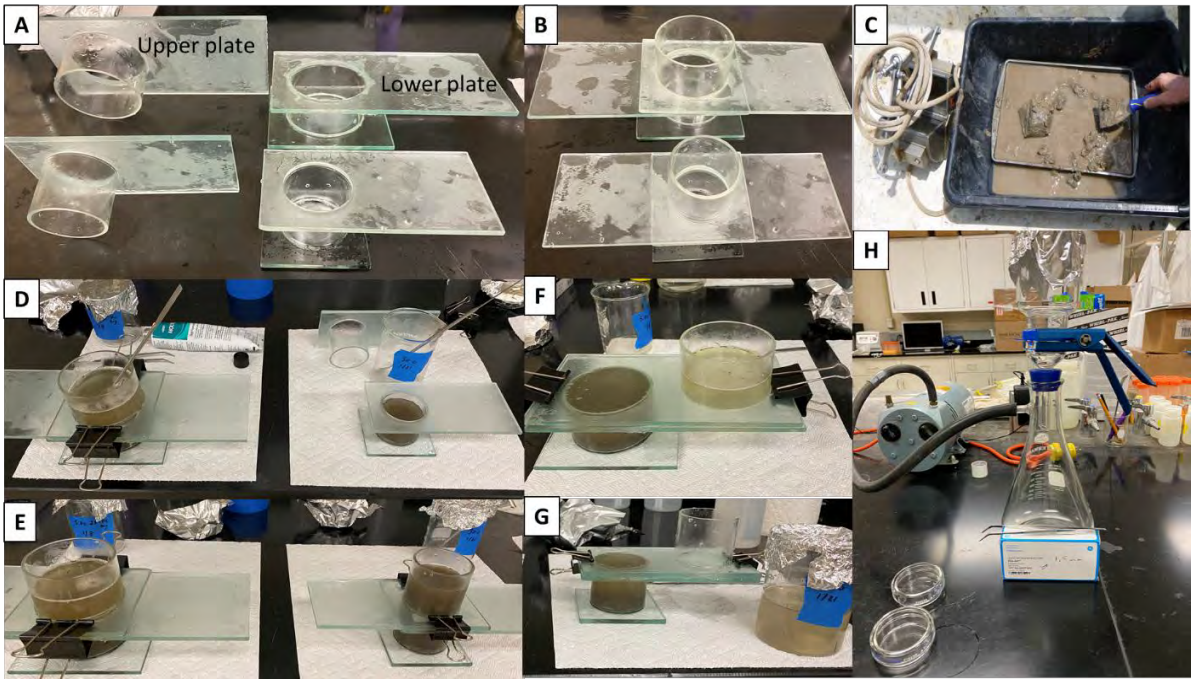

Figure 7. Microplastic separation device designed after JAMSS. A) and B) illustrating the two-part plate components, where the larger and smaller versions hold c.a. 300ml and 150ml of sediment and solution respectively. C) shows our methods for collecting grab samples, where we minimize the use of plastics. D) and E) show the transfer of sieved sediment sample to apparatus with density solution, followed by mixing and settling period. Silicon grease is used to seal the plates. Samples are covered with aluminum foil between all steps. F) and G) illustrates separation step, where plates are slid together to isolate the upper and lower compartments. H) separated upper chamber composition is transferred to vacuum filter using 1.5um filter paper and stored in glass petri dishes for later microscope and FTIR analyses.

3.3 <u>Microscope examination and photography of the filtered material</u> During initial analyses we discovered some sources of consistent contamination from stirring magnets. We reanalyzed the contaminated samples without using the stirring magnets, the lab personnel are using cotton clothes, and we set ambient "traps" to try to identify possible contamination sources.

Once the samples are processed again with careful attention to possible contamination sources, the physical characteristics of plastics particles have been described, and the filters have been submitted to the Marine Science Institute in Port Aransas for plastic type identification using a microscopy FTIR method (Shimadzu AIM-9000).

Dr. Liu laboratory at the University of Texas Marine Science Institute (UTMSI) tested a new method. Shimadzu Scientific Inc. is developing a device that can automatically pretreat solid samples and isolate the plastics. The lab was permitted to evaluate the beta model of this device. The microplastics study laboratory at UT-MSI employed a new column device designed for microplastics density separation (Figure 8) used on 7 selected sediment samples after a filtration on 20 µm and 8 µm filters were analyzed with FTIR.

The 8 µm membrane filter paper was inspected under a wide field microscope to view any larger identifiable plastic particles. Filters were then analyzed by choosing ten squares at random on the gridded filter.

Figure 8. Density separation device (DSD) schematic (left) and during the lab separation(right) (after Löder et al., 2015).

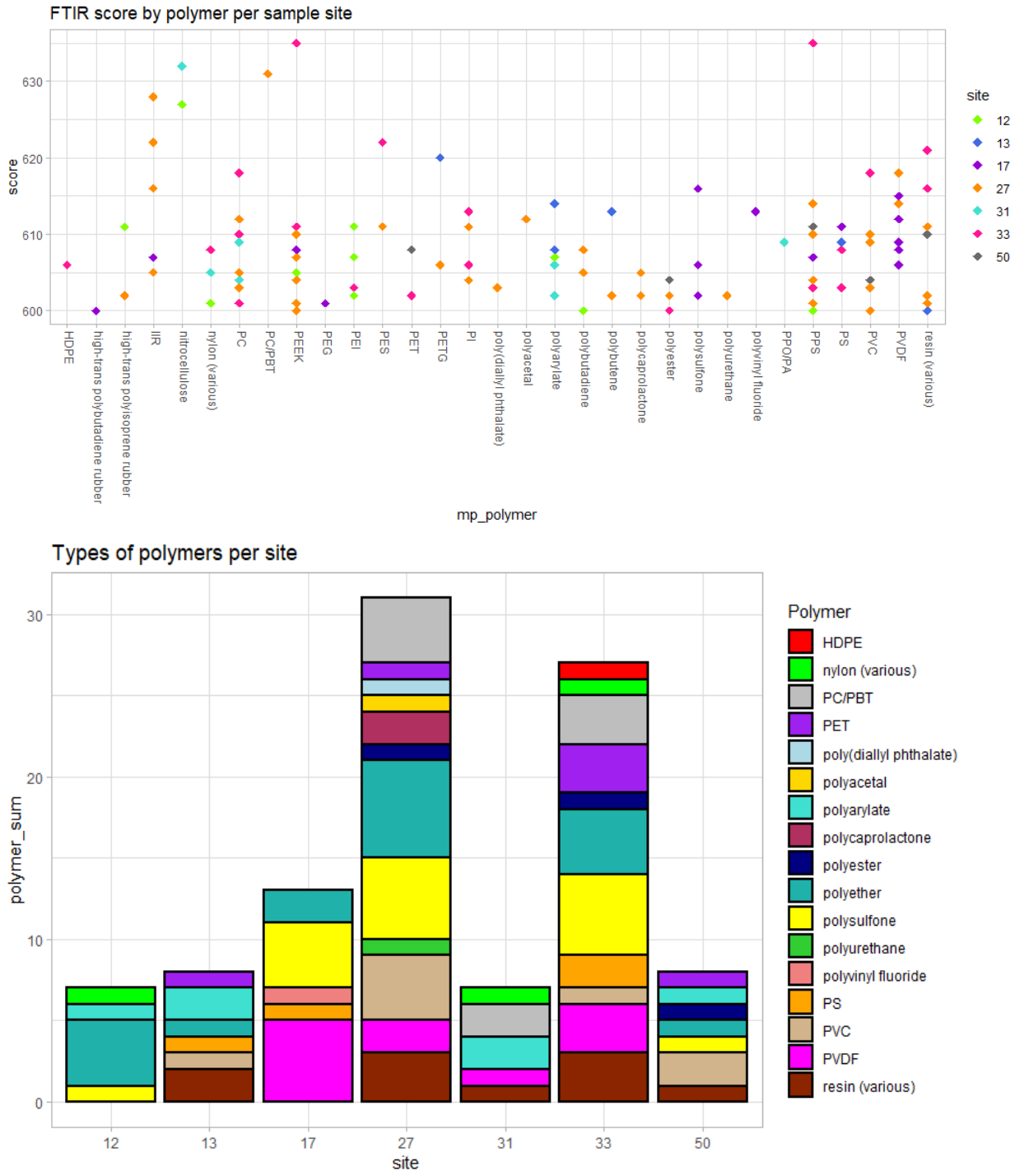

Figure 9: All polymer types identified by FTIR at each site along with their corresponding FTIR score output (top). Amount of common polymer types identified at each site (bottom).

The results of the number of microplastic particles confirmed by the FTIR method (Figure 9) are similar with the microscope identification with more particles in sample locations 33 and 27 (Figure 9, lower graph). However, the FTIR analysis allowed the identification of the plastic types that are extremely variable with about 16 identifiable (with a reasonable confidence) plastic

polymers. The results obtained so far do not point to a particular trend (areas where a given polymer predominates) and it seems that the samples with more microplastics particles also have more polymer types. These observations suggest a depositional environment with a good mix of different sources or an initial heterogenous source.

The microscopy done during the FTIR analysis confirms the dominance of the previously observed morphologies with fibers and fragments being common (Figure 10).

From there, under15x view, any suspected MP particles were analyzed using microscope-Fourier transform infrared spectroscopy (FTIR, Shimadzu AIM-9000) to identify the polymer composition of plastics. Particles that returned a plastic polymer type with a score >600 were considered for further analysis (Figure 9 upper graph). FTIR data was then analyzed using RStudio.

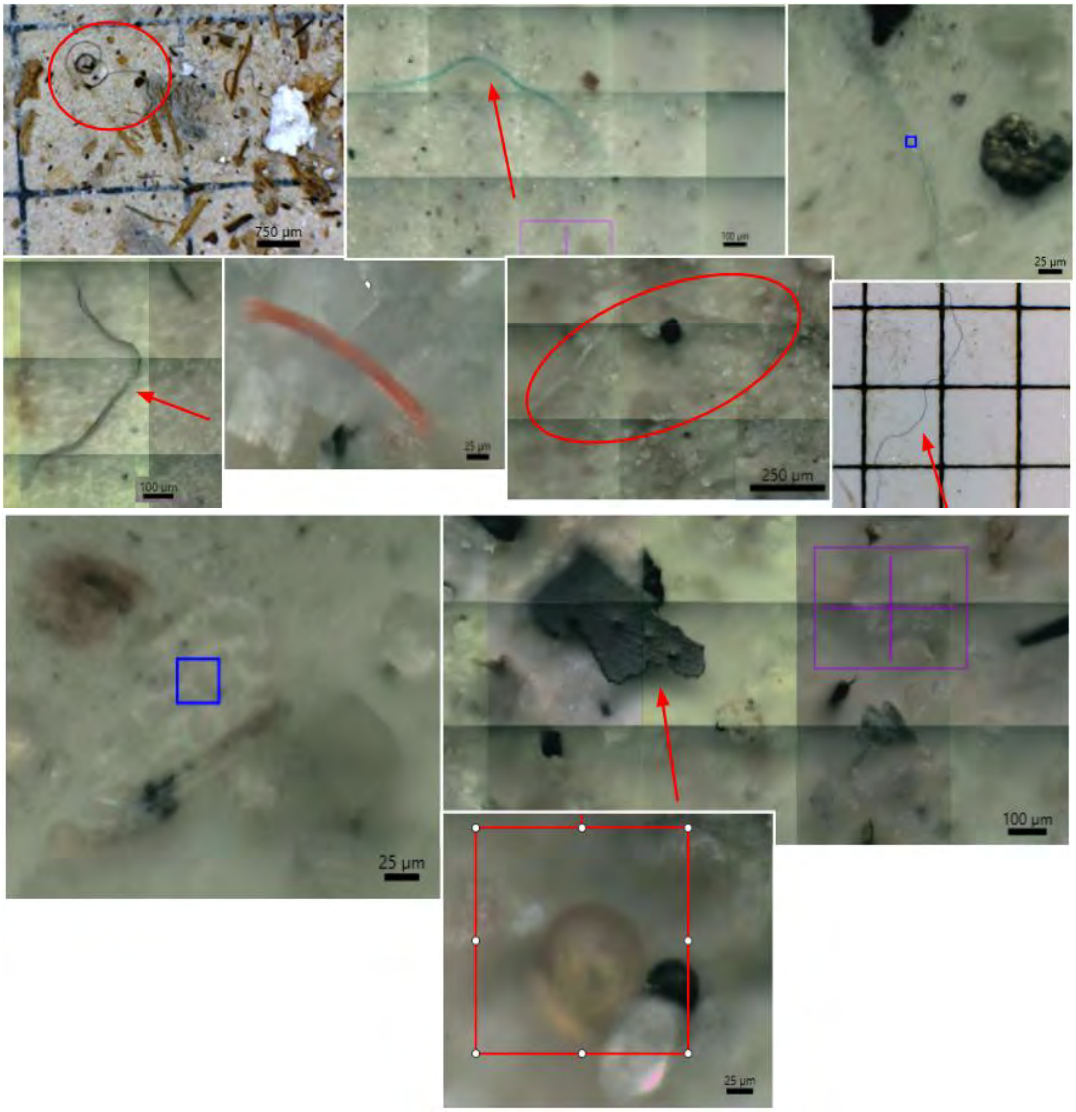

Figure 10: Microplastics morphologies found under inspection of filters including fibers (top) and fragments (bottom) and analyzed with FTIR method.

3.3 <u>CT Scan of the sediment cores</u> In pursuit of a non-destructive "in-situ" method, the Computer Tomography method was tried on some test "made up" sediment cores using Matagorda Bay sediments (Figure 11). The method successfully revealed the known inserted plastic materials (Figure 11). However, the test core was only 4 cm and the approximate location of the inserted plastic material was known. It is more challenging to use a large 30-50 cm core and with an unknown but low concentration of microplastic particles.

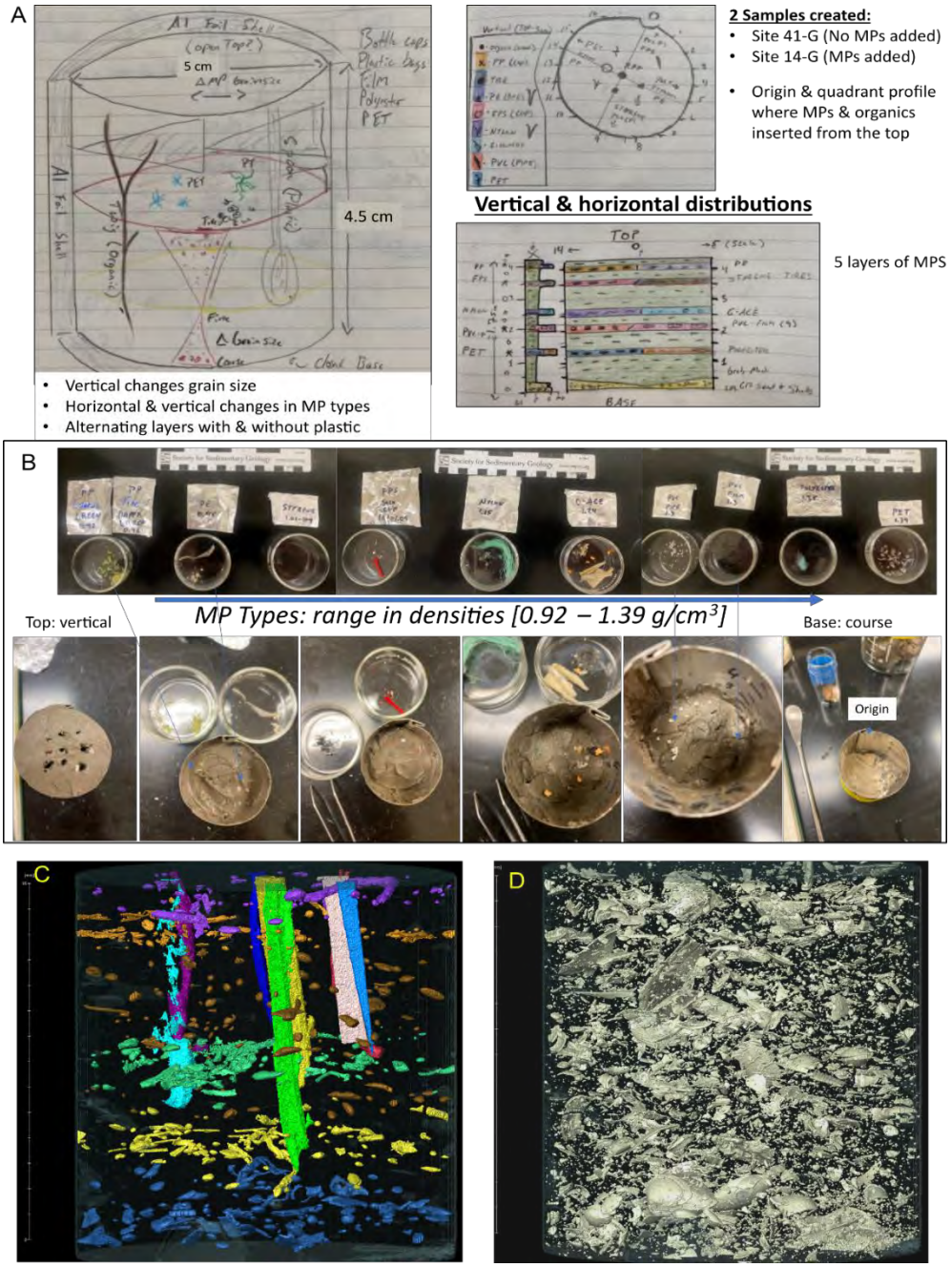

Figure 11. Image of tryout core samples with different plastic types in Matagorda Bay sediments. A- Set up sketch of the plastic material in the core. B- Photos of the different types of plastic used. C- 3-D CT scan image of microplastics. D- 3-D CT scan image of shell fragments.

3.4 <u>Method development for Pyrolysis-GC/MS</u> The previous 'punch' method for analyzing purified samples revealed issues with the heterogeneous distribution of microplastics (Figure 12). Additionally, manually creating calibration curves for 12 polymers and fitting the sample data to each curve was time-consuming. After receiving training at Frontier Lab, we purchased a cryogenic mill and upgraded F-search software. These tools allow for sample homogenization and the simultaneous quantification of all 12 polymers (polyethylene, polypropylene, polystyrene, acrylonitrile butadiene styrene copolymer, styrene-butadiene copolymer, polymethyl methacrylate, polycarbonate, polyvinylchloride, polyethylene terephthalate, polyurethane, Nylon 6, and Nylon 66). With these upgrades, we expect to process all sediment samples from the Matagorda Bay system by the next quarter, which is beyond the scope of the original proposal.

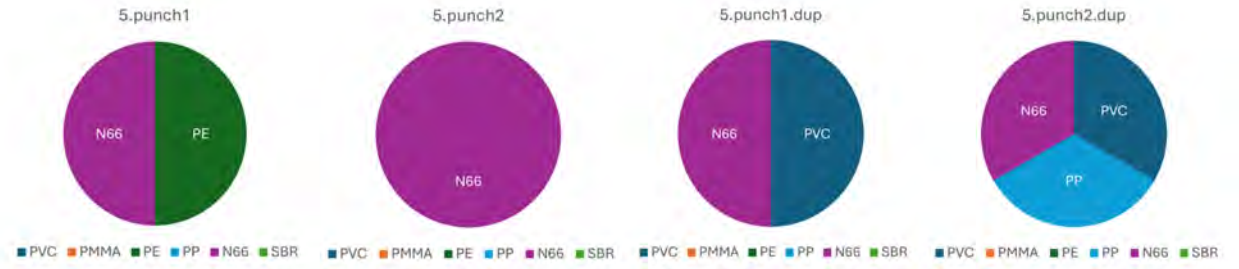

Figure 12. Bar charts displaying the polymer types identified in all of the samples loaded through the Pyrolysis-GC/MS in site 5 of Copus Christi Bay. Four polymers were found in site 5: N66, PE, PVC, and PP.

The detection of microplastics using Pyrolysis-GC/MS was optimized and applied to plankton tow samples collected during the Fall 2023 field trip. Various purification methods were evaluated for isolating microplastics, with nitric acid digestion proving to be the most effective for separating microplastics from biota-rich surface water samples. The isolated microplastics were subsequently analyzed via Pyrolysis-GC/MS, and the results were interpreted using F-Search MPs (Frontier Lab Ltd.), a comprehensive database of pyrolyzates and polymer libraries. This method identified six polymers in the surface water of Corpus Christi Bay: Polyvinyl chloride (PVC), Polymethyl methacrylate (PMMA), Polyethylene (PE), Polypropylene (PP), Nylon 66 (N66), and Styrene-butadiene rubber (SBR), with PVC and N66 being the most prominent, indicating the widespread presence of fibers in the bay system. We are currently establishing a standard calibration curve for 12 polymer standards to quantify the microplastics in the water samples. Once verified, this whole analysis method (Figure 13) will be applied to sediment samples to determine microplastic abundance in the Matagorda Bay system.

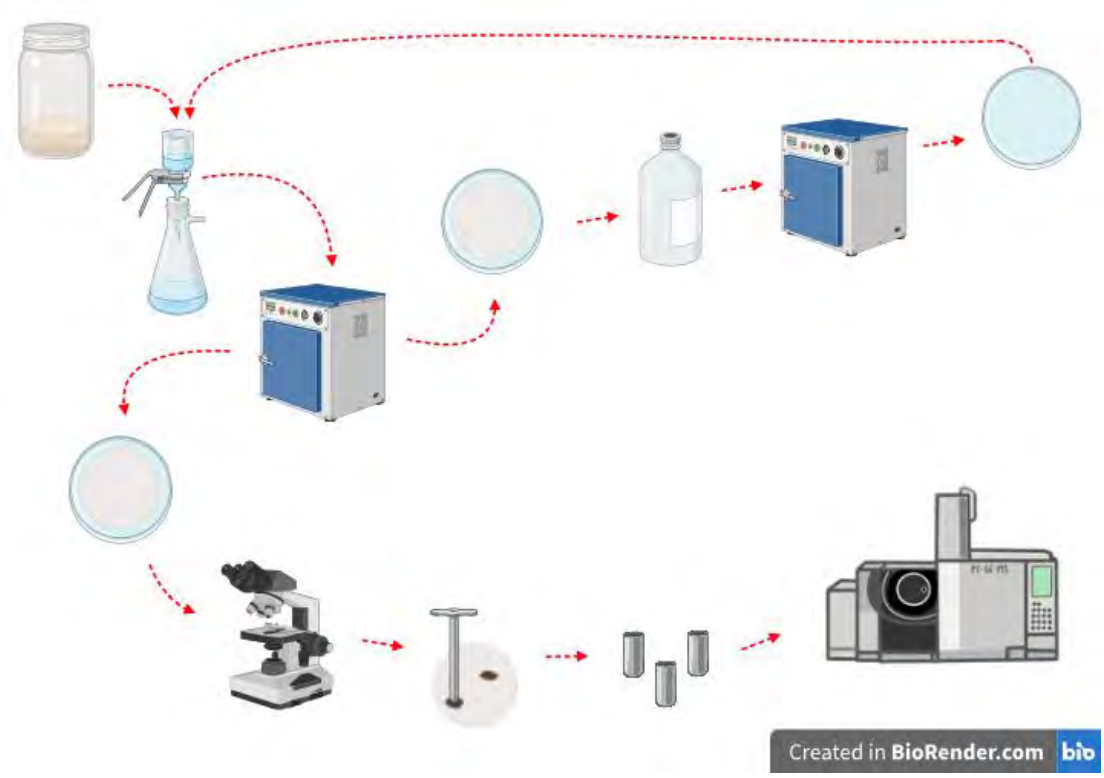

Figure 13. Graphical methods for environmental sample analysis.

Enhanced Detection Method for Microplastic Identification

We further optimized our protocol of quantifying microplastic in the water and sediments collected in Corpus Christi Bay (south-west of Matagorda Bay). Last quarter, we started to use an IQ MILL-2070 cryogenic mill to homogenize samples more thoroughly, and the F-Search MPs 2.1 software and a calibrated plastic standard set. The holistic protocol for quantifying suspended plastics is illustrated in Figure 14, and with Figure 15 showing that plastics largely remained intact after the digestion by the chemical cocktail, nitric acid, and persulfate which can oxidize most of the natural organic matter. This step is critical because without such digestion, the presence of natural organic matter would severely affect the interference in the analysis of microplastics using the pyrolysis GC/MS. Our preliminary data showed that polyethylene is the dominant type of plastic in the Corpus Christi Bay, with a concentration of up to 1.14 µg per liter. Currently we are analyzing the archived samples collected from the Matagorda Bay using this optimized analytical protocol.

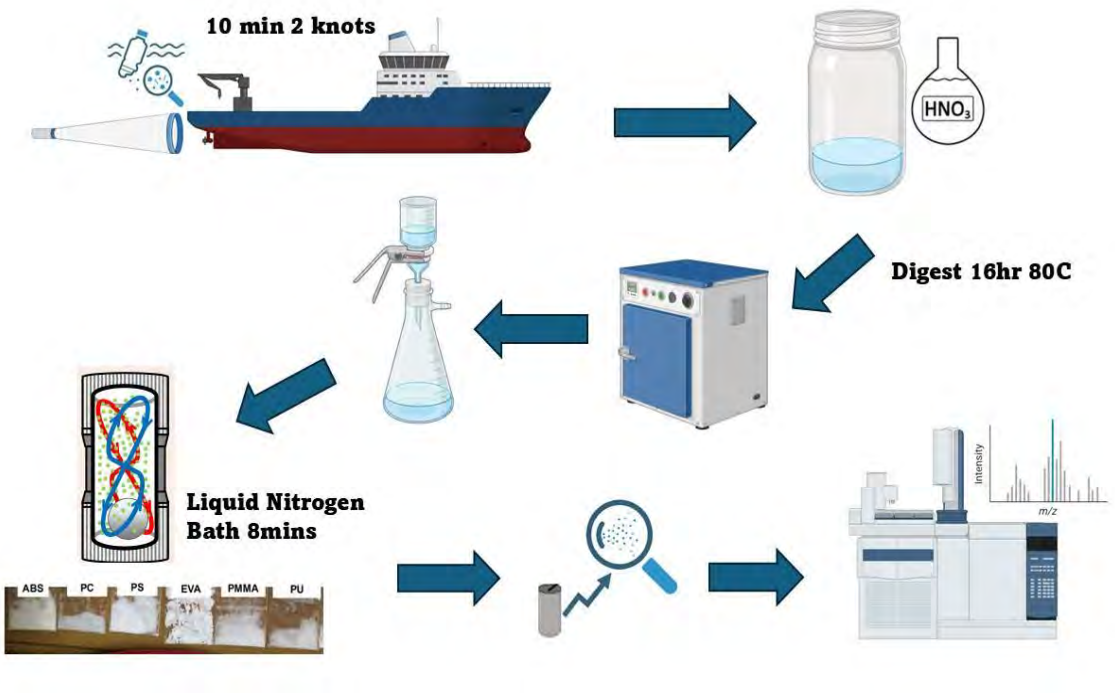

Figure 14. Graphical representation of sampling and analytical protocol of suspended microplastics. The plankton tow typically can filter 10-50k liters of seawater with a mesh size 150 µm. We used nitric acid with sodium persulfate to remove the natural organic matter, while the microplastics remain largely intact. After the cryogenic milling, a subsample can be analyzed.

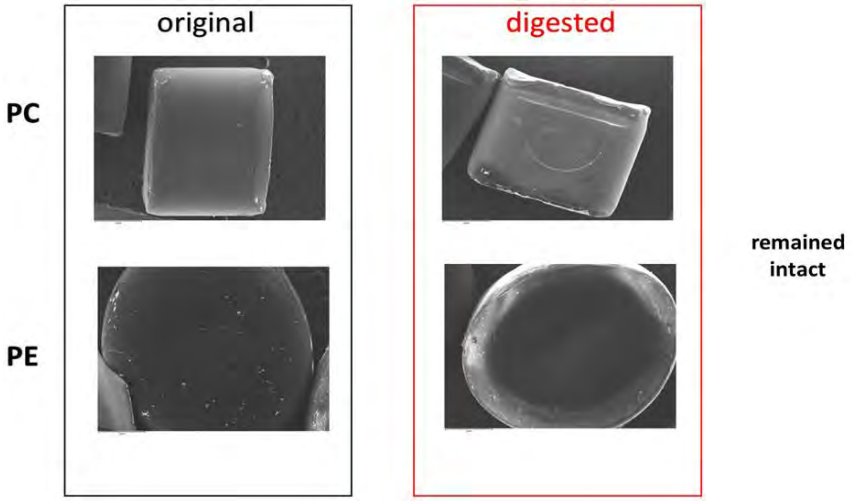

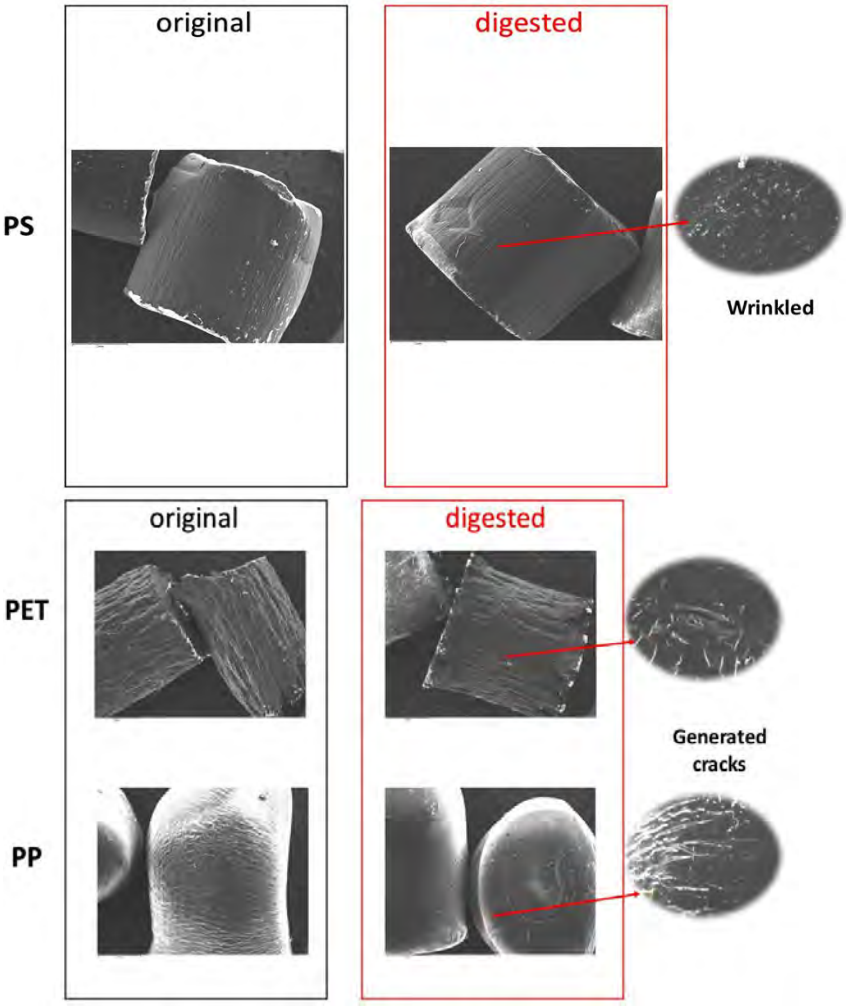

Figure 15. SEM images of 5 plastic nurdle pellets prior to and following exposure to digestion cocktail, demonstrating that the plastics remained largely intact.

4. RESULTS OF MICROPLASTICS ANALYSIS IN SEDIMENT

The material content of filters after the elutriation with LMT (see methods described earlier) have been described using the optical microscope, and the content of individual microplastic particles counted. Main observations are:

(1) microplastics particles observed at the microscope have varied morphologies (fibers, fragments, pellets, and nurdles) (Figures 16 and 17)

(2) there are significant variations between microplastic content; some of the samples seem to have tens microplastics particles per 100g sediments while some samples have only a few microplastics particles per 100 g; However, subsequent FTIR analyses recognize that some of the rounded white-translucid particles are not microplastic particles but frustules of organisms.

; (3) some samples that have large number of microplastics seems to be mixed with white/semi-transparent disks (Figures 16 and 17) identified by FTIR as non-plastics particles.

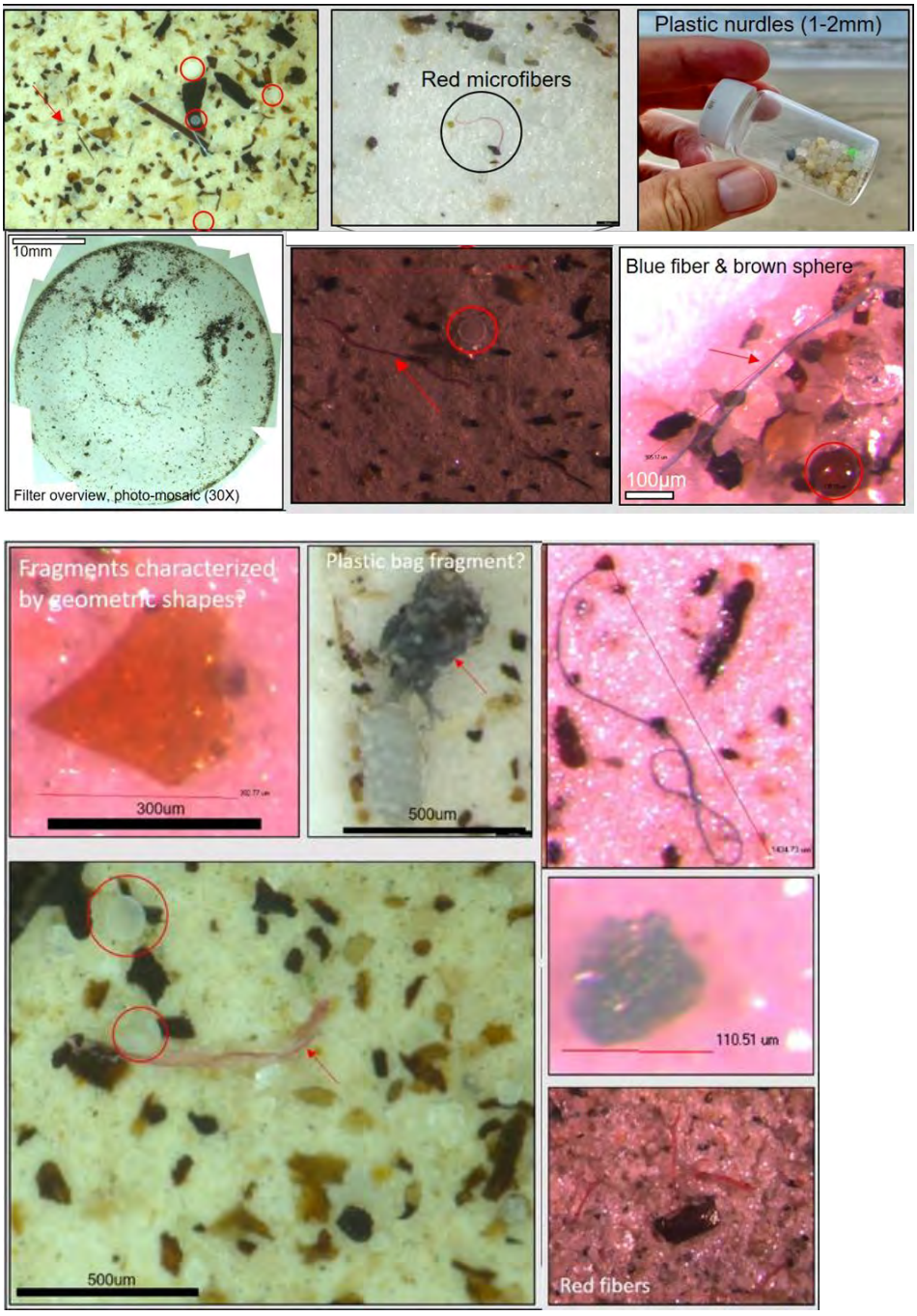

Figure 16. Optical microscope photos. Photos show variable morphology of the plastic particles and dimensions that are commonly around 100 µm.

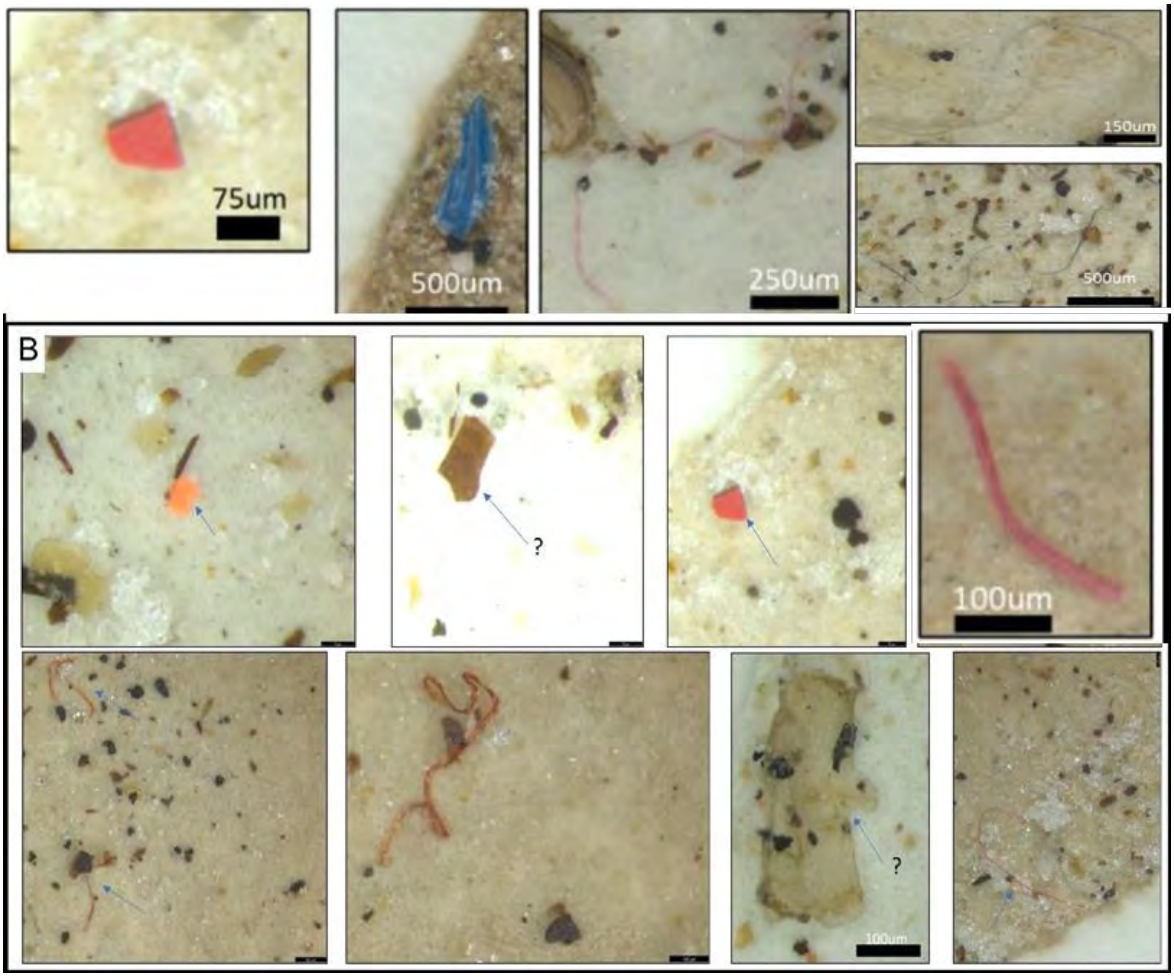

Figure 17. Identification of microplastics using optical microscope. A- method to identify different microplastics morphologies. B- Examples of microplastics, please note the scale of the photos, most fragments are in the range of 100 µm or smaller.

4.1 FTIR analyses on filtered material

Six filters were analyzed at the Marine Science Institute using the FTIR method. The samples were from different locations such as inner bay, central bay or closer to the coast in the tidal delta. The microplastics have been confirmed in all samples analyzed from the inner bays (31G), center of the bay (21G) and in tidal delta (24G) (Figure 18).

The first important observation, under the microscope, is that some of the microplastics have whitish to dark grey colors and are not easily recognized colors (blue, green, red). That suggests counts of the microplastic particles have been underestimated if the color was grey and the shape was not angular or fibrous.

Another key observation is that the measured FTIR signal is noisy, but the microplastic was tentatively assigned when the "match score" got higher than 600 (Figure 18). Clearly, the results of this microscopic FTIR technique should not be used as definite answers, references at the best.

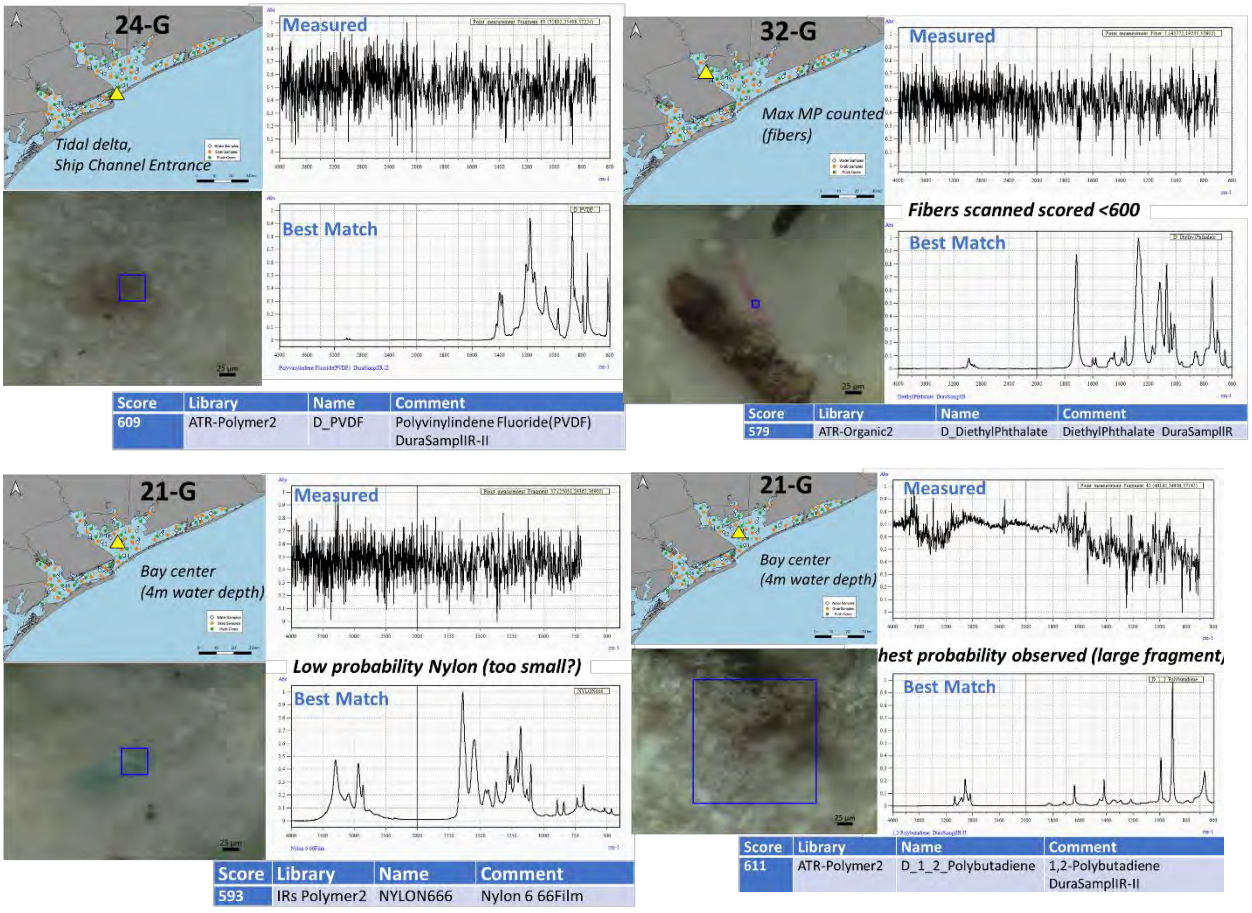

Figure 18. Examples of FTIR results on sediment grab samples 21, 24 and 32. Sample location, microscope photo, FTIR response, and catalog spectra are shown for each sample.

Some initial maps with microplastics by morphology type (Figure 19) individualize areas where fibers or fragments dominate, with an attempt to understand the sources and possible distribution patterns of each microplastic particle type.

Observations related to the higher microplastics content samples (or areas) can be made, and comments on the spatial variability. For example, the micro-fiber distribution map shows there is higher content (tens of particles) in sediment from the outer bay and along the shipping route (Figure 19A). For the micro-fragment distribution map (Figure 19B), it seems to be higher content in the central (deepest?) part of the Matagorda Bay. Microplastics distribution will be discussed in detail later on maps including more sample results considered, together with comparison of the microplastics variability with the distribution of the factors controlling the microplastics dispersion, such as wind direction, bay currents, and water depth.

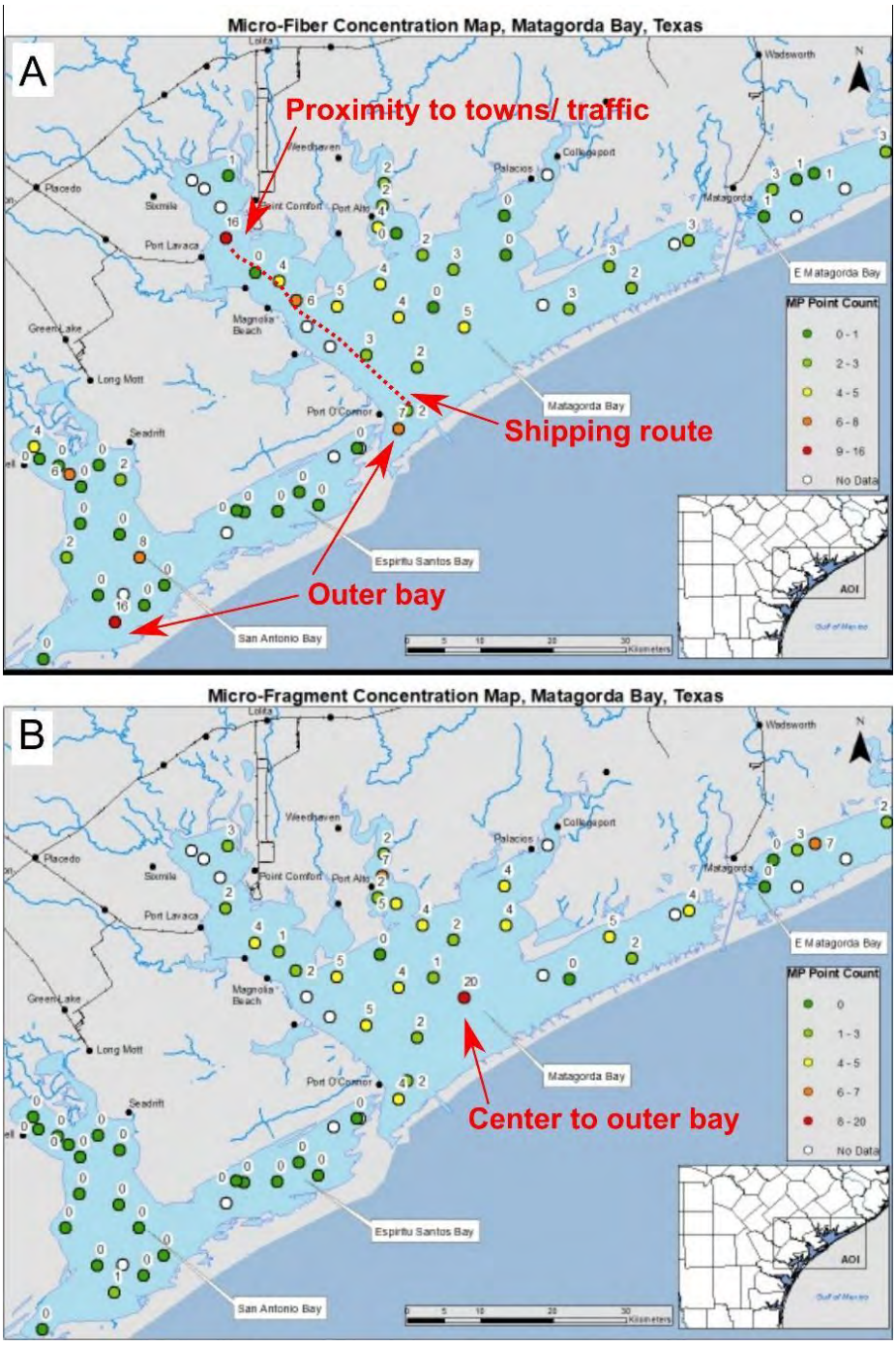

Figure 19. Microplastics distribution by microplastics type. A- Micro-fiber distribution in bay sediment. B- Micro-fragment distribution in bay sediment. The red arrows and text point to high occurrence microplastics areas.

The higher microplastics content in bottom sediments samples of the outer bay and along the shipping channel (Figure 19) has to be linked to the microplastic source and bay dispersal pattern. High human activity areas and rivers discharging in the bay are the source of microplastics (), the sources combined with winds, waves and currents control microplastics dispersal and combined

with bay water depth controls the sedimentation (Figure 20). Long-term wind patterns show a south-southeast predominant direction (toward the land) and a less frequent but higher velocity from northeast (see wind rose Figure 20).

The water depth in the bays (Figure 20) is also likely to control the microplastics settling, and it might be possible to segregate microplastic types based on their densities/shapes. However, these microplastics dispersal controlling factors need more in-depth analyses using river discharges, storm occurrences, and seasonal wind patterns.

Figure 20. Observations pertinent to an initial interpretation of microplastics distribution. Right - possible factors contributed to microplastic variability (longshore currents and wind pattern). Left- Bays water depth, another factor that might contribute to observed microplastics variability.

Sediment cores analyzed in the top few cm improved the bottom sediment microplastic content map. The cores have also been analyzed at middle and bottom depth in addition to the top sediment, to compare the microplastic content at different depths (see Figure 6 for core locations).

Fibers and fragments of microplastics particles seem to have a particular pattern on the microplastics distribution map (Figure 21). There are more fibers in San Antonio Bay, Lavaca Bay, and Matagorda shipping channel, while the central-east part of main Matagorda Bay together with Tres Palacios and Lavaca bays have more fragments (Figure 21). While more observations and measurements on the water currents and sediment transport processes are needed, a first observation is that inner San Antonio and Lavaca bays are areas with more population/ industry activity and microplastics fibers are well known to be sourced from clothing materials or fishing nets.

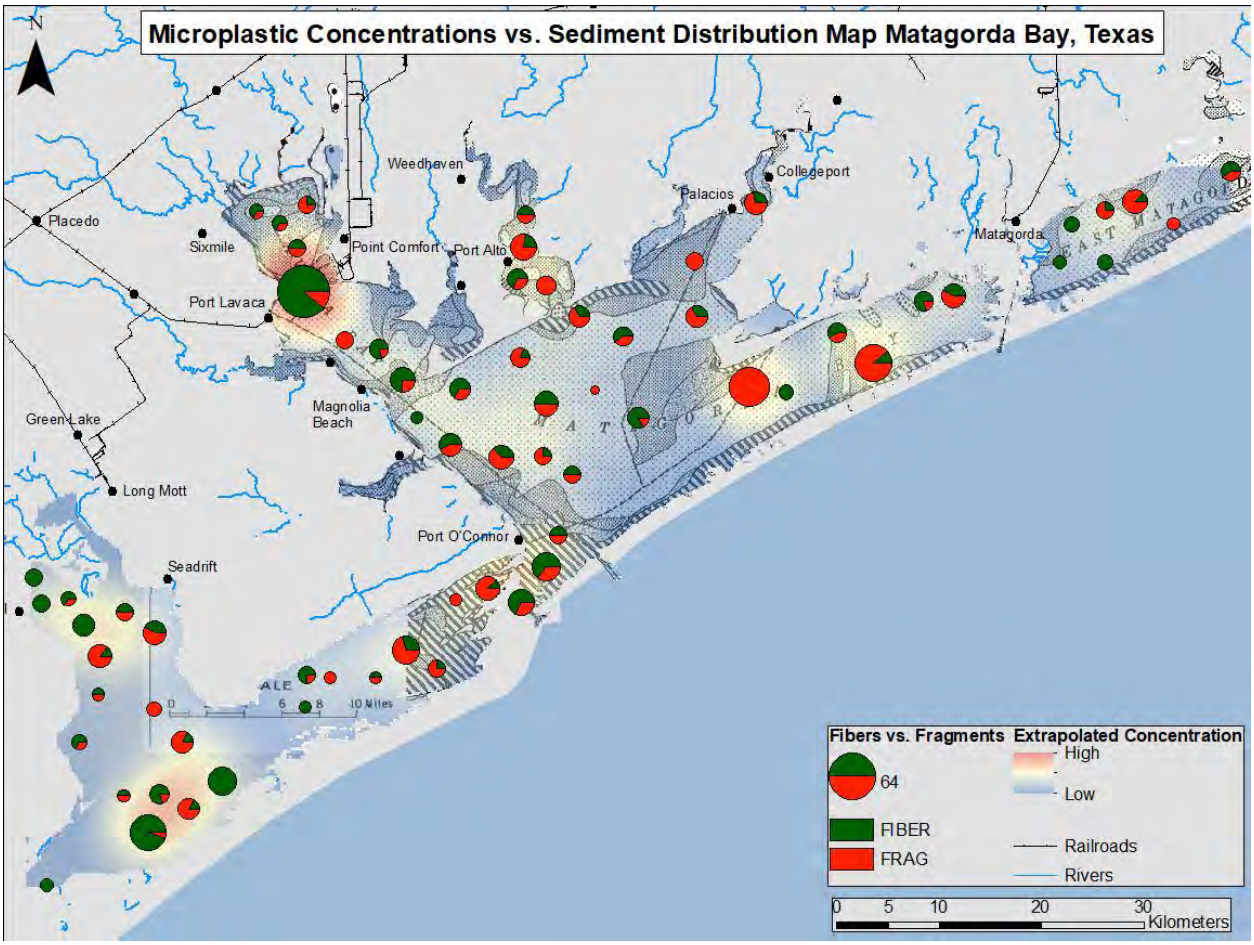

Figure 21. Distribution of microplastics in Matagorda and San Antonio bays sediments separated between fibers (with green) and fragments (with red) morphologies. The background (black and white) pattern shows the grainsize (see figure 2 for legend, and the grainsize pattern map).

4.2 Microplastics in cored sediments

Sediment cores have been opened, sliced (i.e. Figure 22), and for every inch, the sediment was sub-sampled and stored in aluminum-tapped bags for later analyses.

Microplastics were found at the bottom of the cores 22 and 26, analyzed initially, at a depth of about 34 cm and 50 cm (Figure 23). The presence of microplastics at that depth suggests that the sediment was likely deposited after the microplastics appeared in the system (after 1950), or that bay sediment is mixed regularly and redeposited to the depth of sediment sampled in the cores (34 cm and 50 cm respectively). These two possible interpretations have been reinforced by more cores analysed and discussed in conjunction with visual description and grain size analyses.

Figure 22. Sediment core (San Antonio Bay site 26) subsampling (2cm interval).

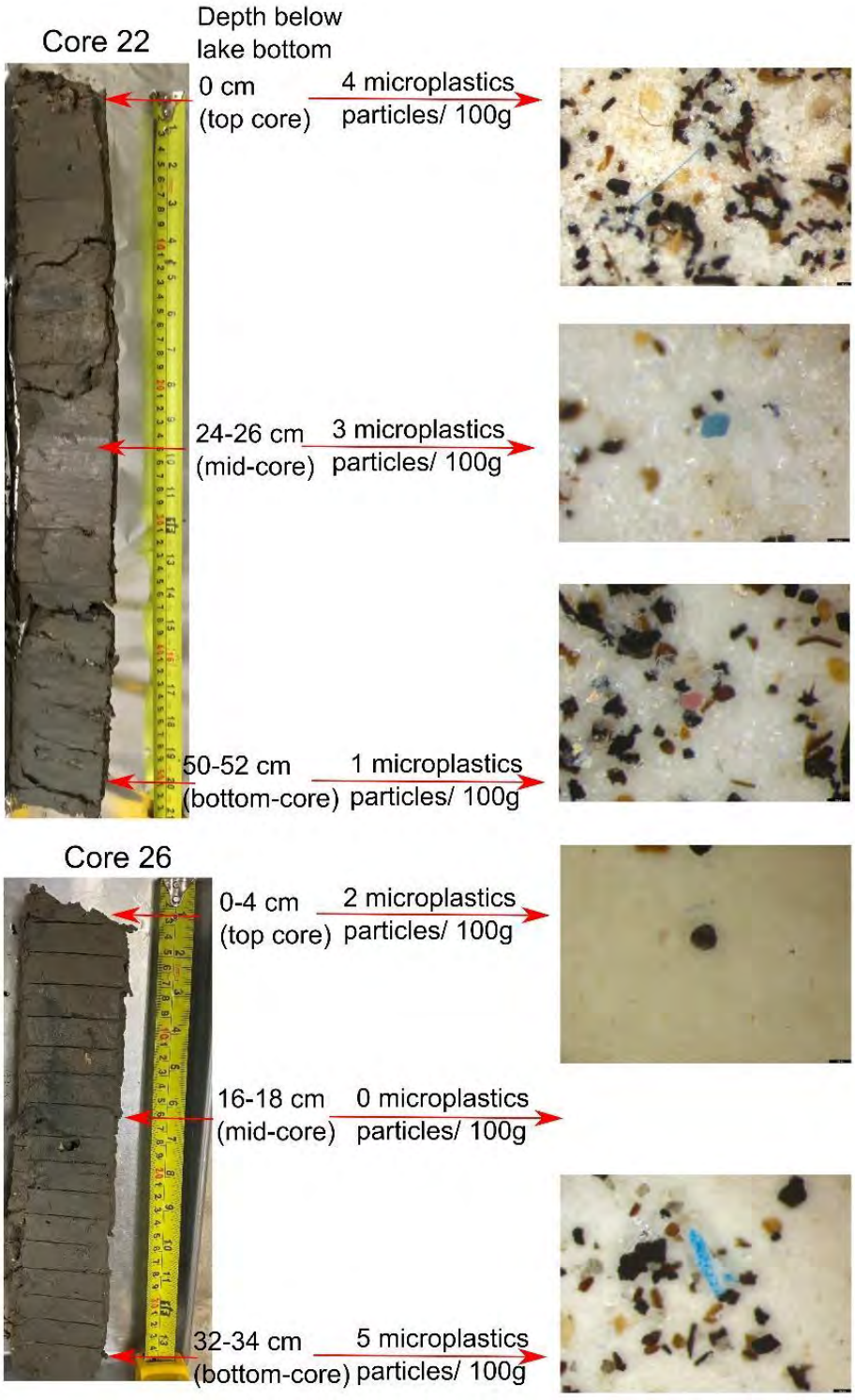

Figure 23. Microplastics content in the mud bay substrate from analysis of 2 cores. For location of the cores, core 22 in Matagorda Bay and core 26 In San Antonio Bay, see figure 6.

Cores 3, and 120 were opened and sediment from top, bottom and middle sampled for microplastics (ee Figure 6 for location of the cores). The sediments in the core were in general, silty-sandy muds (grainsize analysis will reveal the detailed distribution) with diffuse layering (Figure 24). At some levels abundant reworked shelly material can be observed. The lack of layering in the cores opened initially suggests (1) little variability in the grain size of the available sediment in the system, or (2) the continuous mixing of the sediment during deposition. As mentioned above, the microplastics found in cores at a depth of 50 cm indicate their presence deep in the sediment deposits (Figure 25, Table 1). We are not sure yet about the mechanism to emplace the microplastics at 50 cm deep in the sediment below the bay water-sediment interface. There are multiple possibilities to explain the presence of microplastics tens of centimeters deep in the substrate:

1. The sediments were accumulated through time and the deeper buried microplastics represent some of the earlier deposited microplastics, for example deposited 50 years ago (if the sedimentation rate is considered 1 cm per year);
2. There is the possibility of recurrent resuspension and re-deposition of the sediments (microplastics included) through stirring of the unconsolidated sediments through shrimp trawling;
3. Strong storms and hurricanes can also resuspend the sediments due to increase bottom shear stress and locally can form tens of cm deep erosions (i.e., Larm, 1998), the suspended sediments during storm/hurricane events eventually settles depositing the microplastics deeper, at the bottom of a relative thick “storm resuspension” bed;
4. Activity of benthic fauna that live on the substrate or burrow in the substrate can bury the microplastics sediments (through infiltration).

We are not sure which of the mentioned mechanisms, or combination of mechanisms are contributing to the burial, 50 cm or more, into the bay sediment. The microplastics burial through sedimentation is the most conservative explanation and is likely to happen especially in areas with high sedimentation rates such as in front of the Colorado River Delta. However, there are studies that documented strong sediments resuspension through anthropic (Palanques_et_al, 2001, Delappena et al., 2006) or natural mechanisms such as hurricanes (Larm, 1988, Bronikowski, 2004) as well as “down migration” of grains through bioturbation (Näkki et al., 2017). It might be that multiple mechanisms are working in conjunction to the burial of microplastics deeper in the sediments. It will also be helpful to precisely determine the sedimentation rates using multiple radioisotopes such as 210Pb and 137Cs, which could differentiate the magnitude of the resuspension and redeposition.

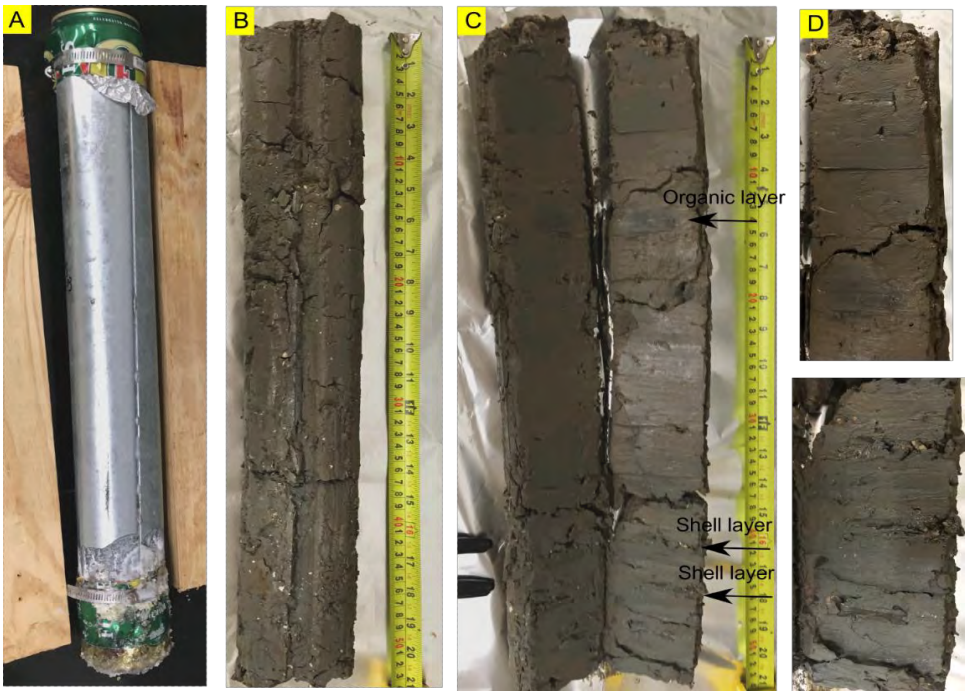

Figure 24. The pushcore 22 form Matagorda Bay. A - Left is the core in the metal sleeve. B – Unsliced core. C - Sliced core notice that arrows are pointing to the organic rich and shell rich layers, D – Close up photos of the shell layers. Note that deposits have an overall structureless appearance, without lamination or other sedimentary structures.

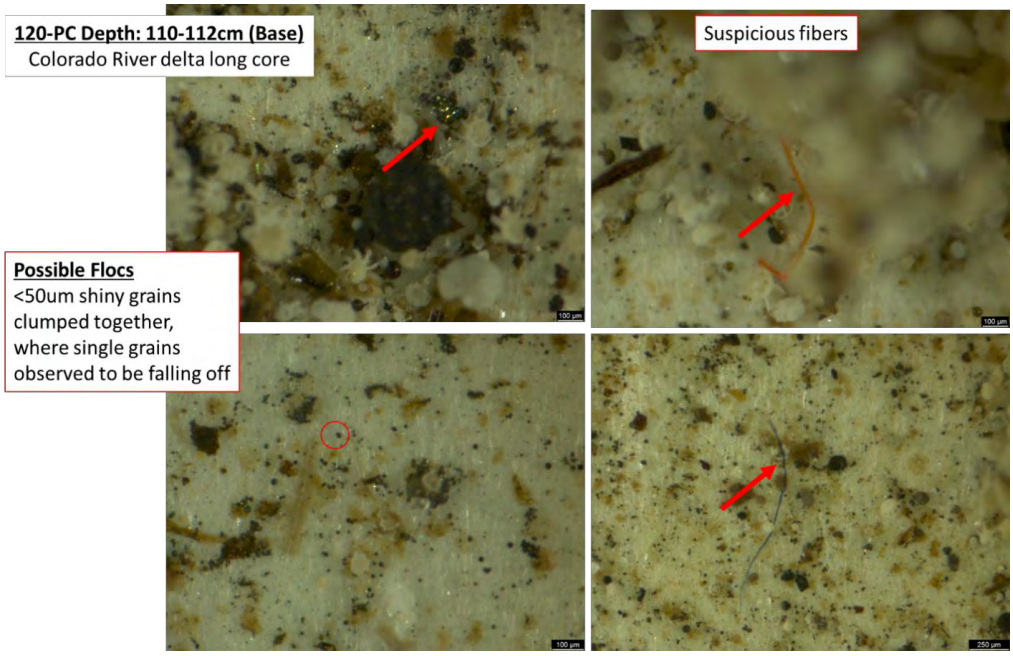

Figure 25. Microscope photographs showing microplastics particles at the base of the pushcores 120 located in front of the Colorado River Delta, eastern map of the Matagorda Bay. See figure 6 for the location of the core. The red arrows are pointing to the observed microplastics. Top left and lower left particles forming flocs that might be microplastics. Scale bar on the photos (black line in lower right corner) is 100 microns with the exception of the lower right image which has a 250 microns scalebar.

Site No.	Lat	Lon	Depth (cm)	MP count	Section
3	28.68036	-95.86956	0-4	3	Top
			40-44	3	Mid
5	28.61996	-96.01996	0-4	19	Top
			36-40	3	Mid
			72-76	3	Base
6	28.60060	-96.07653	0-4	3	Top
			8-12	1	Mid
			20-24	4	Base
7	28.57558	-96.15244	0-4	4	Top
			12-16	3	Mid
			20-24	4	Base
10	28.56405	-96.20224	0-4	3	Top
			8-12	1	Mid
			12-16	6	Base
11	28.63204	-96.28788	0-4	0	Top
			12-18	7	Base
12	28.54032	-96.29970	0-4	3	Top
			28-32	2	Mid
			60-64	6	Base
13	28.64221	-96.38280	0-4	2	Top
			8-12	3	Mid
			18-24	1	Base
120	28.63435	-96.02295	0-4	11	Top
			52-54	2	Mid
			110-112	3	Base
18	28.64881	-96.40559	0-4	6	Top
			8-12	10	Mid
			16-20	1	Base
20	28.61000	-96.44994	0-4	6	Top
			16-20	1	Mid
			28-32	0	Base
21	28.53483	-96.43756	0-4	4	Top
			12-16	2	Mid
			24-28	1	Base
22	28.51065	-96.38309	0-4	4	Top
			12-16	2	Mid
			24-28	1	Base
26	28.33982	-96.57020	0-4	2	Top
			16-18	0	Mid
			32-34	5	Base
27	28.29156	-96.63350	0-4	4	Top
			24-28	0	Base
30	28.34970	-96.75121	0-4	5	Top
			12-16	0	Mid
			24-28	2	Base
31	28.29003	-96.76538	0-4	5	Top
			28-30	4	Base
36	28.52156	-96.36396	0-4	1	Top
			20-24	3	Mid
			40-44	2	Base

Table 1. Table with the microplastic counts on cores at different depths.

After opening more cores, the visual inspection shows homogenous sedimentation in some cores/areas, while in some cores cm-thick shell debris layers, or organic-rich layers have been observed (Figures 26 and 27). The homogenous layers suggest relative constant sedimentation conditions or complete sediment mixing after deposition, while the shells and organic rich layers suggest changing conditions such as an event bed, or seasonal accumulation of organic material (Figures 26 and 27). In some sediment cores analyzed, low amounts of microplastics have been identified at the core bottom (with depth up to 1m, see Figure 26, Table 1).

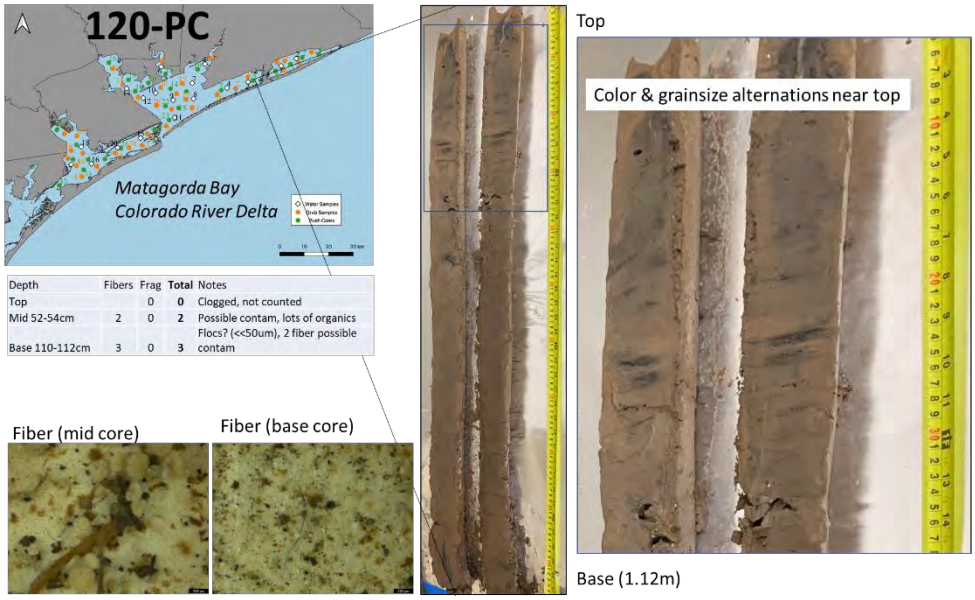

Depth	Fibers	Frag	Total	Notes
Top		0	0	Clogged, not counted
Mid 52-54cm	2	0	2	Possible contam, lots of organics
Base 110-112cm	3	0	3	Flocs? (<<50um), 2 fiber possible contam

Figure 26. Pushcore site 120. Location, core sediment photos and microscope photos. Microplastics fibers observed at the 1m depth.

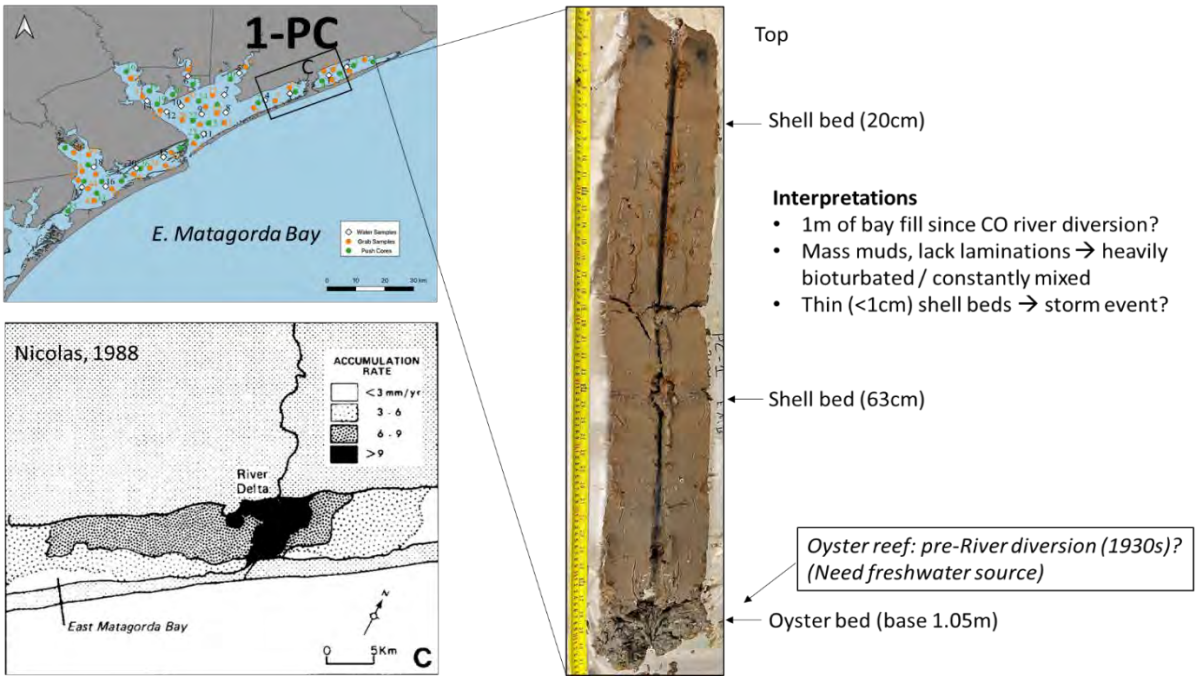

Figure 27. Pushcore site 1. Location and core sediment photo. The core is about 1 m thick. At the base it has an oyster shell bed. Multiple shell beds suggest the recording of possible storm events.

4.3 Visual observations on sediment cores

The cores vary in depth from 20 cm to over 1 m (Figures 28 to 32) and are predominantly muddy, with clay and silt as dominant grain sizes. However, some cores have sandy laminae and sand lenses, some are rich in organic material (for example, cores 4 and 5 in Fig. 28), or have layers of shell fragment (for example, cores 34 WP66 and 34 WP82 in Fig. 31), and most cores have mm-sized shell fragments dispersed throughout muddy deposits. It is common to have sand beds mixed with fragmented oysters (e.g. core 14 in Fig. 30). In some instances, larger oyster shell fragments are present (core 25 in Fig. 30 or core 35 in Fig. 32). In a few cores, bioturbation (organisms disturbing the substrate sediments) can be recognized by the presence of rounded and subrounded geometries filled with coarser sediments (core 15 in Fig. 30). What the cores seem to lack, or are obviously missing in core photos or through visual observations, are fine-laminated sediments with typical clay-silt or silt-sand alternations (see Figs. 28 to 32). The thin-laminated deposits, also called varves, are typically formed in low-energy bays and lakes, and the variability in laminae (mud-sand or organic-rich vs organic-poor or shell-rich vs shell-poor) represents seasonal changes in energy levels or environmental conditions. The lack of laminae and the lack of seasonal changes record are likely consequences of the relatively shallow depth of the bay (less than 4 m), in which sediments are either (1) mixed by fauna through bioturbation, or (2) continuously reworked by wind-generated waves and bay currents, with sediments resuspended in the water column and transported throughout the bay, or (3) repeatedly stirred by anthropic activities such as fishing and shrimping, disturbing bottom sediments.

Figure 28: Photos of sediment cores 1, 2, 3A, 3B, 4, and 5 from East Matagorda. The top-left map indicates the location of the cores. Cores are dominated by muddy sediments with some thin laminae of sand or shells. Note that cores 4 and 5 have more organic content (fragments or dark grey mud) and are also located closer to the Colorado river outlet, which is the source for the organic material.

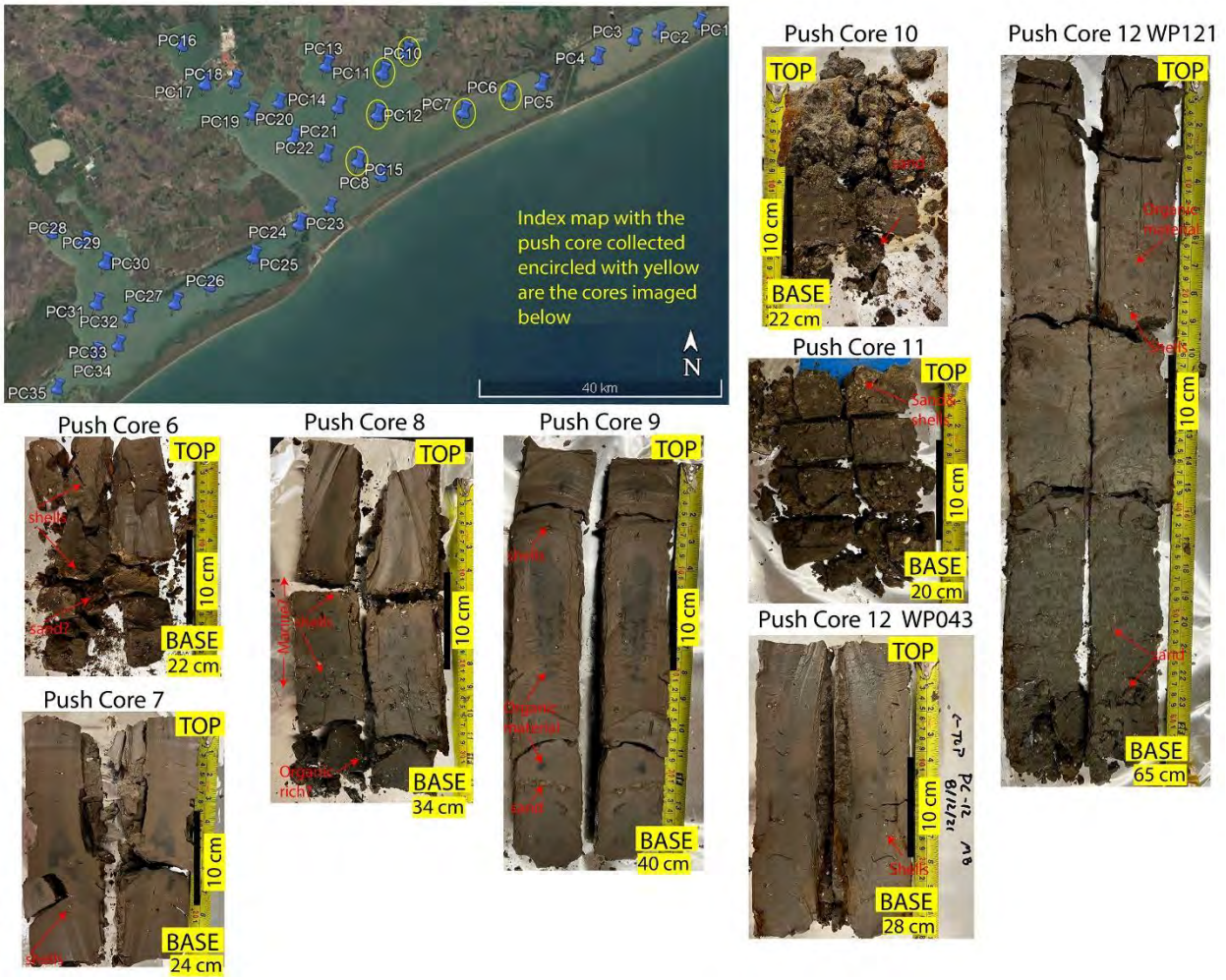

Figure 29: Photos of sediment cores 6, 7, 8, 9, 10, 11, 12 (at two locations) from Matagorda Bay. The top-left map indicates the location of the cores. Cores are dominated by muddy sediments, with two exceptions, cores 10 and 11, which are muddy sands. These two cores are located in the northeastern part of Matagorda Bay at the mouth of Tres Palacios Bay, where the shoreline is erosive. This area is also dominated by intense shipping activity, where re-occurring dredging for channel maintenance and ship-induced sediment resuspension might affect the sediment grainsize deposited in the bay.

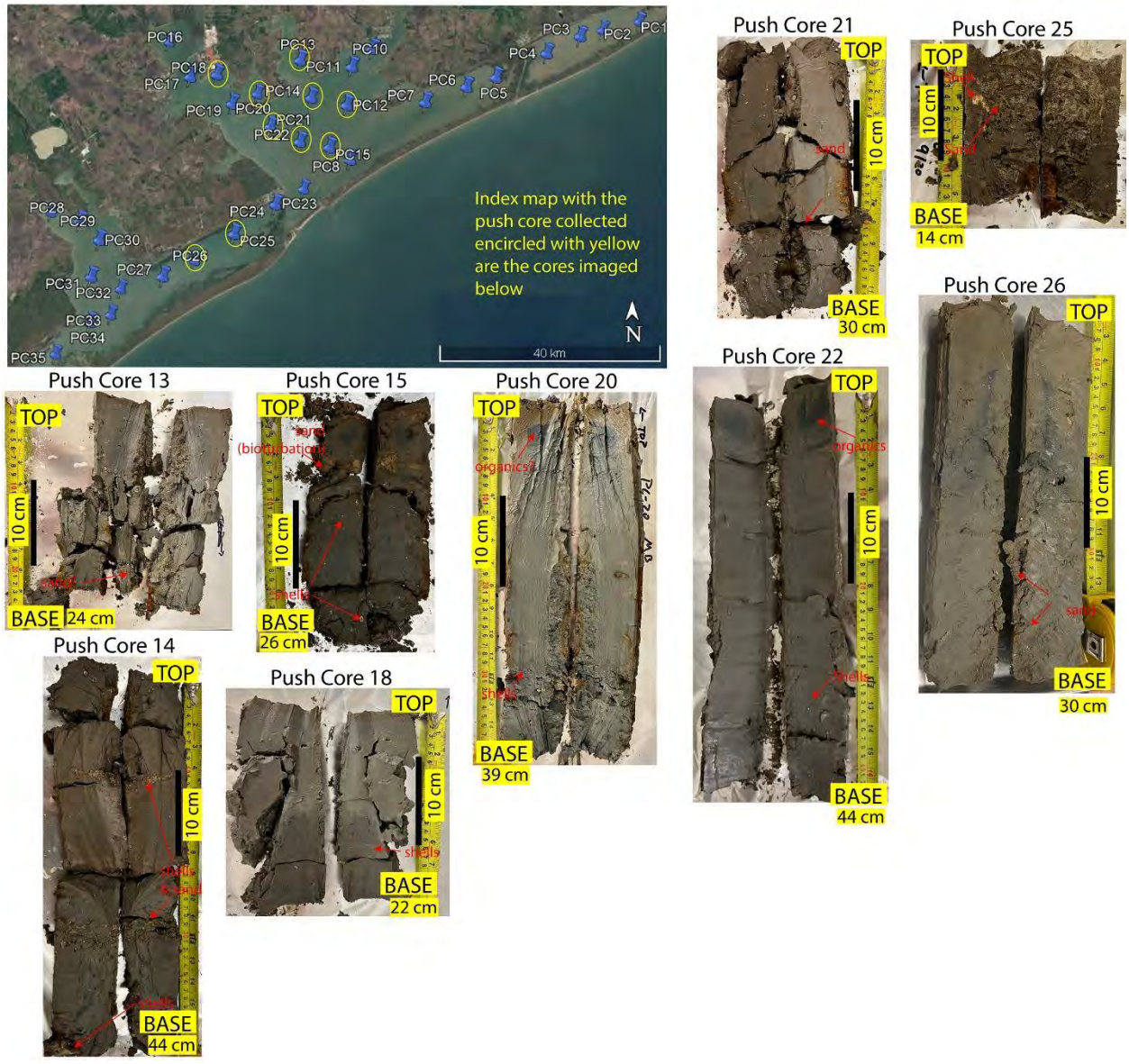

Figure 30. Photos of the sediment cores 13, 14, 15, 18, 20, 21, 22, 25, 26 from Matagorda Bay. Top left map indicates the location of the cores. Cores are dominated by muddy sediments with two exceptions, cores 24 and 25, which are muddy sands. These cores are located proximal to Pass Cavallo, where a flood tide delta composed of marine sands dominates the area. Well preserved and obvious bioturbation filled with sand is visible in core 15.

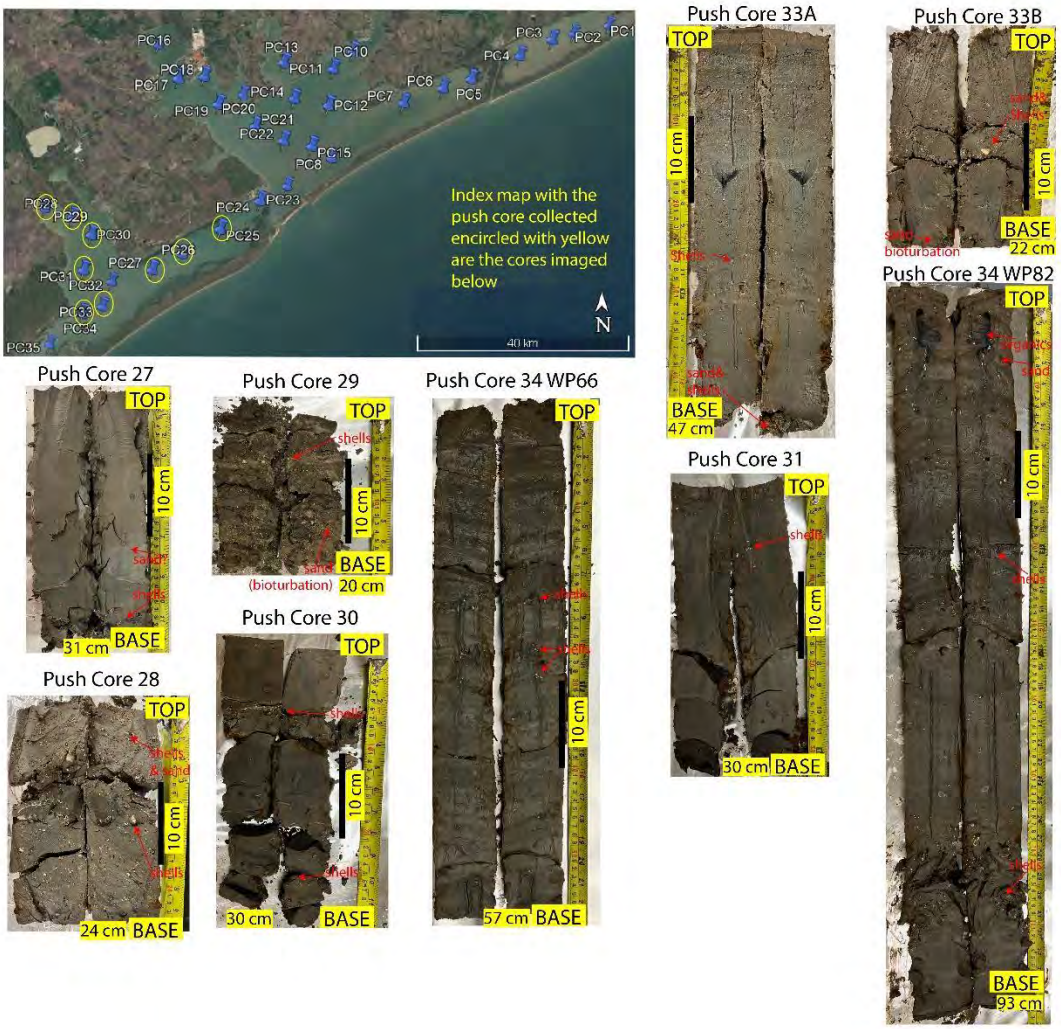

Figure 31. Photos of the sediment cores 27, 28, 29, 30, 34 WP66, and 34 WP82 from San Antonio Bay. Top left map indicates the location of the cores. Note that core 29 has multiple sand intercalations. Cores 30 and 34 WP82 have some clear shell fragments and (probably?) sand-rich intervals indicating higher energy flow events.

Figure 32. Photos of the sediment cores 35, 36, 37 (San Antonio Bay) and 120 (Matagorda Bay – Colorado river mouth). Top left map indicates the location of the cores. Cores are dominated by muddy sediments with varied degrees of brown to grey alteration. Core 120 (PC-5 location on the map) was collected at the mouth of the Colorado River, and is characterized by homogenous silt and clay indistinctly layered at the base, which transitions to finely laminated organic-rich beds near the top. These observations of A) massive or indistinct bedding may relate to regular mixing at the mouth of the river, and B) punctual (i.e., seasonal) drought and flooding events.

4. 3 Grain size analysis in cores

Understanding the accumulation and dynamics of microplastics in bay sediment is crucial, and key to this is analyzing the grain size and total organic content (TOC) of the sediment.

Grain size analysis on cores 11, 13, 21, 31, 35, 36, and 37 was conducted at 2cm or 4cm intervals based on perceived bed grain size variability from visual descriptions. The Mastersizer 3000, which uses laser diffraction to measure particle size distribution, was employed for this analysis (Malvern Panalytical, 2023).

The grainsize results from cores were presented as histograms (grain-size class frequency) as they vary with depth (Figures 33 to 39). The results shows that sediment grain size is primarily dominated by silts (grains between 4 and 60 microns, see reddish-brownish colors on figures 33 to 39), but there are some notable observations related to grainsize variability. While silt is the dominant grain size, some sampled cores (e.g., core 11, Fig. 33) exhibited dominance by very fine and fine sand. Another interesting finding is the presence of multiple high-frequency "peaks" in different grain size classes in many samples. For instance, samples at the surface (0 cm) and at depths of 4 cm and 8 cm in core 13 (Fig. 34) displayed three grain size peaks in clay, silt, and very fine sands. Many other samples in different cores have bi-modal or tri-modal distributions. This observation on grainsize distributions suggests that sediments have been transported by different processes and eventually ended up mixed in the same deposits, possibly due to bioturbation or anthropogenic factors.

Some cores show variability in grain size with depth. If no thin (mm) thick laminae were observed in the photos (Figs. 28 to 32), changes at the cm or dm scale have been observed. For example, in core 21 (Fig. 35), while the core is predominantly silty, the bottom three samples (at depths of 24 cm, 26 cm, and 28 cm) are dominated by very fine sand. While most samples exhibit a tripartite distribution (clay-silt-very fine sand), some cores show variations with a higher peak of coarser sediments (very fine and fine sand).

The distribution of the predominant grain size (i.e., silt) is roughly similar to the findings of the last comprehensive sediment survey in the Matagorda Bay (e.g., McGowen, 1979). Although the correlation between grain size, TOC content, and microplastics will be done in further data analysis, no correlation was observed between sediment grab samples for which both microplastics and grain size have been analyzed.

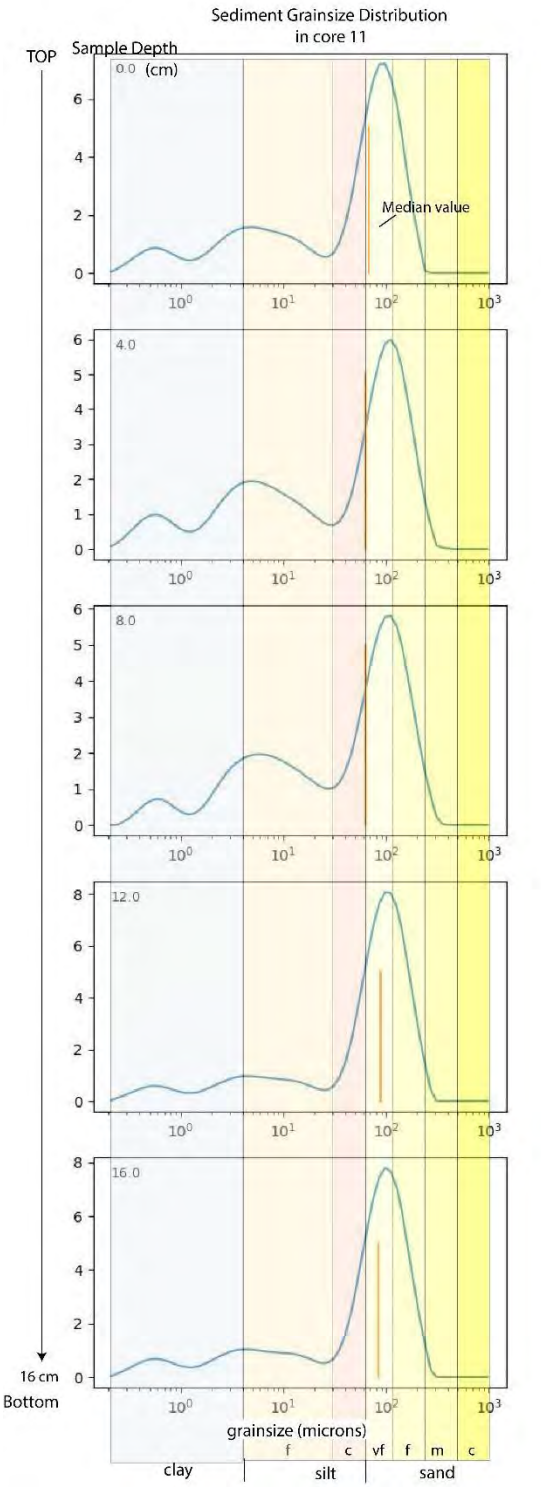

Figure 33. Sediment grain size in core 11. Multiple frequency histograms represent sediment samples at given depth in the core. On the X axis grainsize classes are separated and color coded to be easier to observe. The vertical orange line on each graph represents the median (d50) grain size value.

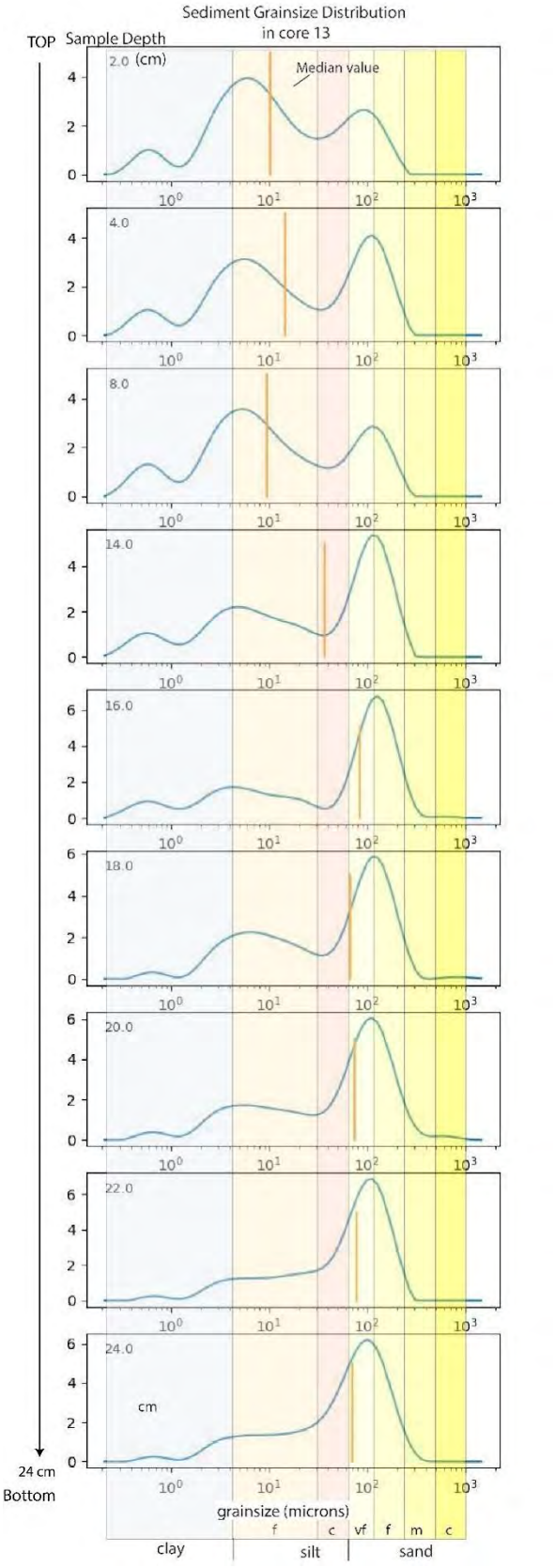

Figure 34. Sediment grain size in core 13. Multiple frequency histograms represent sediment samples at given depth in the core. On the X axis grainsize classes are separated and color-coded to be easier to observe.

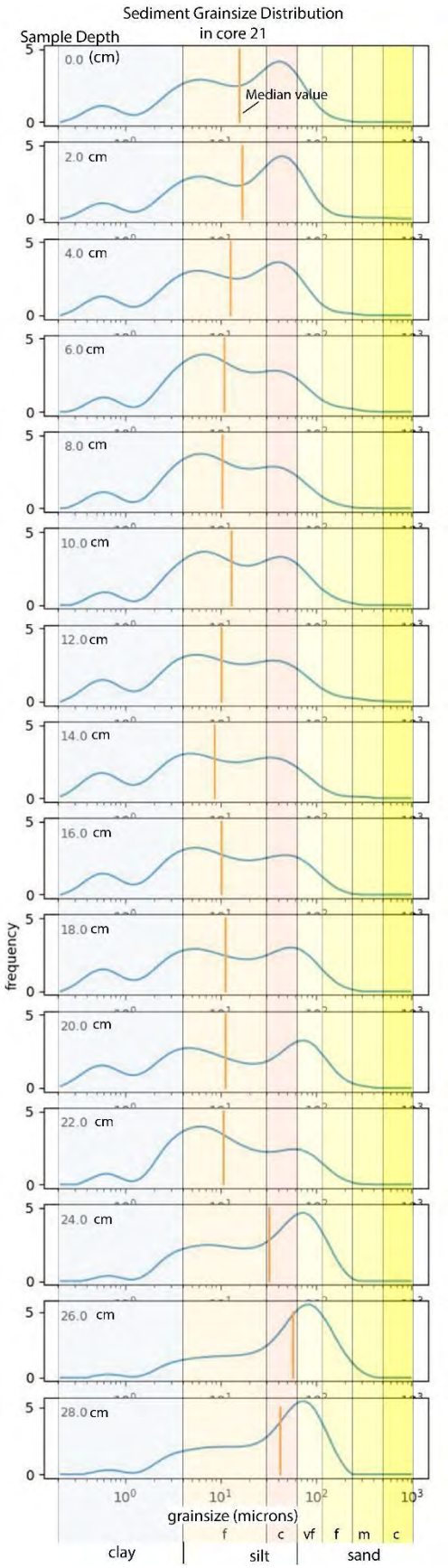

Figure 35. Sediment grain size in core 21. Multiple frequency histograms represent sediment samples at given depth in the core. On the X axis grainsize classes are separated and color-coded to be easier to observe.

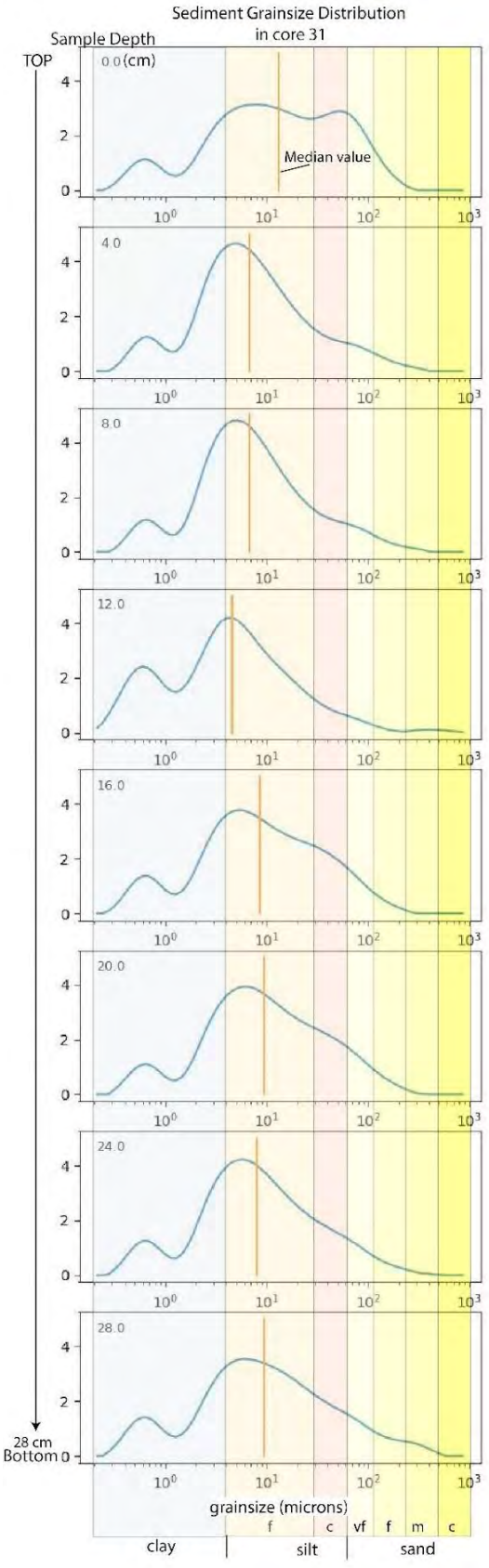

Figure 36. Sediment grain size in core 31. Multiple frequency histograms represent sediment samples at given depth in the core. On the X axis grainsize classes are separated and color-coded to be easier to observe

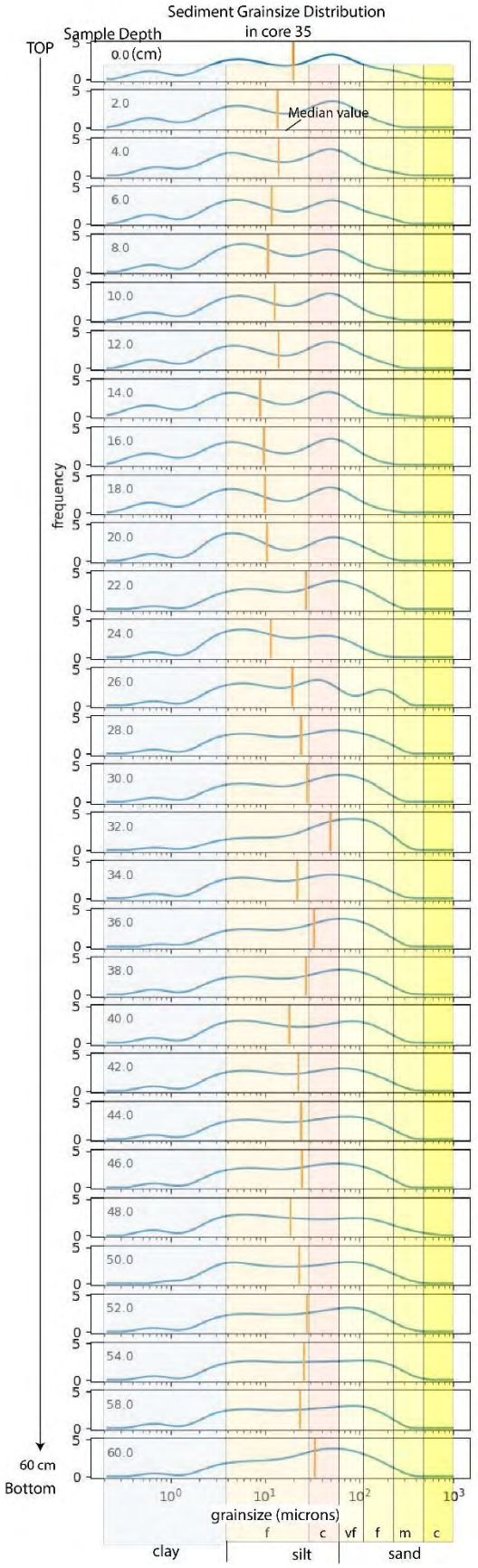

Figure 37. Sediment grain size in core 35. Multiple frequency histograms represent sediment samples at given depth in the core. On the X axis grainsize classes are separated and color-coded to be easier to observe

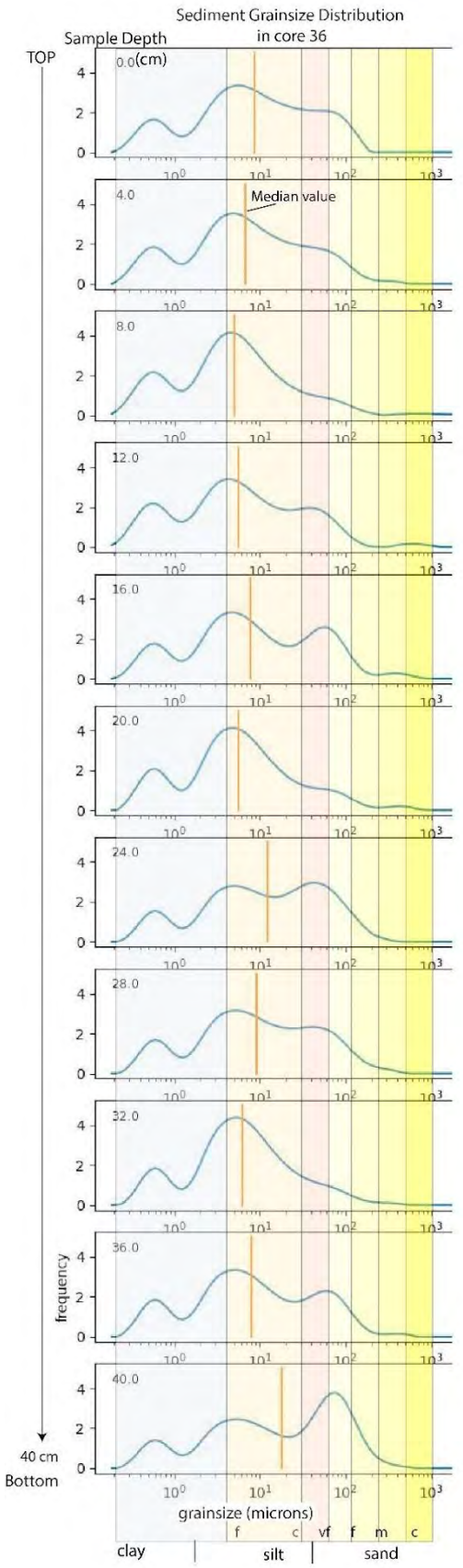

Figure 38. Sediment grainsize in core 36. Multiple frequency histograms represent sediment samples at given depth in the core. On the X axis grainsize classes are separated and color-coded to be easier to observe

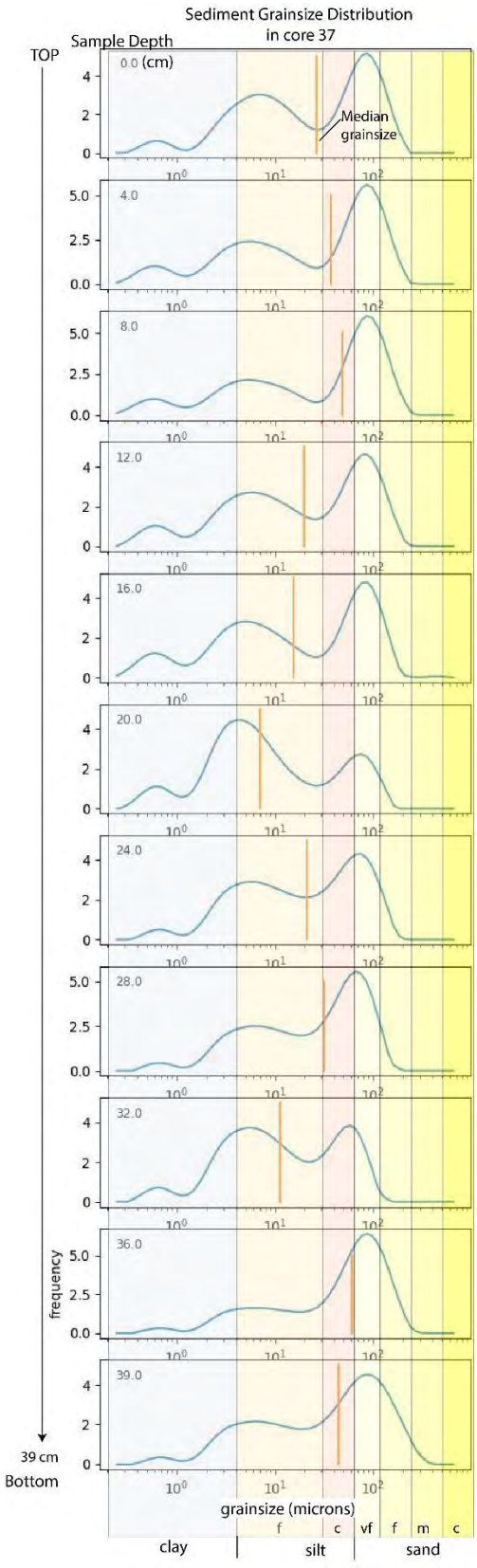

Figure 39. Sediment grainsize in core 37. Multiple frequency histograms represent sediment samples at given depth in the core. On the X axis grainsize classes are separated and color-coded to be easier to observe

4.4 Grain size and total organic carbon in sediments

Grainsize and total organic carbon (TOC) in the sampled sediments is important for understanding the microplastics dynamics and accumulation in the bays. One of the initial hypotheses was that microplastics will be found more in finer sediments and in organic enriched sediments. The grain size and the total organic content (TOC) in the sediment is strongly influenced by clastic material input (microplastic included) to the bay, and water circulation patterns in the bay. If we are able to establish some rules of what type (grainsize, TOC content) of sediments the plastics might concentrate in, we can improve the prediction of microplastics occurrence. Again, the initial hypothesis was that microplastic content will be higher (1) in finer-grained sediments and (2) in organic-rich deposits, which may pertain to overlapping material densities (ca. 0.9-1.5 g/cc).

Here, we compared microplastic concentrations from grab samples to values related to percent sand on cumulative curve distribution at D10, D50, and D90 grain sizes (that is sediment sizes at 10%, 50%, and 90%). The bay sediment ranges from clay (most D10 values are around 10 microns) to fine sand (D90 values at 125-250 microns) (see Figure 40A). Our observations indicate that the bay is dominated by silt-size sediments and it seems the sediment grain size accumulated during last decades is unchanged since it was extensively mapped in the late 1970s. The distribution of the predominant grain size (i.e., silt) is also roughly similar to the last comprehensive survey (Figure 42) (e.g., Mud; McGowen, 1979). The distribution of the samples varies with some samples showing a unimodal distribution with a peak in the clay-silt range and other samples having a peak in the fine sand range. Interesting to note is that many samples have bi-modal distribution (like sample G_47 in Figures 40B, 41B) suggesting different sediment transport and deposition processes. The observed bi-modality of the sediment distribution is similar to the observations made in cores. The grain size and TOC analysis on 63 shallow sediment bed (grab) samples produced the distribution maps. The results show the Matagorda Bay sediment is dynamic (with different grain size distribution modes in different locations), but the grain size range, dominated by silt, is similar. However, if any association between grain size and microplastic concentration can be found then we also know the prevalent areas for microplastic accumulations.

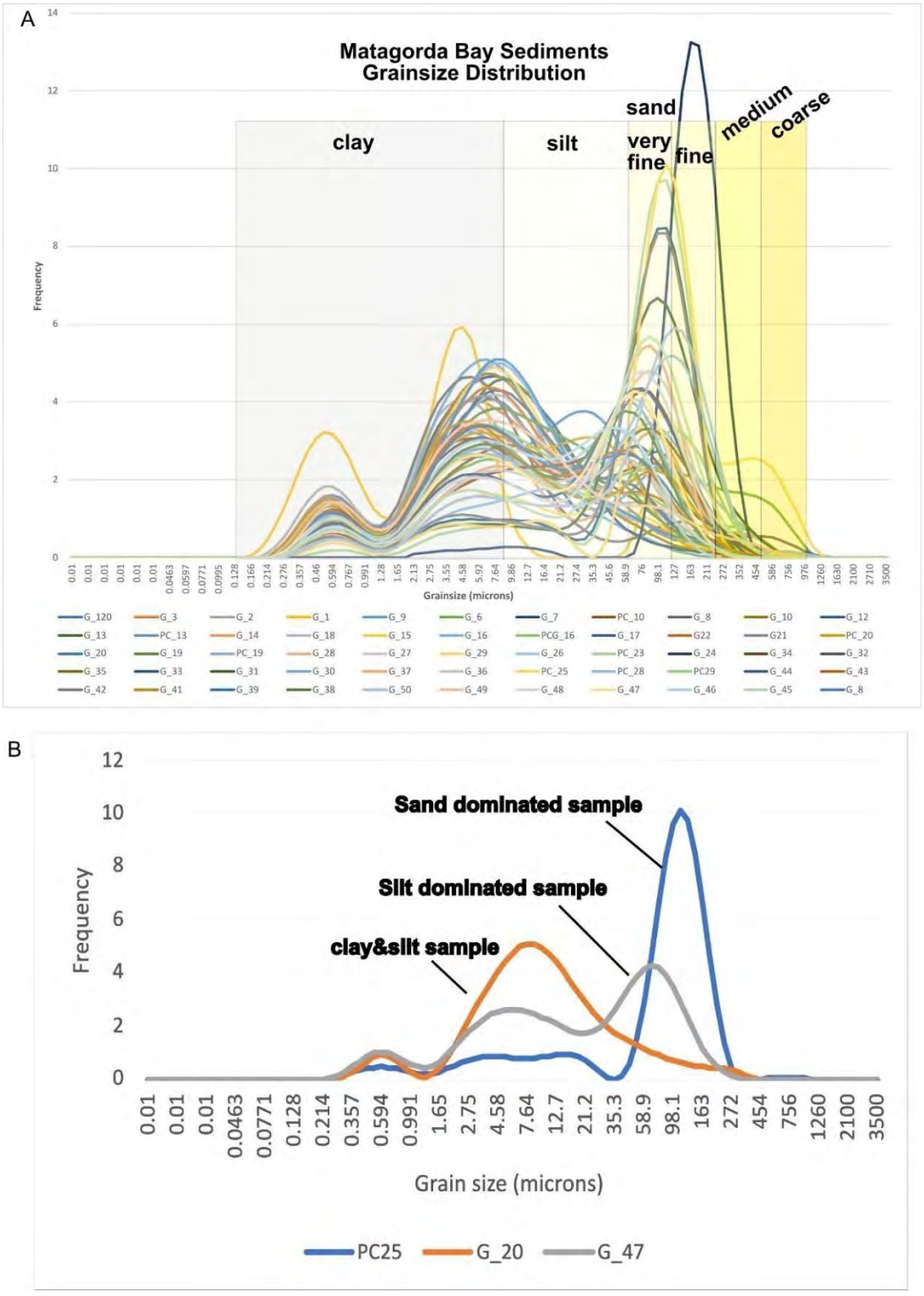

Figure 40. A – Multi-sample grainsize distribution. Notice the range is from clays to silt to very fine sands with many samples showing two grainsize "peaks" (bimodal) in the same sample. However, the grainsize distribution between samples varies. B – Samples with different distribution modes. Note some samples have unimodal distribution with a peak in clay-silt range and other samples have a pick in fine sand range.

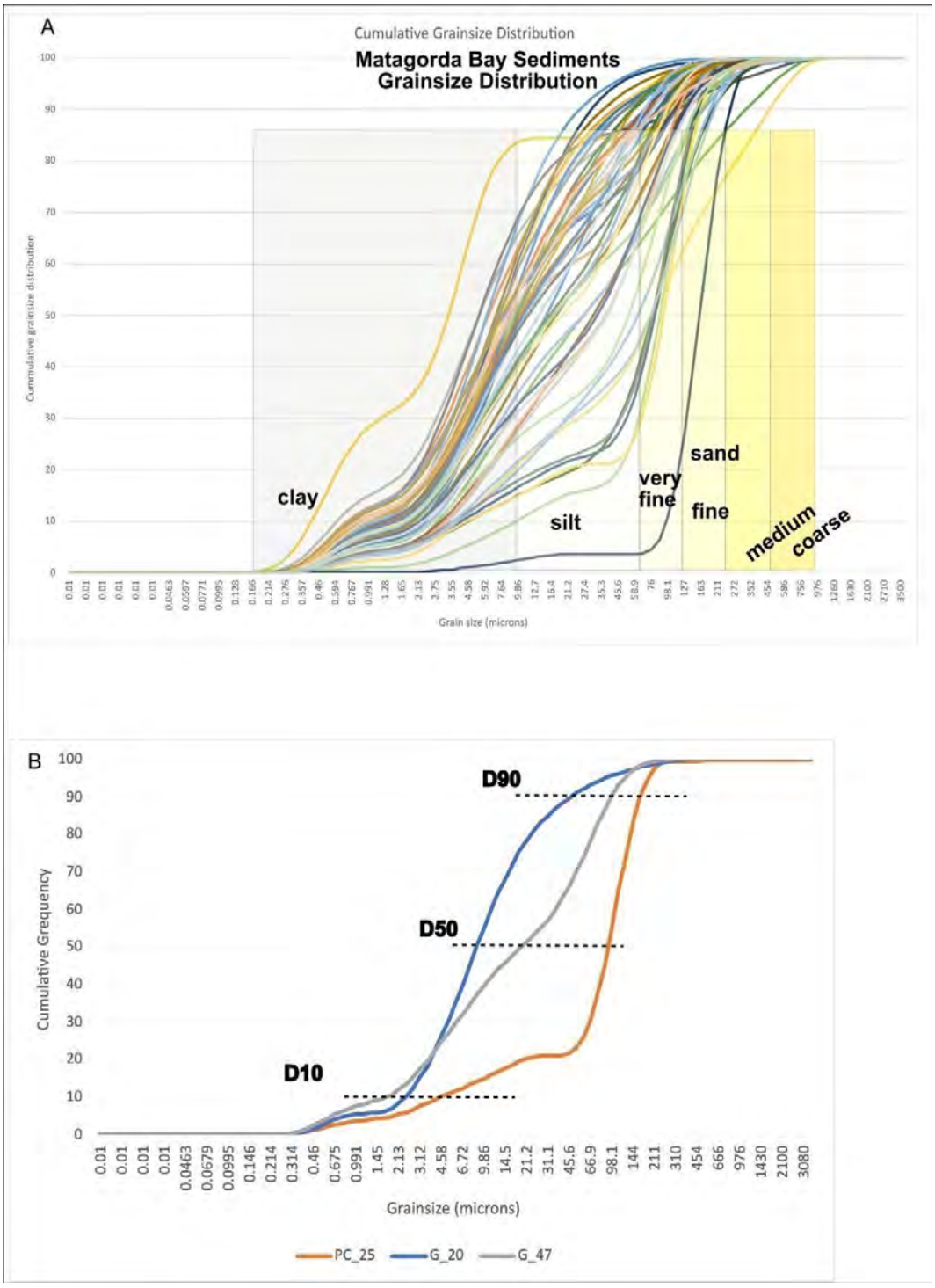

Figure 41. Cumulative distribution graphs of the same samples from Figure 40. A – Multi-sample grainsize distribution. Notice the range is from clays to silt to very fine sands. However, the grainsize distribution between samples varies. B – Samples with different distribution modes. Note some samples have unimodal distribution with a peak in clay-silt range and other samples have a pick in fine sand range. The steepest curve location indicates the higher frequency grainsize range.

Our grainsize results indicate higher microplastics concentrations within silt-dominated bay areas (Figure 43).

However, it seems that grainsize is a poor prediction for microplastic content in this silt-dominated depositional environment. The total microplastic concentration versus the grainsize distribution shows a relatively poor correlation, but with the highest microplastic concentration in fine (silty) sediments (Figure 44A). However, there are fine grainsize samples that have low microplastic concentrations as well (Figure 44A). If the microplastics are separated by type (fibers and fragments) and plotted against D10, D50 or D90 distributions the correlation is still low (Figure 44B).

When we compare relative concentrations of microplastic in the sediment versus in the water column (next section of the report), initial results indicate approximately 1,000- times more plastic resides in the bay sediment.

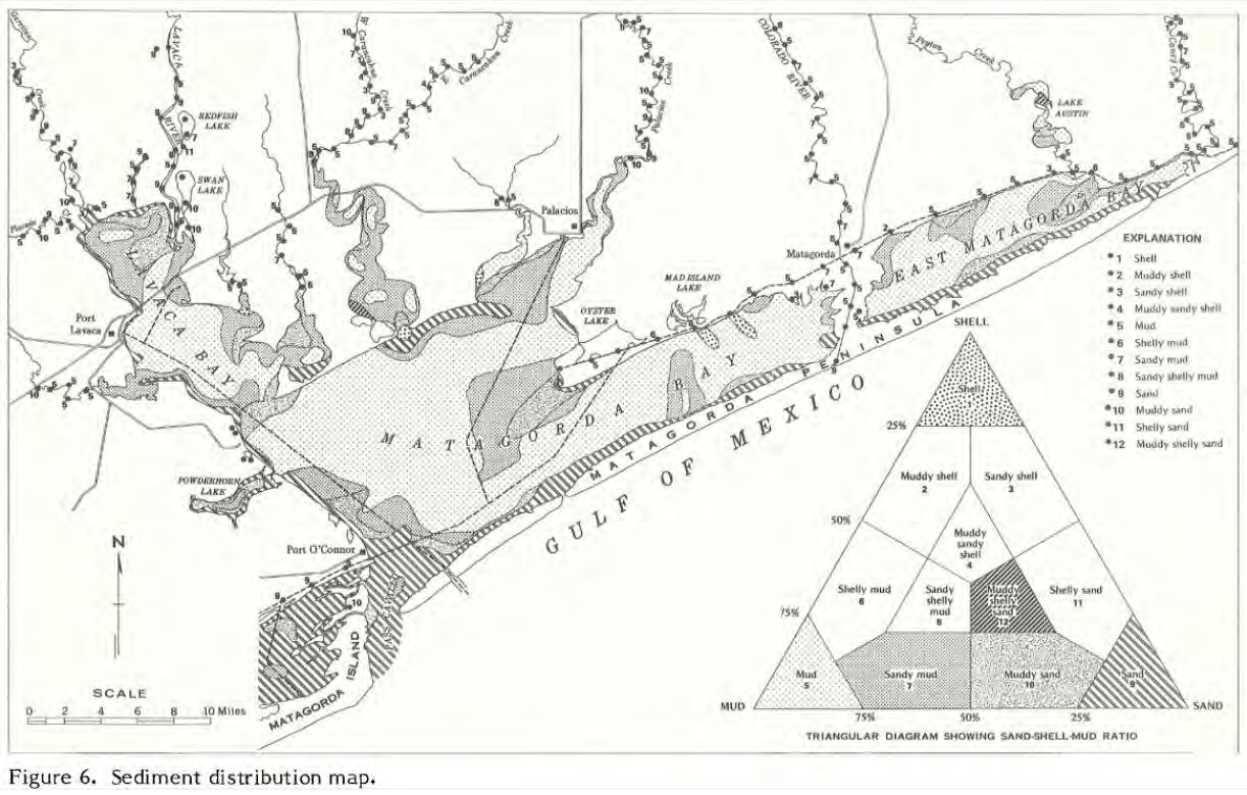

Figure 6. Sediment distribution map.

Figure 42. Sediment grainsize distribution map in San Antonio and Matagorda bays (McGowan, 1979).

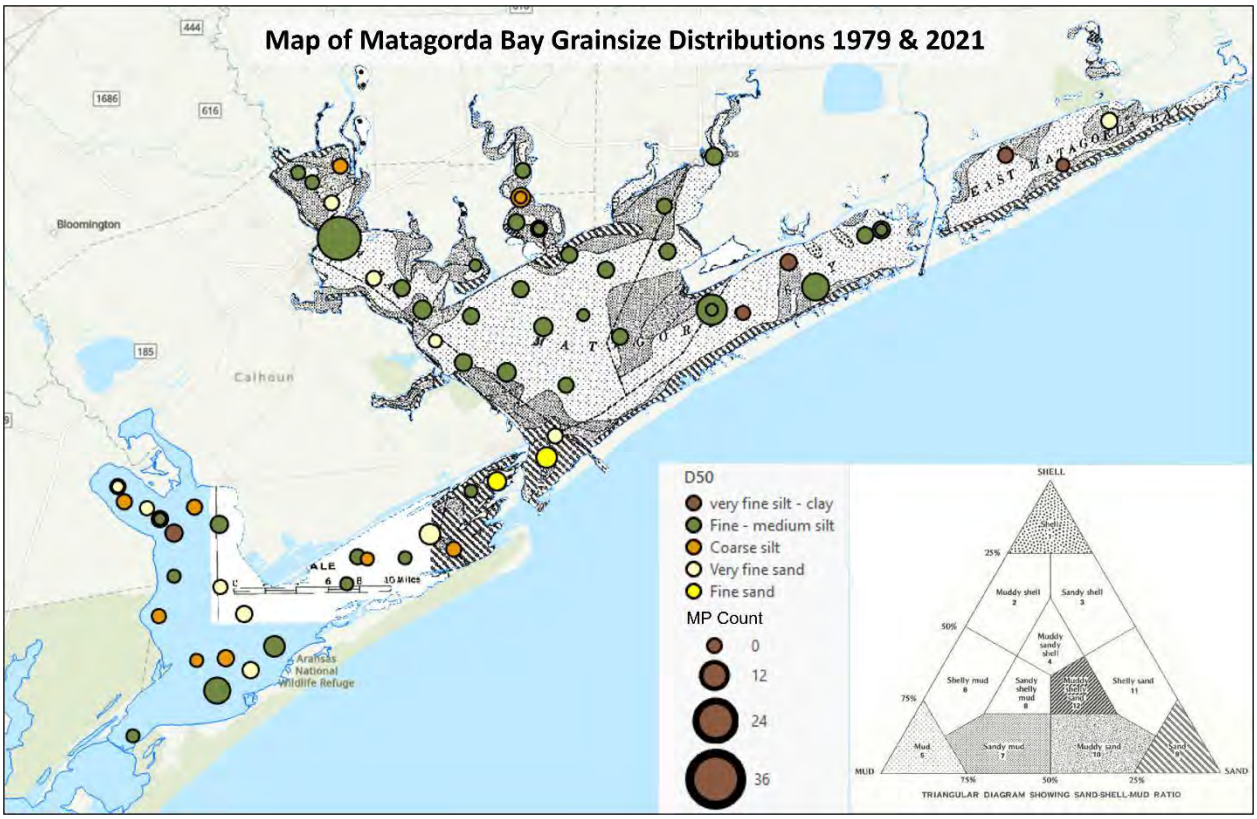

Figure 43. Map of Matagorda Bay grainsize distribution and microplastic concentrations from shallow bed grab (circles, collected in 2021) samples overlain with the sediment distribution map (modified from McGowen, 1979). The map illustrates higher microplastic concentrations proximal to urbanized areas (e.g., Port Lavaca) and in fine to medium silt-dominated bed material.

Total Organic Carbon (TOC) distribution in Matagorda Bay and establishing its level of association with microplastics is important because the organic material might be food for many organisms and the presence/association of microplastics with that might affect the trophic chain. Matagorda Bay grab samples have been analyzed for TOC content (Table 2). We found that the highest TOC occurs proximal to Lavaca River and Pass Cavallo. Interestingly, these values are significantly higher than the TOC values found in McGowan's (1979) study, where most samples contained less than 0.5% TOC. This stark contrast may be related to the different lab methods used (i.e., *Loss on Ignition* (this study) versus *Wet Combustion* (McGowan, 1979). From the processed samples, we can say that TOC is not associated with microplastics as there is not a good correlation between the values.

Figure 44. Sediment grain size versus microplastic (MP) concentration. A – All microplastics found plotted against D10-D50-D90 values. B – Microplastics concentration separated by type (fiber, fragments) versus grainsize values at D10, D50 and D90.

The distribution (mapping) of Total Organic Carbon (TOC) in Matagorda Bay was analyzed for all 65 grab samples and the tops of cores have been analyzed for TOC content (see Table 2). Additionally, sediments in cores 11, 13, 21, 31, 35, 36, and 37 have also been analyzed for TOC.

The overall variability in TOC values ranges from 0.2% to 3%, with most values falling between 0.8% and 2.2% TOC (refer to Fig. 45). These values are higher than the TOC values reported in McGowan's (1979) study, where most samples contained less than 0.5% TOC. This difference might be explained by the increase of organic material accumulation in the bay caused by increased restricted circulation with the ocean. However, as previously mentioned, it also may be attributed to the different laboratory methods used, specifically *Loss on Ignition* in this study versus *Wet Combustion* in McGowan (1979) study.

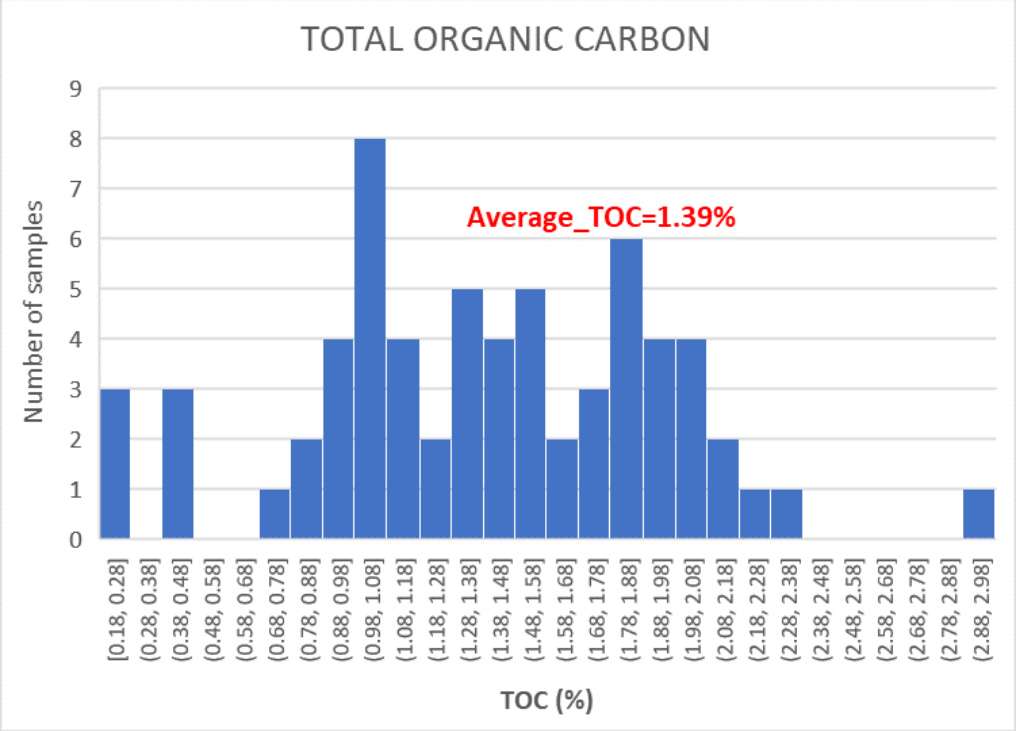

Figure 45 illustrates the distribution of Total Organic Carbon percentages in sediments at the bottom of the bay in grab samples and at the top of cores. The average TOC value is 1.39%.

SITE_NO	BAY_ID	GRAB_PCB	Weight Before (g)	Weight After (g)	LOI	TOC
25	SB	PCB	59.8309	59.0369	0.794	1.33
26	SB	PCB	59.4724	58.3169	1.1555	1.94
28	SB	PCB	57.1987	56.1167	1.082	1.89
29	SB	PCB	55.36	54.6306	0.7294	1.32
32	SB	G	52.7662	52.3874	0.3788	0.72
33	SB	G	52.9247	52.3687	0.556	1.05
35	SB	G	50.6248	49.4437	1.1811	2.33
36	SB	G	51.5946	50.6745	0.9201	1.78
37	SB	G	56.2862	55.4035	0.8827	1.57
38	SB	G	55.9598	55.3496	0.6102	1.09
39	SB	G	52.5624	51.9734	0.589	1.12
41	SB	G	56.659	56.1425	0.5165	0.91
42	SB	G	59.5536	58.8661	0.6875	1.15
43	SB	G	46.7374	46.1225	0.6149	1.32
44	SB	G	52.2988	51.6473	0.6515	1.25
45	SB	G	51.6719	51.0994	0.5725	1.11
46	SB	G	56.1625	55.1934	0.9691	1.73
47	SB	G	56.5523	55.8051	0.7472	1.32
48	SB	G	58.6492	58.0644	0.5848	1.00
49	SB	G	52.4013	51.5383	0.863	1.65
50	SB	G	54.8959	54.3625	0.5334	0.97
51	SB	G	59.6847	59.1105	0.5742	0.96
52	SB	G	53.9178	53.3664	0.5514	1.02
73	SB	G	55.9343	55.1293	0.805	1.44
79	SB	G	56.9131	56.8125	0.1006	0.18
6	MB	Water	46.6795	45.9756	0.7039	1.51
7	MB	G	51.9011	50.8297	1.0714	2.06
8	MB	G	50.6071	49.6669	0.9402	1.86
9	MB	G	49.1325	48.1601	0.9724	1.98
10	MB	G	47.9518	47.0551	0.8967	1.87
10	MB	G	59.1221	58.5391	0.583	0.99
12	MB	G	49.9354	49.2055	0.7299	1.46
13	MB	PCB	58.3742	57.7621	0.6121	1.05
13	MB	G	46.3092	45.7599	0.5493	1.19
14	MB	G	56.5449	55.7415	0.8034	1.42
15	MB	G	48.0055	47.0025	1.003	2.09
16	MB	PCB	53.0486	52.3661	0.6825	1.29
16	MB	G	49.4001	48.297	1.1031	2.23
17	MB	G	54.9539	54.071	0.8829	1.61
18	MB	G	47.6635	46.9388	0.7247	1.52
19	MB	PCB	59.336	59.0892	0.2468	0.42
19	MB	G	53.119	52.9863	0.1327	0.25
20	MB	G	56.425	55.2731	1.1519	2.04
21	MB	G	51.5643	50.6395	0.9248	1.79
22	MB	G	54.2982	53.8235	0.4747	0.87
23	MB	PCB	59.8593	59.3363	0.523	0.87
24	MB	G	50.0816	49.8865	0.1951	0.39
26	MB	PCB	48.7119	47.8236	0.8883	1.82
27	MB	G	52.3903	51.8768	0.5135	0.98
28	MB	G	53.472	53.2568	0.2152	0.40
29	MB	G	50.726	50.589	0.137	0.27
31	MB	G	58.1134	57.5524	0.561	0.97
32	MB	G	49.1332	48.2477	0.8855	1.80
33	MB	G	53.1903	52.6454	0.5449	1.02
34	MB	G	59.6734	58.7797	0.8937	1.50
120	MB	PCB	55.6482	54.5683	1.0799	1.94
1	EM	G	56.0222	55.4349	0.5873	1.05
2	EM	G	51.5035	50.5335	0.97	1.88
2	EM	G	51.4799	50.3838	1.0961	2.13
3	EM	G	51.4084	50.7088	0.6996	1.36
3	EM	PCB	50.6933	49.6578	1.0355	2.04
4	EM	PCB	54.9181	53.2876	1.6305	2.97
4	EM	G	46.714	46.0099	0.7041	1.51
5	EM	PCB	57.6937	56.6953	0.9984	1.73
44	EM	G	57.619	56.6009	1.0181	1.77

Table 2. Total Organic Carbon for the grab samples collected in Matagorda Bay (MB), East Matagorda Bay (EM), and San Antonio Bay (SB).

Samples including bay grab sediments and push core tops, as well as shoreline transects from Lavaca Bay and Matagorda Peninsula have been plotted on the map (Figure 46A). Updated microplastic results show higher concentrations near Port Lavaca and proximal to the Colorado River mouth.

Total Organic Content for each of the surface samples was completed and spatially interpolated to compare with the last comprehensive study by McGowan 1979 (Figure 46B). TOC results illustrate higher values proximal to the Colorado River mouth and near the center of Matagorda Bay. The TOC trend results (high vs. low values) in the bay are similar to the previous (McGowen et al., 1979) study.

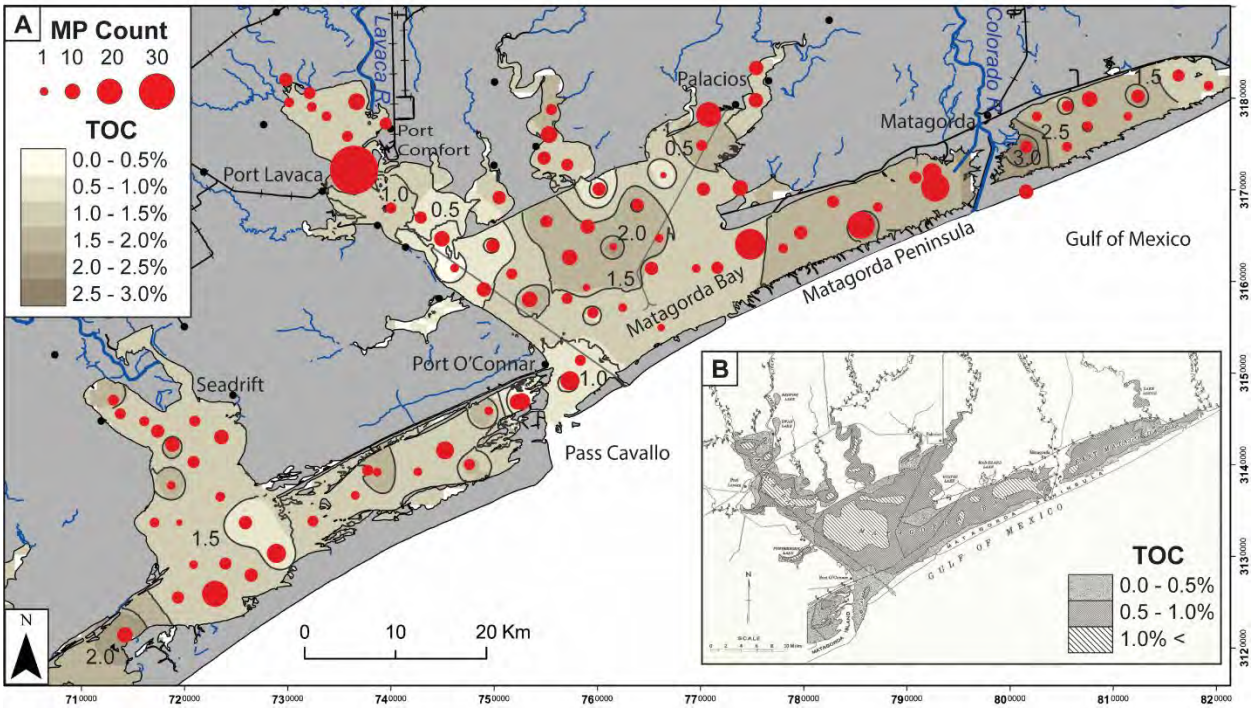

Figure 46. A) Total Organic Content and microplastic distribution map from bay sediment samples. B) Previous TOC map (modified from McGowan, 1979).

5. WATER RESULTS AND ANALYSIS OF MPs

5.1 FTIR analysis of suspended particles: Suspended particles were collected using a plankton tow (150 µm) at 11 sites in Fall 2021. Surface water samples (<1m) were collected at all sites, but at sites 3, 4, 6, 9, 18, and 20, deep water samples (2-3 m) were also collected. The particulate samples were filtered using an ASTM metal sieve with a pore size of 150 µm and dried in an oven for 2 days at 60℃. About 20-25 mL of 30% hydrogen peroxide were added to the dried residues and incubated in the oven for 2 days at 60℃. The samples were then filtered with MCE Green Grid membrane filters with a pore size of 5 µm. About 1 mL of 6 mol/L of HCl was added to the

membrane filters to remove the possible carbonate on the filter. The membrane filters were left to dry for a day and then were analyzed using an AIM-9000 FTIR microscope.

Out of the 195 suspected microplastics observed at all sites, there were 169 fragments, 23 films, 2 spheres, and 1 fiber (Figure 47). Fragments were the most abundant, while fibers were the least. Sites 1, 2, 9, 17, 18, and 20 had replicates, so the average was calculated along with the standard deviation (Figure 48). Site 18 had the highest abundance of microplastics, while Sites 4,5,6, 9, and 10 had the lowest abundances.

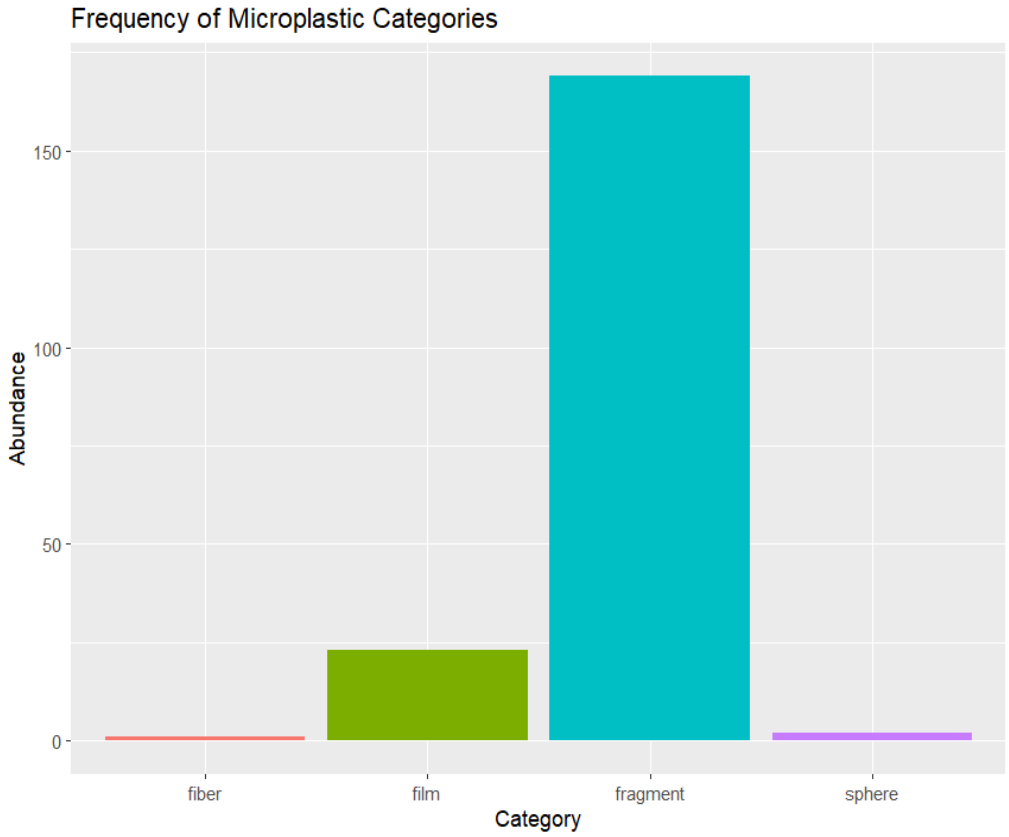

Figure 47: A bar graph that shows the abundance of each category of microplastic shape for the microplastics that were found in all samples. The categories shown are fragments, films, fibers, and spheres.

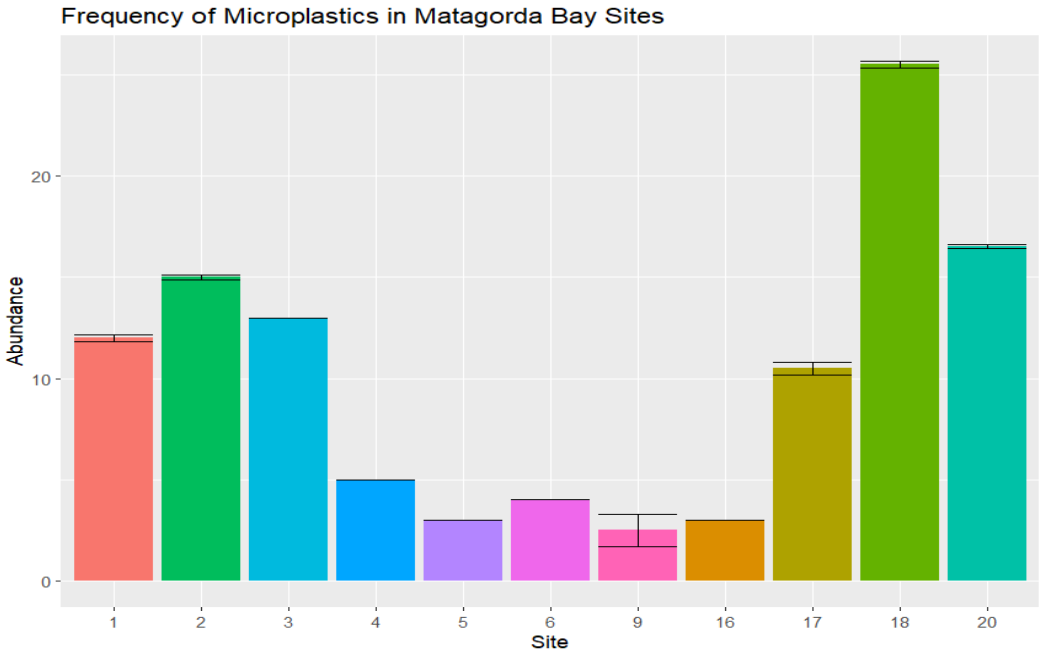

Figure 48: A bar graph that shows the abundance of microplastics for each of the eleven Matagorda Bay sites. The figure includes microplastics found in both surface and deep water samples. Standard error bars are included for sites that had replicates.

Microplastics were identified in all surface water samples (Figure 49). Microplastics were more abundant at Sites 2, 1, 3, 17, 19, and 20 than Sites 4, 5, 6, 9, and 16. Microplastics were also found in all the deep-water samples (Figure 50), but Site 3 was not included since the analysis of samples from this site is still on going. Site 9 had the highest concentration of microplastics for deep water samples. Sites 1, 3, 17, and 20 have intermediate concentrations of microplastics. Sites 4 and 6 had the lowest concentrations of microplastics for deep water samples.

The type of polymers in microplastics were identified with the microscopy FTIR based on reflectance. A high variety of polymers were found (18 types), including polyacrylonitrile-butadiene-styrene (ABS), epoxy, polycarbonate (PC), polyphenylene sulfide (PPS), and rubber etc. (Figure 51). Rubber had the highest abundance out of all polymer types. polyphenylene sulfide and epoxy also had high abundances. There was a similar distribution pattern among the sample sites (Figure 52). Common polymers such as rubber, polyphenylene sulfide, and epoxy appear throughout most of the sites except for some of the sites that had very low abundances of microplastics such as sites 4, 5, 6, 9, and 16.

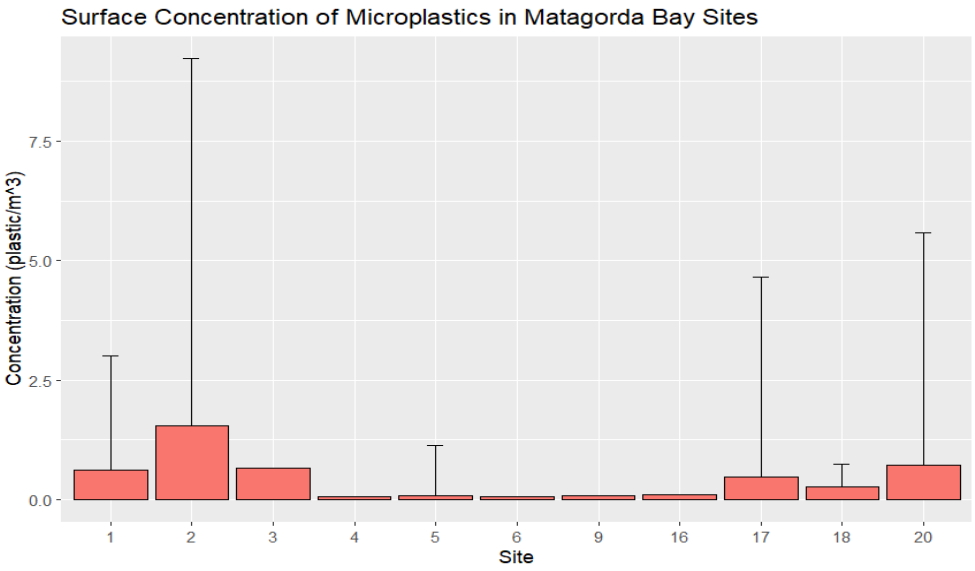

Figure 49: A bar graph that shows the surface water concentrations of microplastics in eleven sites as microplastics per m^3. Standard error bars are included for sites with replicates.

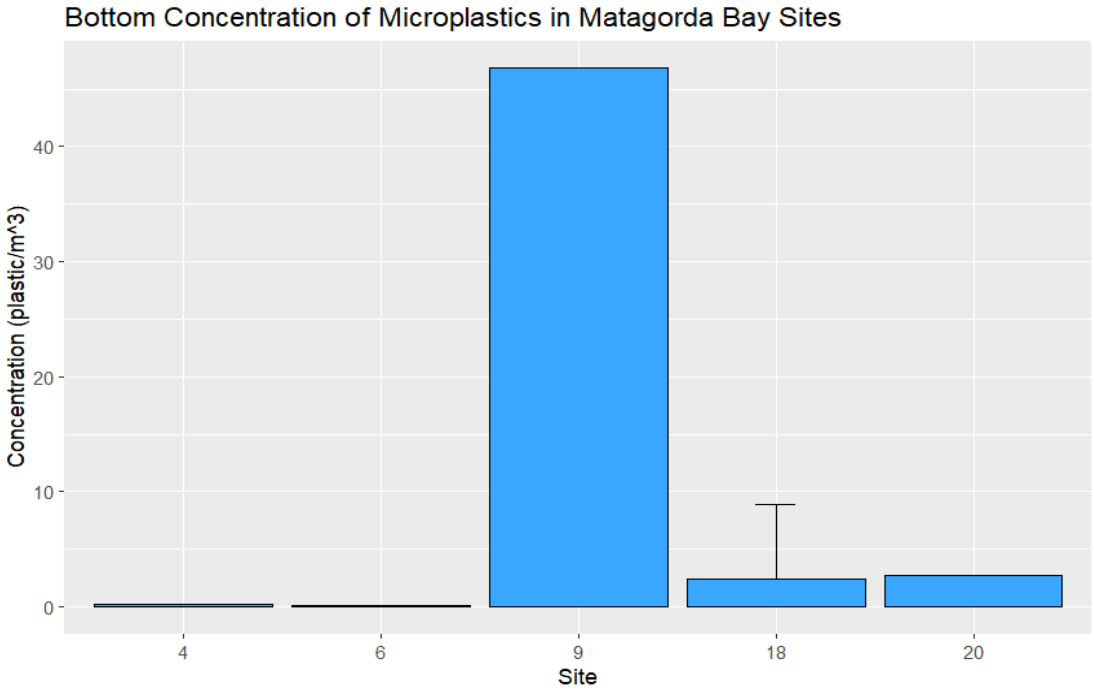

Figure 50: A bar graph that shows the deep water concentrations of microplastics in five sites as microplastics per m3. Standard error bars are included for sites with replicates.

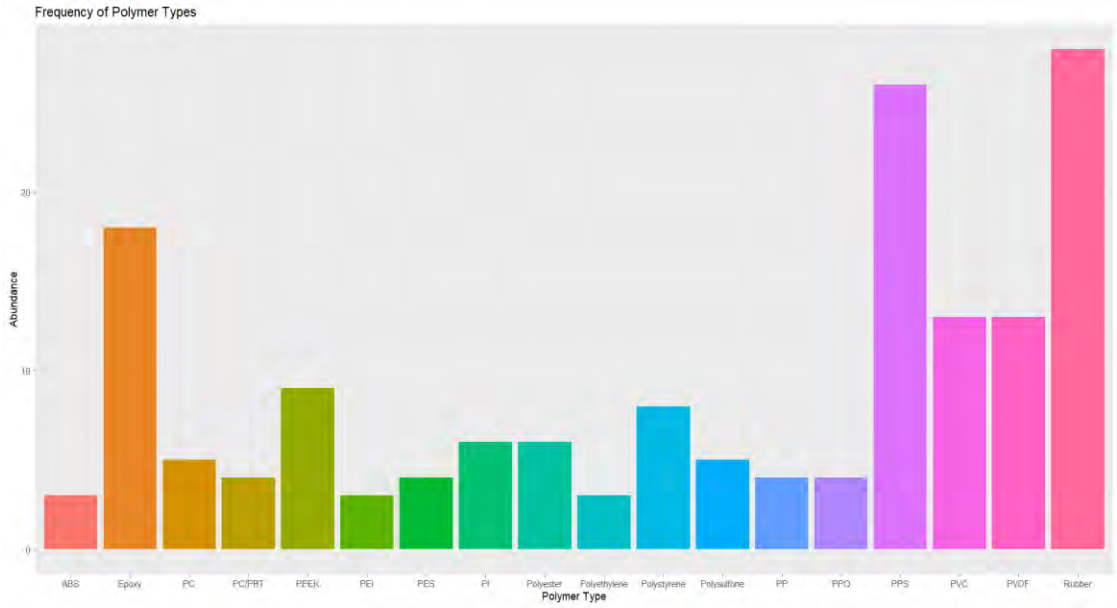

Figure 51: A bar graph showing the abundance of 18 polymer types that were found in all sites and samples. The graph only includes polymers that occurred more than twice in the samples.

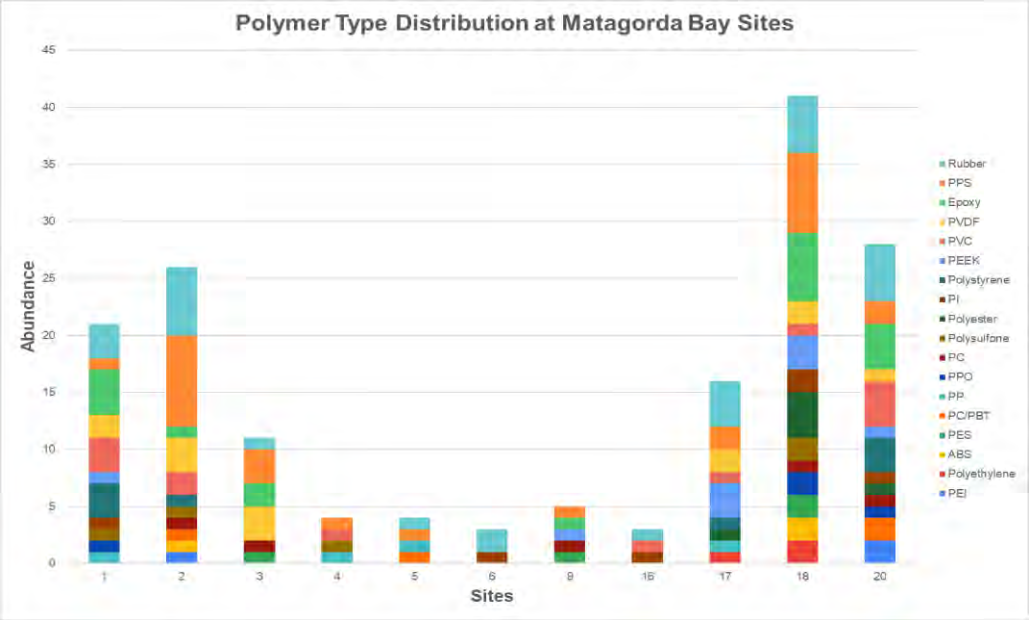

Figure 52: A stacked bar graph showing the distribution and abundance of 18 polymer types across all Matagorda Bay sites. The graph only includes polymers that occurred more than twice in the samples.

Fibers tend to be found in higher abundances in other bays and estuaries in Texas and can even make up to 77% of microplastics (Watford 2021). However, in Matagorda Bay, fibers were found in very low abundance, with fragments dominating the samples instead. This may be due to the low human populations in the cities around Matagorda Bay, relative to other bays with high

populations, such as Chesapeake Bay. Another possibility is that the mesh size of the plankton tow was too large for fibers to be caught in. Other studies used smaller filters, like membrane filters that had a pore size of 0.45 μm. In future experiments, smaller mesh sizes could be used in sample collection to see if there is a difference in fiber abundance. It is also interesting that rubber, polyphenylene sulfide, and epoxy are abundant in Matagorda Bay, likely due to their resilience, high molecular weight, and consistent input. Polyphenylene sulfide is used in filter fabric for boilers, electrical insulation, and gaskets. Epoxy is used in metal coatings, electrical components, and adhesives. Rubber is used in products such as tires and hoses. Future work is needed to elucidate the sources of these plastics and their potential toxicity to marine organisms. Again, caution needs to be taken with the identification of the polymers considering the low resolution of the microscopy FTIR, as mentioned above.

6. SPATIAL ANALYSIS

An analysis of the spatial variability of microplastics in the bays and an attempt to understand possible correlations with other factors such as water depth, sediment grainsize, total organic content has been made.

Analysis of the microplastics distribution in Matagorda Bay shows little correlation between the microplastics content and possible control factors such as total organic carbon, grainsize, water depth, distance to the shore. The correlation between different potential control factors is also low when microplastics are considered by morphology (fibers or fragments) (Figure 53).

Microplastic Correlation Matrix	
FIBER	0.87
FRAGMENT	0.46
D10	0.12
D50	0.07
D90	0.14
TOC	0.08
SHORE DISTANCE	0.14
DEPTH	0.11

Figure 53. Correlation matrix coefficients between microplastics content and factors that might be linked to the microplastics deposition.

Another finding resulting from analysis of the microplastics from Matagorda Bay sediments is that microplastics fragments are larger than the grainsize of the sediments they associate with. This observation suggests a higher mobility of microplastics (Figure 54). The high microplastics mobility supports the idea that these are easier to get resuspended and eventually exported out of the bay to the Gulf of Mexico via natural or man-made inlets.

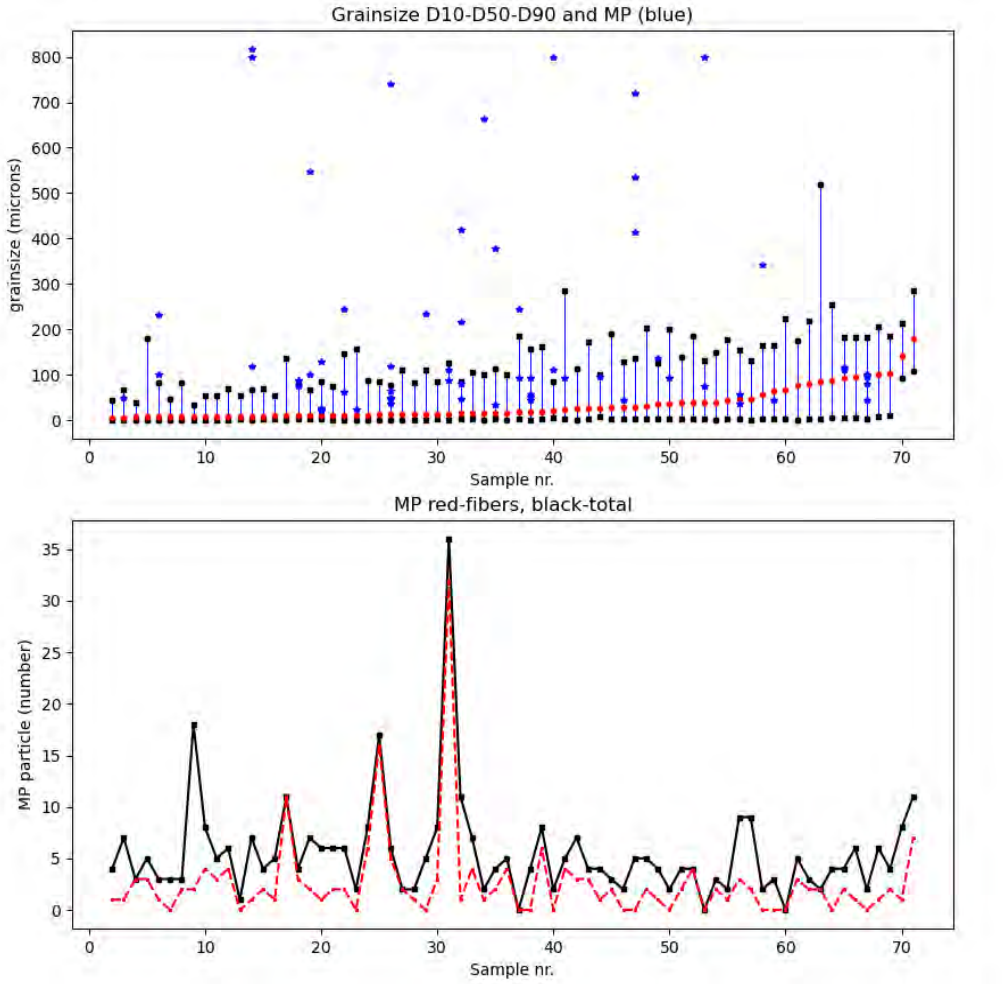

Figure 54. Sediment grain size and microplastic particle sizes in sediment samples from San Antonio, Matagorda and East Matagorda bays.

7. MATAGORDA BAY BATHYMETRY CHANGES THROUGH TIME (1888 to present)

We digitized old marine navigational charts (bathymetry maps) of Matagorda Bay to understand sediment accumulation patterns, sediment that also includes microplastics. The historical sedimentation patterns would give us information about the long-term accumulation of sediments (including microplastics) and also about the dominant sediment transport processes in the bay (wave, currents, wind).

Sediment accumulation from bathymetry maps was also examined to better understand sediment long term/historical transport and dynamics in Matagorda Bay. Historical nautical charts from 1888, 1934, 1954, 1970, and 1981 (see Fig. 55) were digitized using ArcGIS software and re-gridded (see Fig. 56). Historical water depth values were subtracted between the different digital gridded maps and the modern NOAA depth soundings to quantify temporal changes and highlight the bay fill evolution.

The bathymetry differences map between 1888 and the present (see Fig. 57) indicates that Matagorda Bay has become shallower with more than 2 meters of sediment accumulation (red areas in Fig. 57), while some areas (green areas in Fig. 57) showed deepening behind the barrier. Most of the area towards the northeast accumulated sediments from the Colorado River, resulting in the bay becoming shallower. Interestingly, it appears that the bay has deepened behind the barrier bar, likely due to erosion of the bay shoreline, higher sediment compaction, subsidence in the area, or a combination of these factors (refer to Fig. 57).

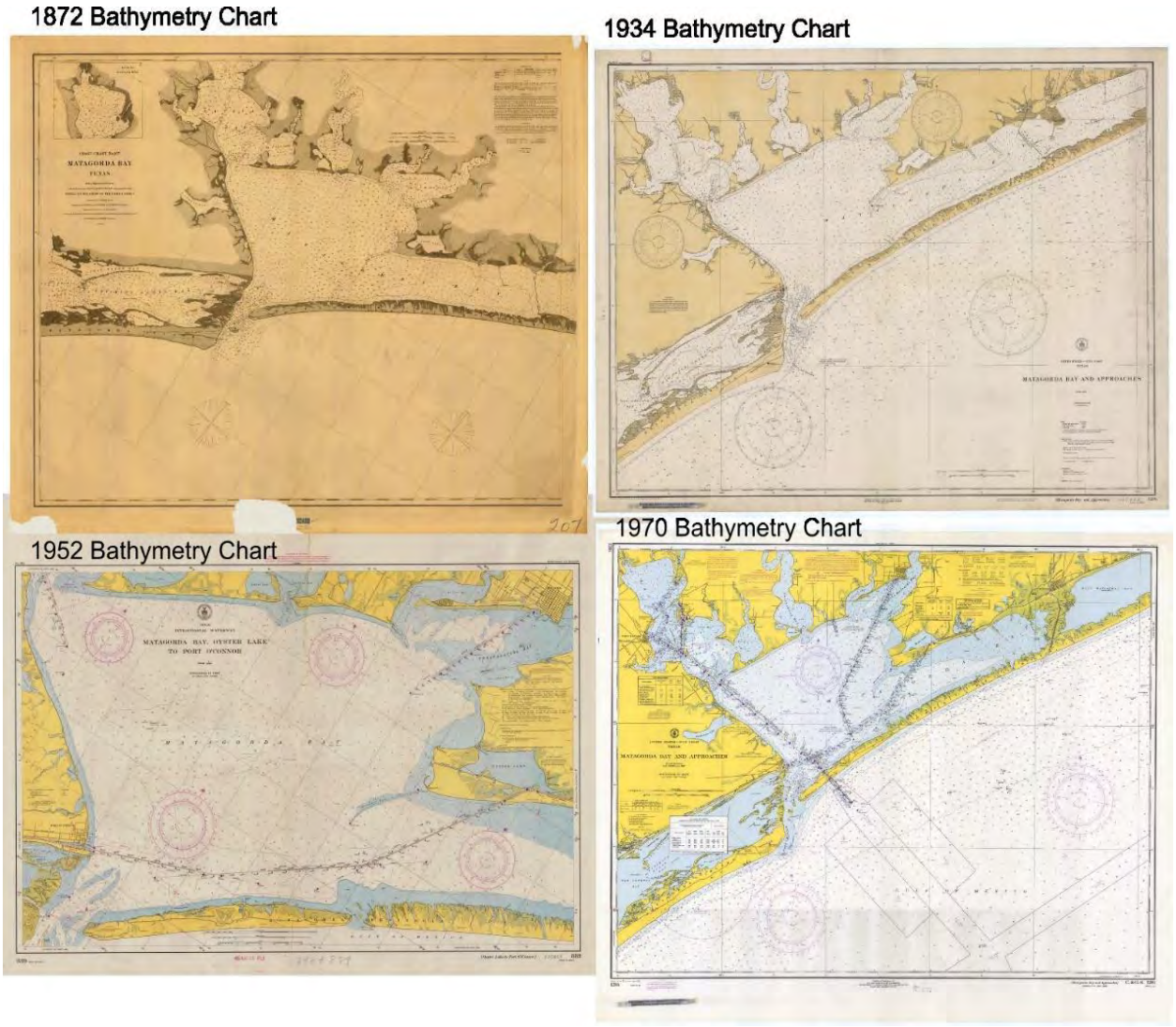

Figure 55 Historical navigation charts of Matagorda Bay from 1872, 1934, 1952 and 1970 that were digitized, re-gridded, and used to observe the sediment accumulation/erosion patterns. Maps from 1888, 1981, and the present are not shown.

Figure 56. Digitized and re-gridded navigational bathymetric chart from 1888, depth units in meters.

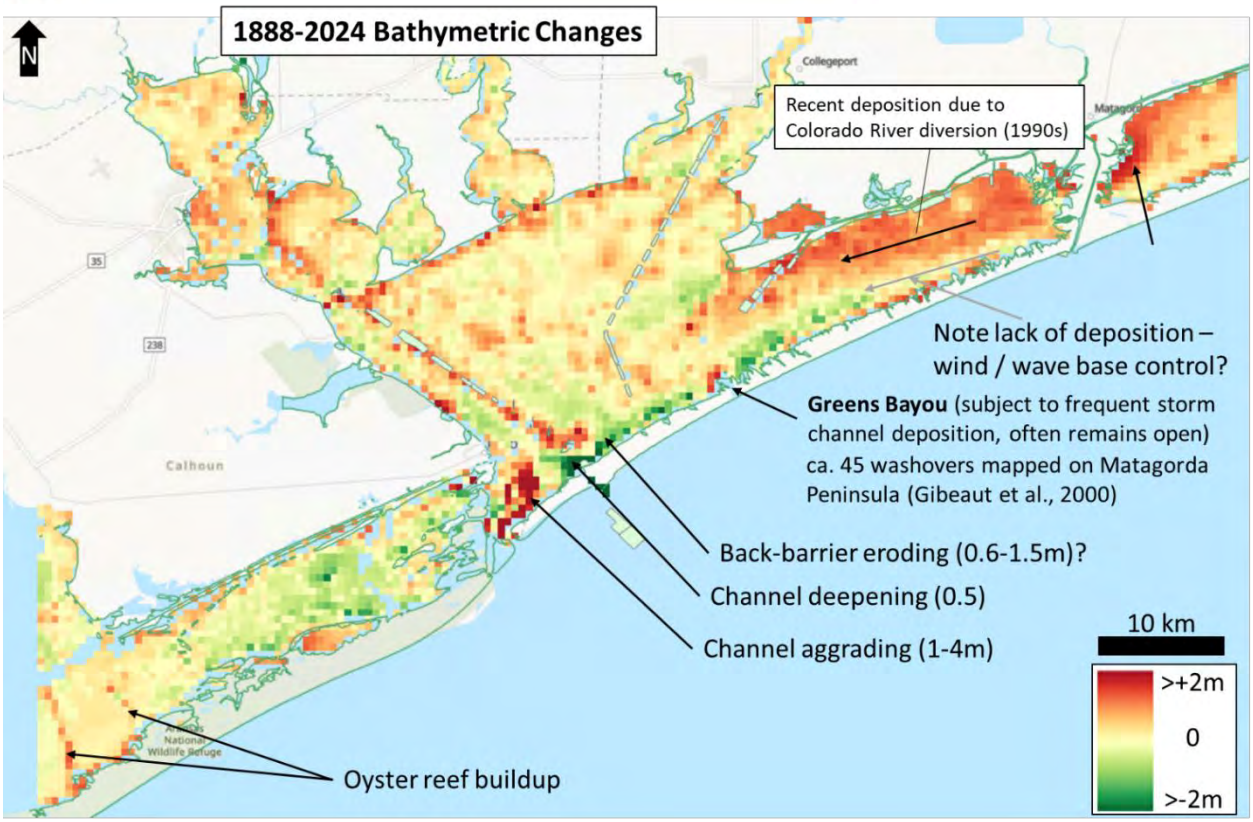

Figure 57. Map showing the water depth changes between 1888 and 2024 bathymetric maps. In areas with red bay got shallower, the sediments have been accumulated, in areas with green the bay deepened, likely the sediments were eroded. Pale green rectangles indicate dredge spoil locations adjacent to ship channels (from NOAA, 2024).

Long-term (over 100 years) sediment accumulation in Matagorda Bay using historical bathymetry maps suggests a highly dynamic bay that had parts which preserved the same depth or even got deeper (Figure 58). Long-term sediment accumulation patterns (1888-2024) indicate deposition associated with the modern Colorado River diversion and orientation of prevailing winds, as well as locations of dredge spoils from the Matagorda ship channel and Intercoastal waterway. "Static" bed elevation within the bays is postulated to be linked with sea level rise, which is documented to have increased by 20 cm over the same time period (Figure 58B). Net increase in water depth is hypothesized to be linked with subsurface structures and fluid extraction, where depth changes form linear features in proximity to known growth faults and developed oil and gas fields (Figure 59). For example, a known growth fault on Matagorda Peninsula studied by Feagin et al., (2013) linked the 40-year 0.75 m displacement with fluid extraction from the salt dome field in East Matagorda Bay. Further, enhanced subsidence may be associated with deposition by the Colorado River, where rapid sediment loading may activate preexisting growth faults. Historical seaward shoreline retreat along the barriers, coupled with net deepening along back-barrier shorelines may also indicate that these barriers are undergoing subsidence. The implications of enhanced subsidence along active land-building areas (deltas) and coastal armoring features (barriers) subject coastal populations to elevated risk of inundation by storms and future sea level rise.

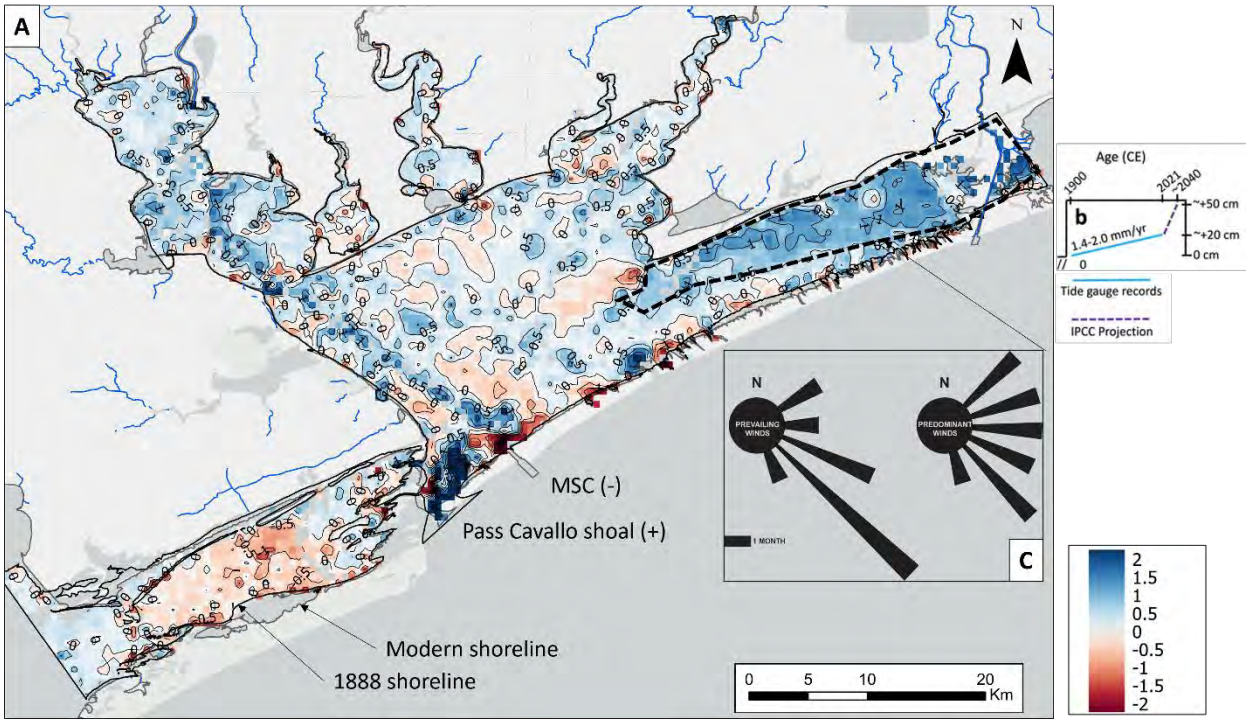

Figure 58. A) Historical bathymetric difference map constructed from 1888 and 2024 navigational charts, where blue and red (values are in meters) indicate areas that underwent deposition and erosion, respectively. B) Modern and projected sea level rise data, modified from Anderson et al., 2023. C) Prevailing and predominant wind directions, modified from McGowan 1979, used to explain the modern deposition of Colorado River sediments within downwind location (black polygon).

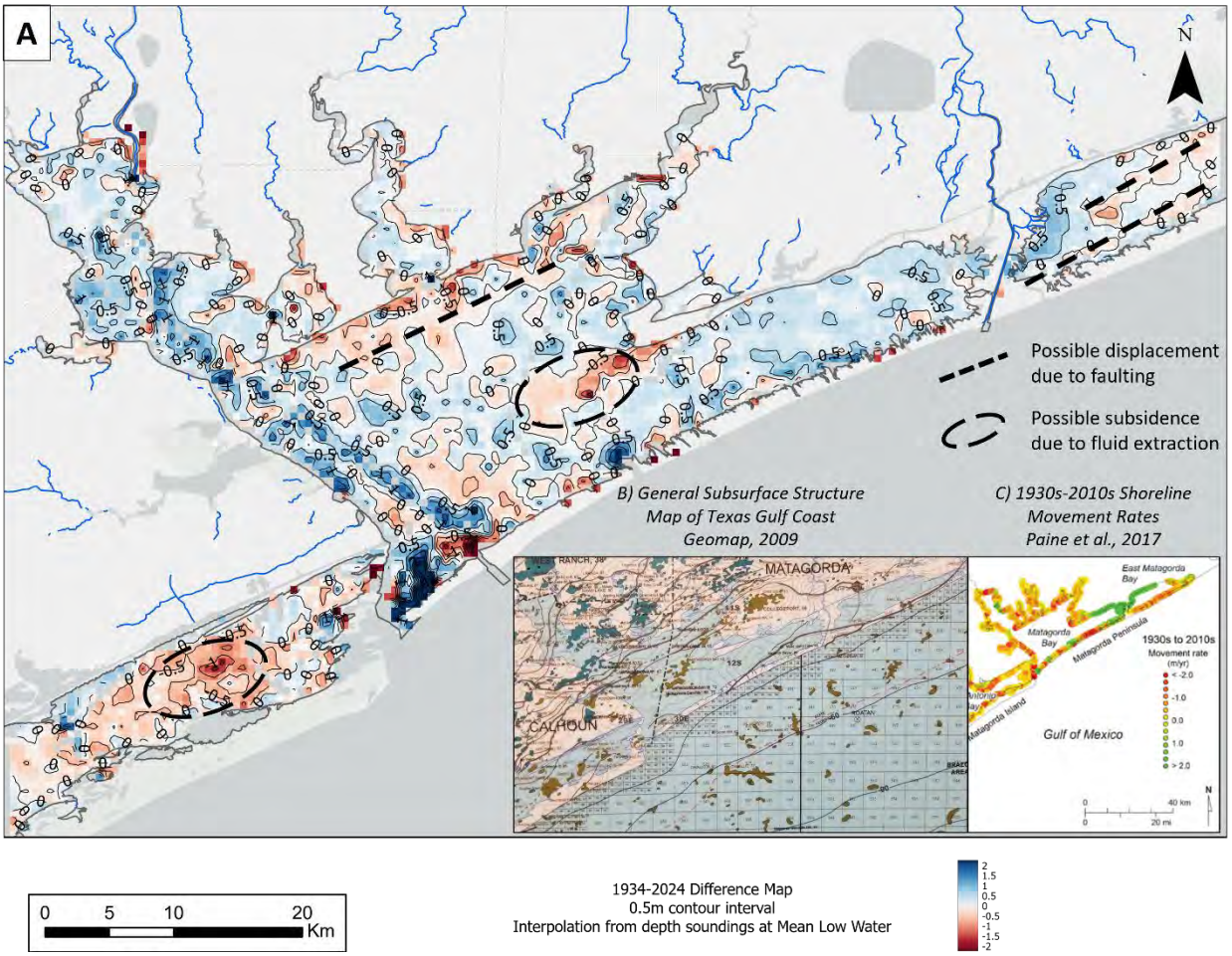

Figure 59. A) Historical bathymetric difference map constructed from 1934 and 2024 navigational charts, where blue and red indicate areas that underwent deposition and erosion, respectively. B) General structure map of Matagorda Bay, showing Cretaceous structures and oil and gas fields, which are hypothesized to be linked with bathymetric changes by active growth fault slip and subsidence related to fluid extraction. C) Historical shoreline movement from Paine et al., 2017, illustrating areas where recent storms penetrated the barrier and produced overwash deposits in the bay observed in the bathymetric difference map (i.e., at Greens Bayou).

8. SEDIMENTATION IN COLORADO RIVER DELTA

Following the observation that the largest sediment accumulation is in the eastern part of the Matagorda Bay, in December 2023, we conducted fieldwork and collected data in the Colorado Delta area. The Colorado River Delta and adjacent area, located in the eastern part of Matagorda Bay formed a sedimentary accumulation that strongly accelerated after 1992 when U.S. Army Corps of Engineers built a canal for river flow diversion. Since 1992 the Colorado River prograded a delta into the bay with a few kilometers of progradation of the shoreline. The delta deposits are up to 4 m thick (bay water depth prior to delta formation). The Colorado River is likely a source of microplastics because its catchment contains large urban areas. However, it is not clear how

much microplastics is actually preserved in the delta deposits. During this field work we attempted to understand the delta deposits architecture and to collect cores and grab samples, sidescan and CHIRP (Compressed High-Intensity Radiated Pulse) data were collected to enhance our understanding of bathymetry and sedimentation in the Colorado Delta (see Figs. 60 and 61). Sediment coring was unsuccessful. The CHIRP and sonar recording shows that the Colorado Delta channels are very shallow (less than 0.5 m deep) at the mouth, forming a mouth-bar sedimentary deposit (Figs. 61 and 62). The sediment is mostly silt with low amounts of clays suggesting an active transport of the finer sediments toward the central part of the bay.

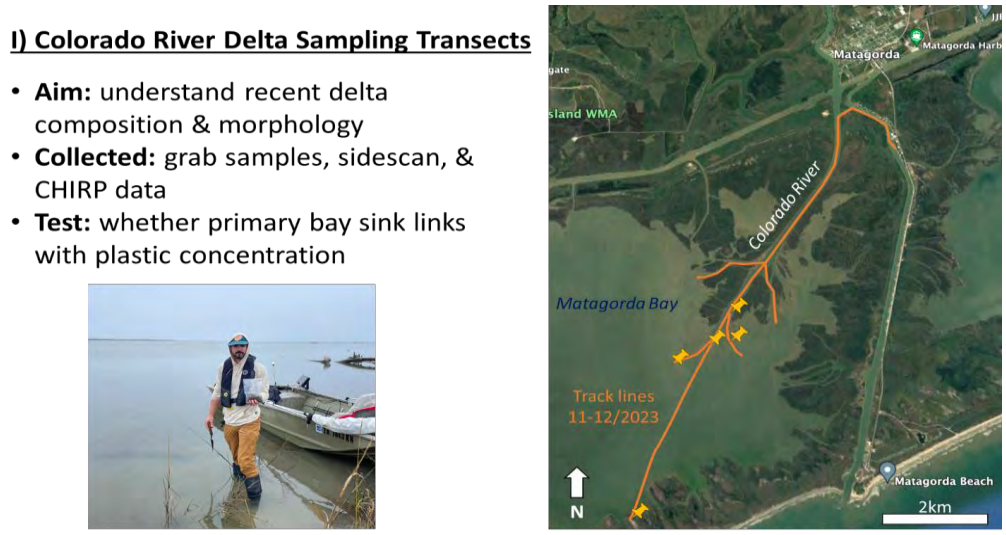

Figure 60. Data collected during December 2023 field work. The lower left photo shows sediment data collected in the delta front area of Colorado. On the right are the lines of Chirp data and sediment sample locations.

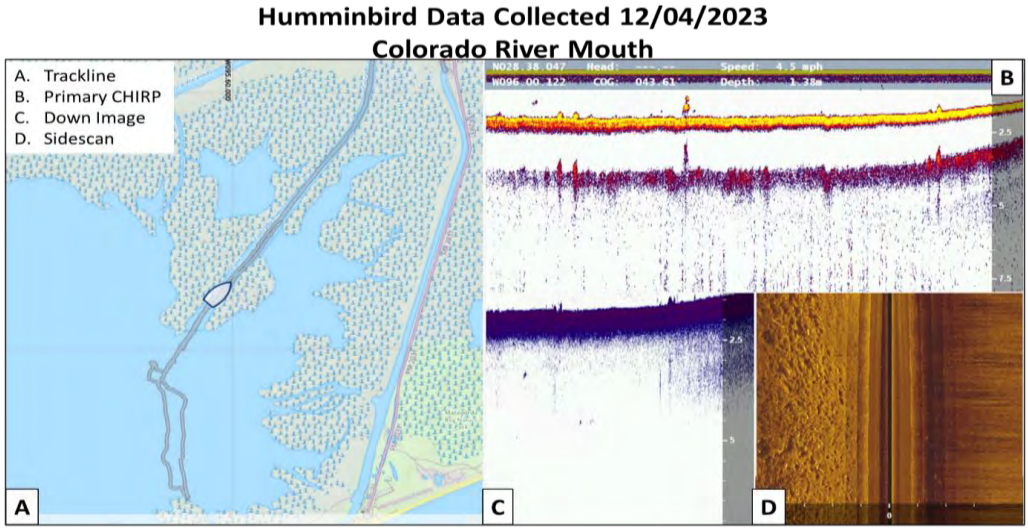

Figure 61. Example of CHIRP and Sidescan data collected along the Colorado Delta distributary channel.

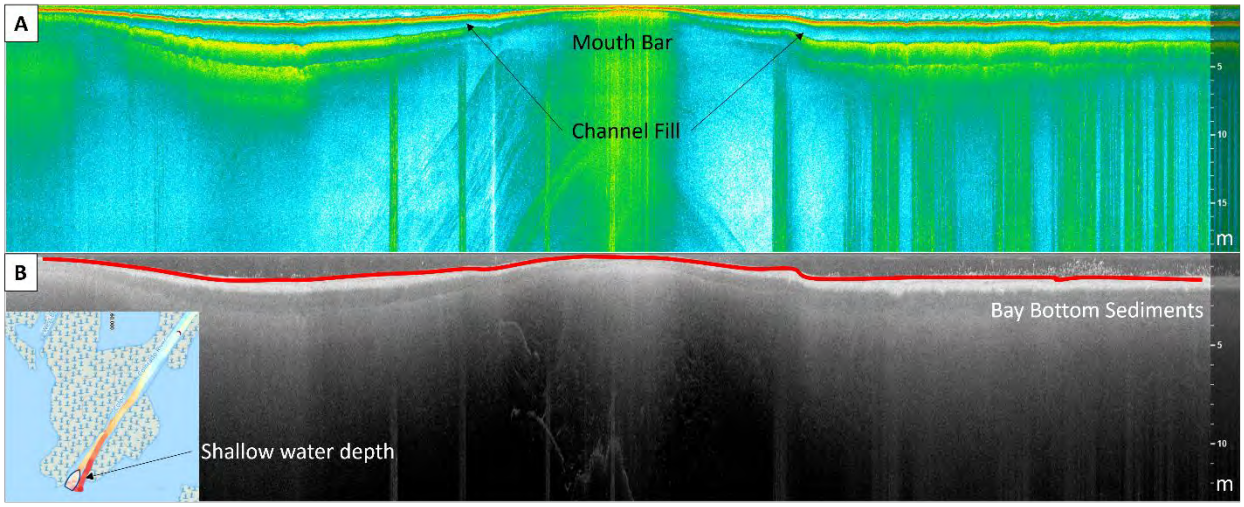

Figure 62. Example of CHIRP (A) and Downscan sonar (B) data collected along the Colorado Delta distributary channel.

9. PRESENTATIONS AND PUBLICATIONS

Microplastic data findings, such as location of the sampling and concentrations, have been reported as a dataset to *NOAA – National Center for Environmental Information – Marine Plastics*. We hope the results will be added on their microplastics map, which is publicly available online at:

https://www.ncei.noaa.gov/products/microplastics

William Bailey presented the poster "*Characterization and Distribution of Microplastics in Texas Bays*" (shown below as a figure) at the **American Geophysical Union Conference** held in San Francisco, California in December 2023.

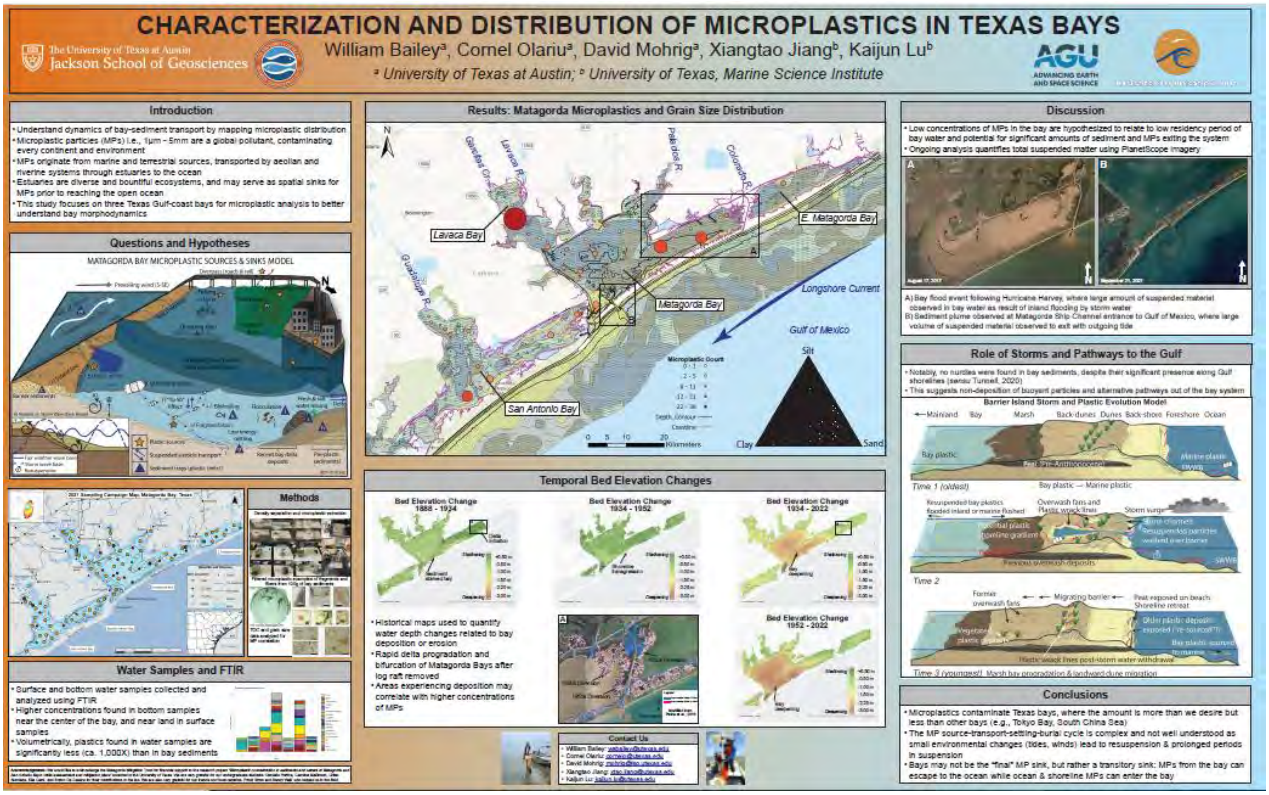

The ongoing work related to the post-Hurricane Beryl – Matagorda Peninsula erosion-deposition of sediments and plastic debris distribution was presented at the "**Texas Plastic Pollution Symposium**" in Houston on April 3rd, 2025. The poster titled "Dynamics of Marine Litter Post-Hurricane Beryl: Assessing the Ultimate Fate of Flotsam" by *William Bailey, David Mohrig, Cornel Olariu, and Kutalmis Saylam* discussed plastic debris fate during strong storms, a topic highly relevant to the project studying the microplastics in sediments of Matagorda and San Antonio bays because is trying to understand the sediment (microplastics included) exchange between bays and Gulf of Mexico during the storms.

The key results on microplastics in sediments have been published in an article "Microplastics in Bays along the Central Texas Coast" in the journal of *Environmental Science & Technology*. Article link: Microplastics in Bays along the Central Texas Coast by Bailey et al., 2025

The main findings reported in the article are:

(1) relative low concentrations (ca. 10s−100s particles per kg sediment or 20−200 × 104 items/ m3. By comparison with coastal environments and other studies the microplastics content in Matagorda sediments is relatively low (see Figure 63).

(2) there are negligible correlations between analyzed deposit constituents and microplastics (R2 for grain size = −0.14 to 0.12, organic content = 0.08, water depth = −0.11, distance to shore =

−0.14) (see figure 2). The low correlation makes it difficult to pinpoint a controlling factor in microplastic transport and sedimentation.

(3) the relatively low microplastics concentration could be explained by the dynamic role of wind-driven mixing and openness to the Gulf of Mexico, which leads to the high flushing rate of sediment and microplastics out of the bays.

(4) larger microplastic particles (fragments: 178 ± 93 μm, fibers: 0.5 to 2.0 mm) were consistently deposited with finer sediments, indicating high transportability of the microplastic particles (see figures 3 and 4). Microplastic resuspension into bay waters has significant implications for limiting microplastic accumulation within bay sediments.

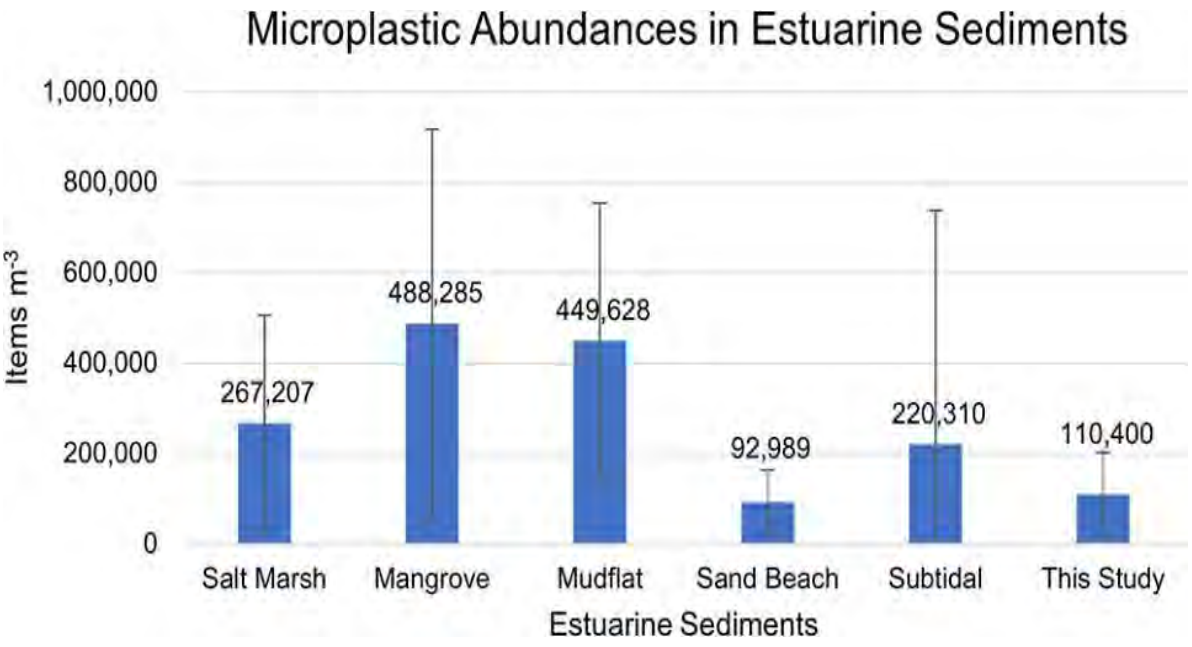

Figure 63. Comparison of microplastic abundances in estuarine sediments from reviews by Biltcliff-Ward et al., 2022 and Bailey et al., 2025 (where items per cubic meter equals mean ± SD MPs per 100 g w.w. × 20,000). Figure from Bailey et al., 2025.

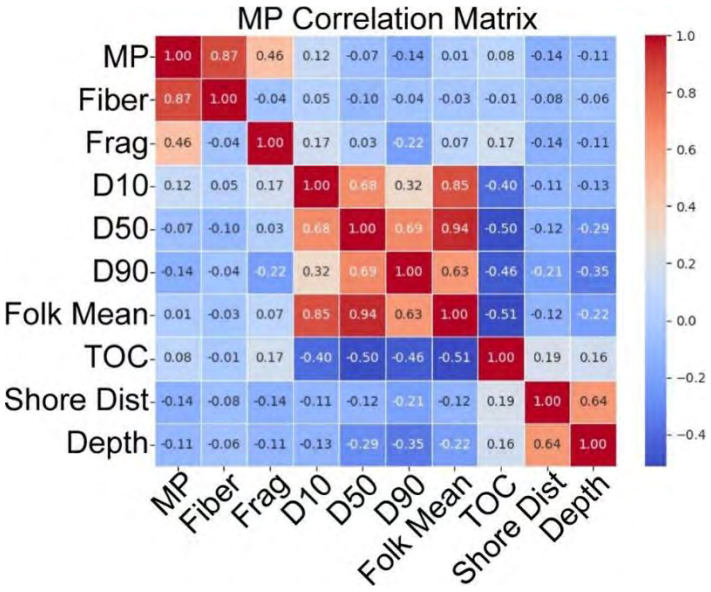

Figure 64. Correlation matrix between MP (total microplastics), fibers, fragments (Frag), sediment grain size (D10, D50, D90, Folk Mean), total organic content (TOC), distance to nearest shoreline (Shore Dist.), and water depth (Depth). Results of this study show negligible correlation between microplastics and all other parameters. Figure from Bailey et al., 2025.

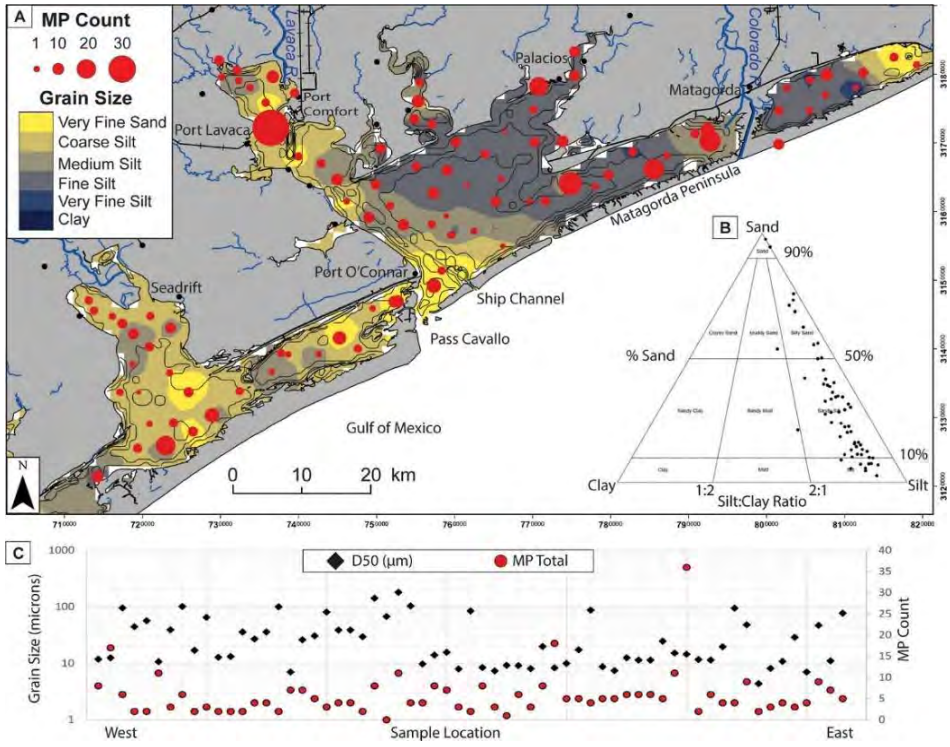

Figure 65. Results maps A) of MP counts from 100 g (w.w.) sediment overlain with modern grain size (D50) assemblage; B) Ternary diagram showing distribution of fine-grained sediment samples constructing a linear distribution of coarsening approximately North–south from landward river mouths to the tidal inlet at Pass Cavallo (sand composition). C) Graph plots median grain size (D50) and MP counts for each location spatially arranged from west (left) to east (right). Note there is not an obvious trend between MP number and D50 (grain size). Figure from Bailey et al., 2025.

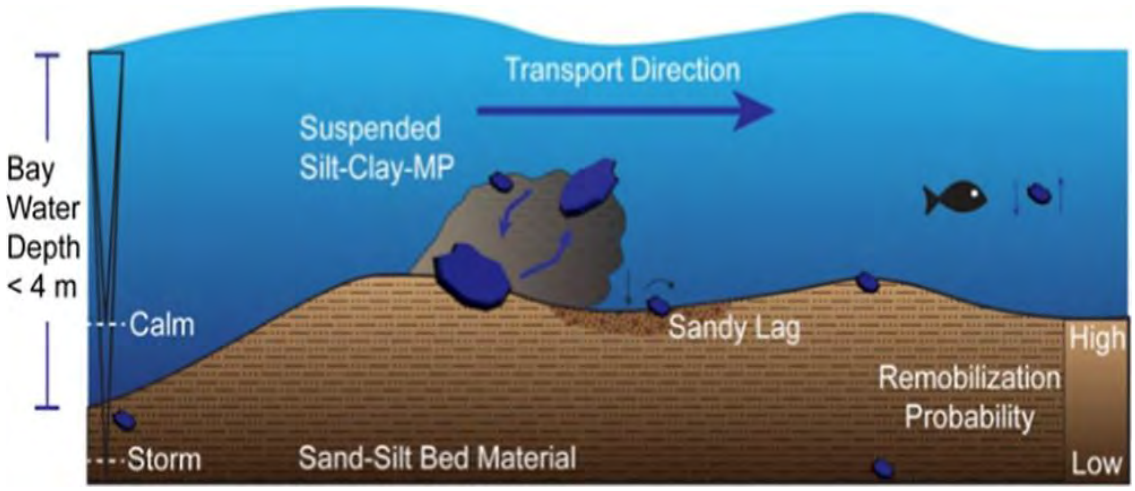

Figure 66. Schematic model of microplastics relative mobility in a heterogeneous MP and sediment mixture. Dailey ("calm") wind/wave-current conditions (indicating minor bed scour) illustrating shallow wave base and deeper "storm" ("seasonal or infrequent") scour scenarios for bed and MP remobilization to show resuspension probability for variable depth profiles and that MP particles larger than "background" sediment grains can be re-entrained from the bed when exposed to currents. Turbulent burst of grains shown schematically, where grain size of MPs compared to the bed shown in figure 65C (above). Figure from Bailey et al., 2025.

10. OTHER ENDEAVOURS THAT SPROUTED OUT OF THE MATAGORD BAY PROJECT

A numerical model simulating suspended material has been used to understand the dynamics of microplastics in Matagorda Bay. The hydrodynamic model, ANUGA, inputs bathymetry, velocity, winds, tides, and river stage into the particle tracking model (DORADO) to compute the paths and the time of particles in suspension that eventually reveal the fate of the particles (microplastics). Further, this model uses a parameter (theta) as a proxy for the particles' buoyancy, which can be adjusted to simulate the range of suspended materials' (i.e., sand, silt, mud, organics) sensitivity to depth (Figure 67). "Steady" and "unsteady" conditions are incorporated into the model to variably adjust for changes in tides, winds, and river stage during the model's simulation.

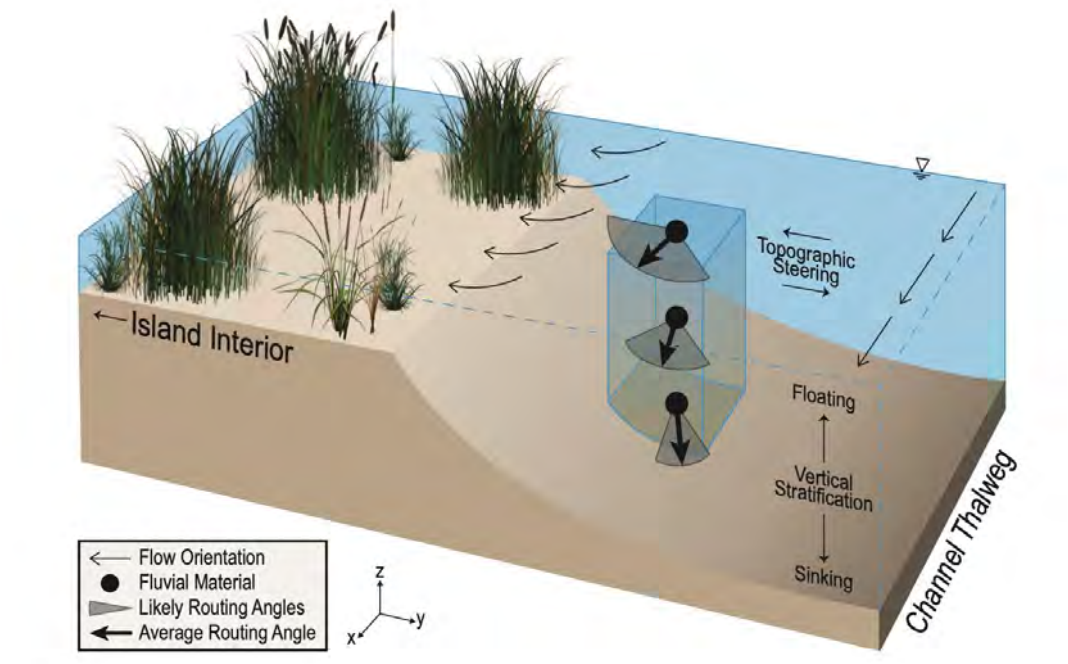

Figure 67. Conceptual schematic model by Wright et al. (2022) illustrating the connection between topographic steering and vertical stratification and the resulting sorting of materials in space.

The particle tracking model was used to simulate island nourishment in Wax Lake and Atchafalaya deltas (Wright et al., 2022), and ongoing work aims to apply the same methods to Matagorda Bay. Future work will simulate microplastic spill events from different locations (e.g., Port Comfort, Colorado River) to calculate residence periods for suspended particles in the bay and quantify the time for particles to escape the bay waters (**Figure 68**).

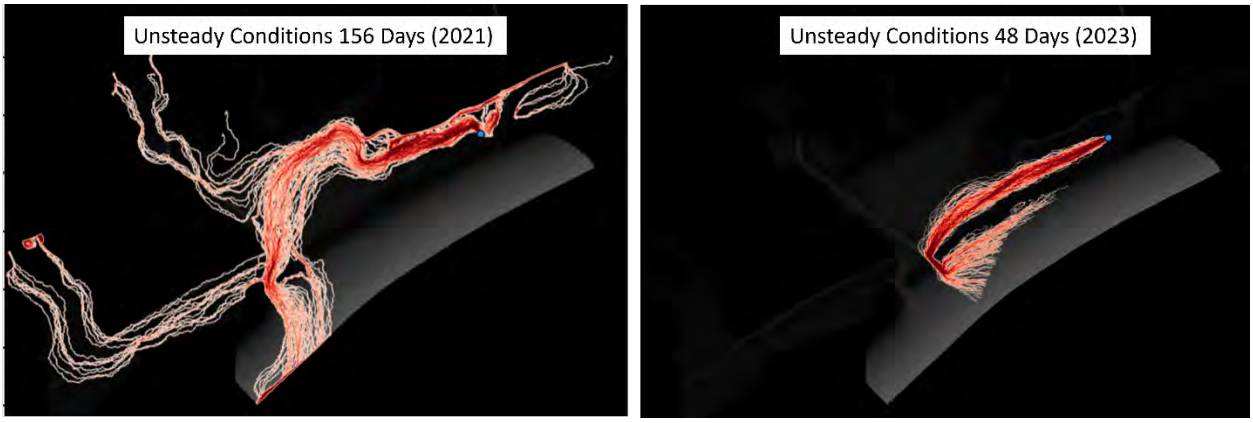

Figure 68. Example of numerical particle tracking model residence time output results for two scenarios where buoyant particles were seeded at the mouth of the Colorado River into Matagorda Bay. Left) Unsteady conditions ran for 156 days (May 15 to October 1, 2021) to simulate the period when sediment and water samples were collected. Right) Unsteady conditions ran for 48 days (May 1 to July 1, 2023) to simulate a period when longshore current reverses.

10.1 International Collaboration

PhD student Will Bailey visited the University of Perpignan in France to collaborate with a group doing similar research on two lagoons in the Mediterranean. As part of the Chateaubriand STEM Fellowship, an international collaboration between the French and US universities, he applied our methods developed at the University of Texas at Austin to an unstudied region in southern France. Ongoing microplastic analyses will test for correlations with grain size, total organic content, and wind direction to further our understanding of coastal plastic concentrations (**Figure 69**).

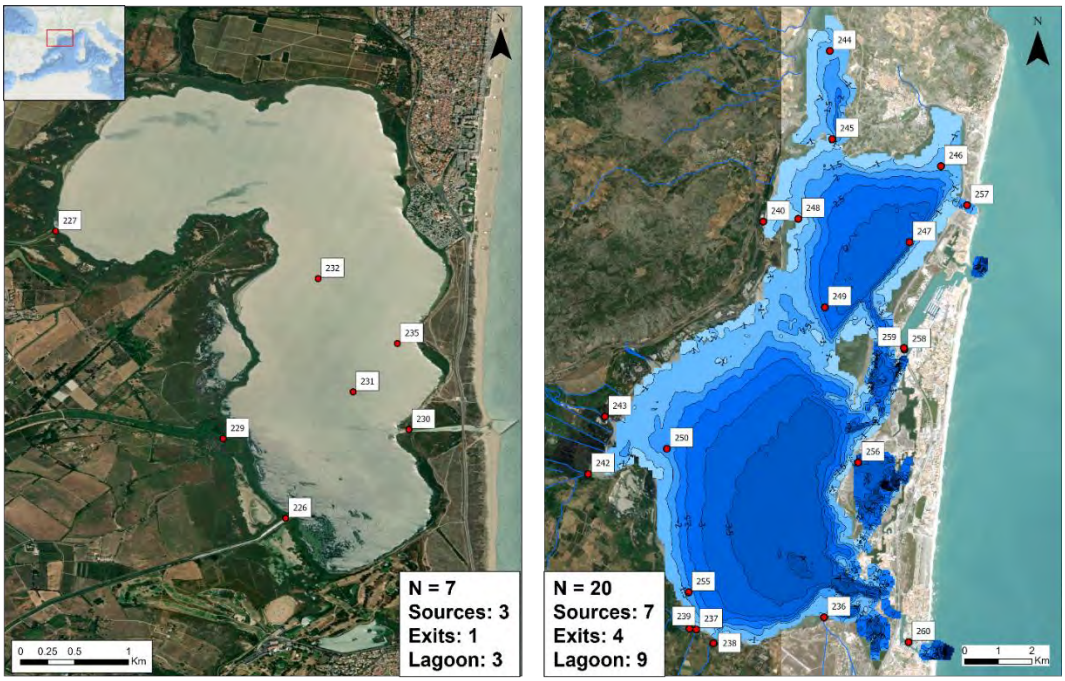

Figure 69. French Mediterranean lagoons were sampled for microplastic concentrations. Left - Canet Lagoon. Right- Leucate Lagoon, where push cores (60 cm) were collected. Sediment core locations form transects between fluvial sources ("sources") and connections with the sea ("exits"). Intermediary locations ("lagoon") test for gradient between sources and exits with the prevailing offshore wind regime.

10. 2 Hurricanes affecting beach sediments and plastics

Hurricane Beryl made a landfall in the proximity of Matagorda Bay on July 8th 2024. A post-Hurricane Beryl field trip to the Matagorda coast was undertaken with the scope to assess the Gulf of Mexico water flood into the coastal bays and the potential plastics transport during the flooding (Figure 70). The data collected will be analyzed in the future but initial observations suggest the hurricane related floods do transport microplastics from the beach (marine side of the barrier) into the bay.

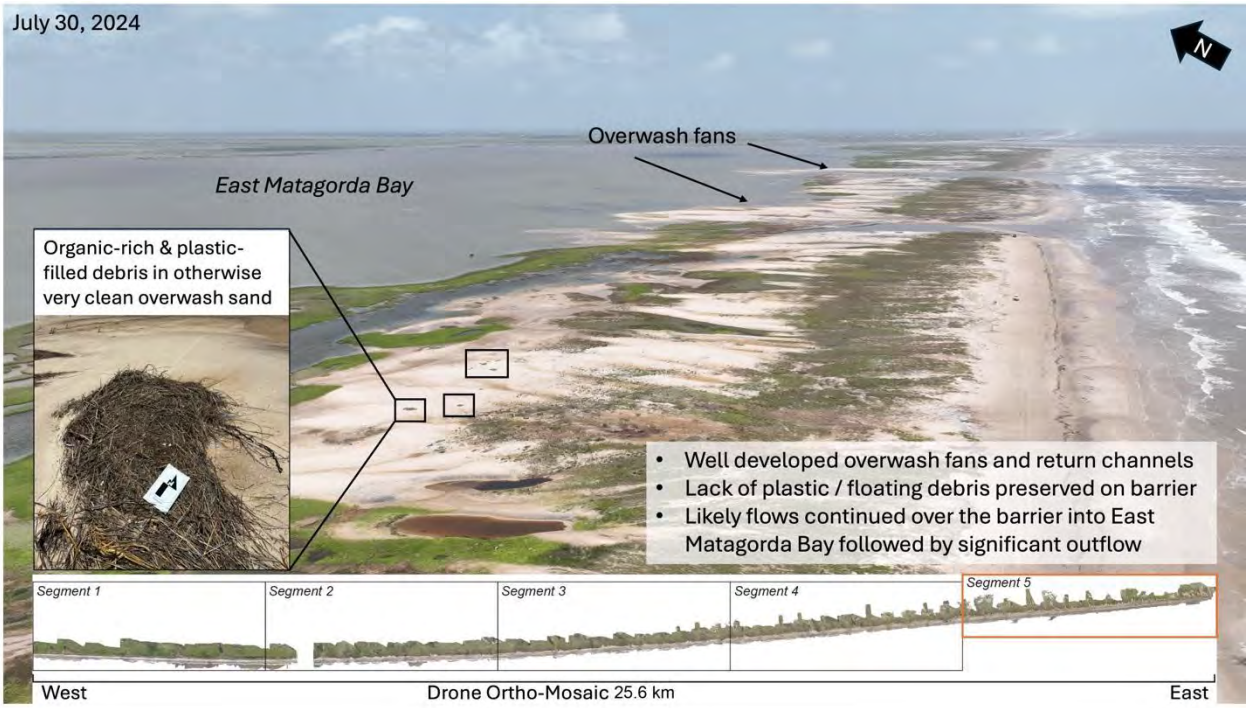

Figure 70. Unmanned-Aerial-Vehicle (drone) photo of the coast along the Matagorda peninsula showing the hurricane related flood line and associated plastic-rich deposits.

Work regarding the post-Hurricane Beryl – Matagorda Peninsula data initial results found plastic debris (i.e., micro- & macro-plastic) to be highly concentrated within highwater wrack lines that onlap beach topography and vegetation (Fig. 71 to 73). These results suggest significant plastic sourcing to bay waters in areas without topographic barriers (i.e., the area which developed new overwash fans and return channels). Future work will utilize LIDAR data collected by the Bureau of Economic Geology of the University of Texas at Austin. Pre- and post-storm LIDAR analyze shows topographic change in area landward of shoreline and try to correlate net depositional areas with plastic-rich deposits.

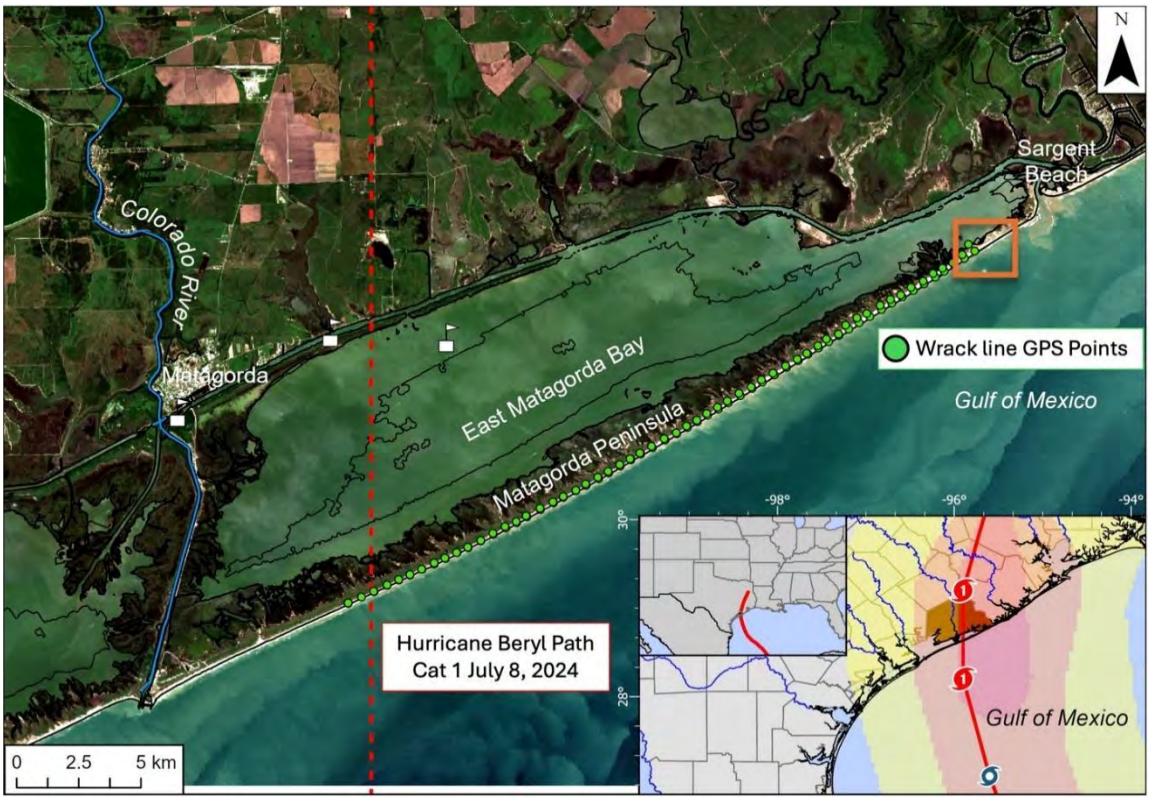

Figure 71. Post-Hurricane Beryl field campaign overview map illustrating storm path and locations of measured points along Matagorda Peninsula with plastic-rich deposits. Inset rectangle indicates location of new overwash fans in lower relief part of the barrier (Figure 72).

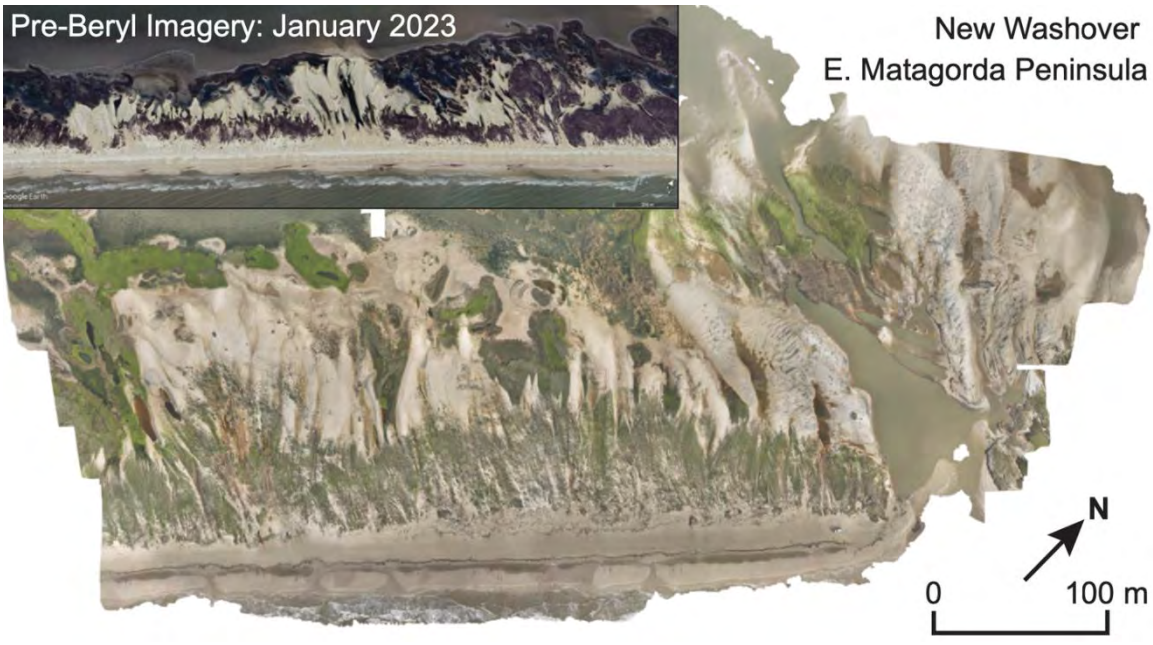

Figure 72. New overwash fans and flood-return channels, which lacked plastic-rich deposits and likely transported debris into East Matagorda Bay.

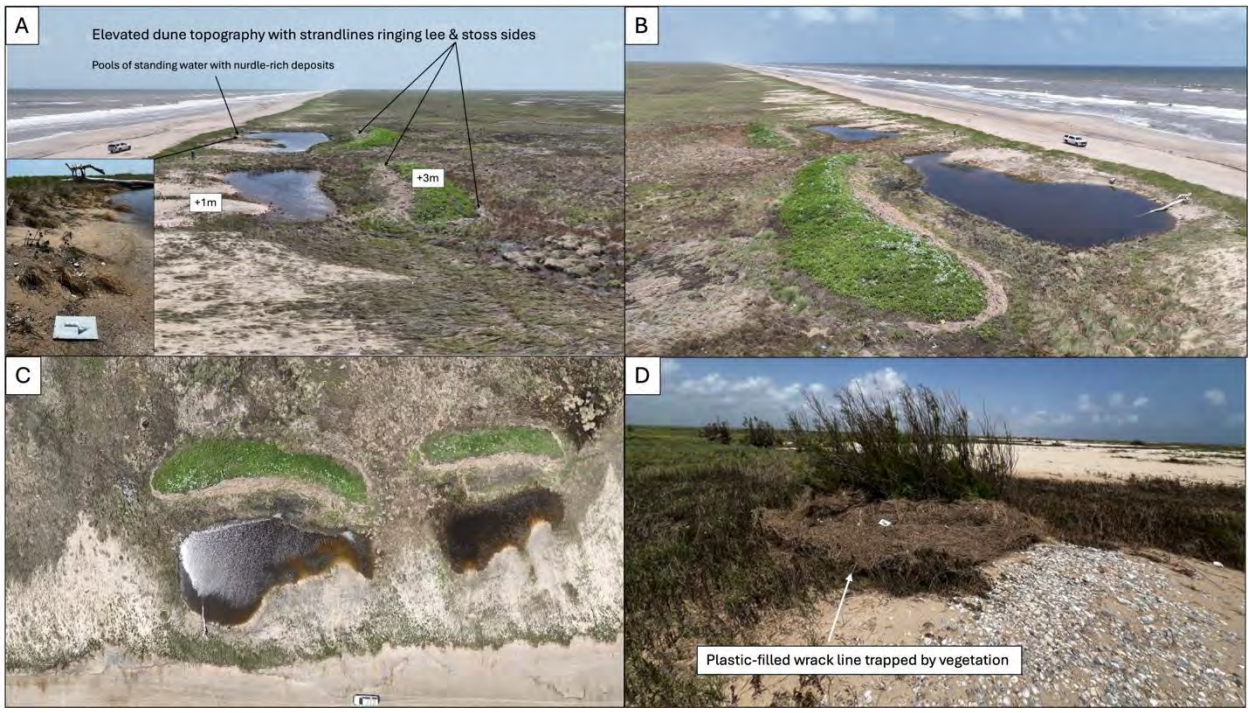

Figure 73. A-C) Plastic-filled deposits onlapping barrier dune topography and D) preserved vegetation acting as a filter for floating debris.

11. CONCLUSION

The benefit of the project is the establishment of a long-needed reference map for microplastic content in sediments of the Matagorda Bay and adjacent San Antonio Bay. Water samples were also analyzed for microplastics and concentrations consistent with the microplastics found in sediments were reported. The map of the microplastics in sediment would be considered as a reference point for future trends/evolution of the microplastic pollution in the bay. Any future changes in microplastic content could be compared against the comprehensive map distribution found here. The mapping of the surface sediments of the entire bay did not identify any past and recent "hotspots" for microplastic accumulation. However, higher microplastic content has been found in Lavaca Bay, mostly fibers, which is closer to larger urban settlements. Another area with higher microplastic content, mostly fragments, is in the eastern part of the Matagorda Bay in front of the Colorado Delta and "behind" the Matagorda Peninsula. The source in this area can be the Colorado River of the beach material transported over the barrier during the storm-related floods. The comparison of possible factors controlling the microplastics concentrations did not result in a strong correlation and we could not identify a main control. The microplastic particles have larger sizes than the sediment it is found into which suggest a higher mobility of the microplastic particles. Higher mobility is explaining the lack of "hot spots" because the microplastics (given their low specific gravity) are remobilized by river floods or storm surge events and redeposited in the bay. The entire bay sediments are "well mixed". The high mobility also explains the

relatively low concentration by comparison with other published datasets and suggests the microplastics are transported further into the Gulf of Mexico.

The higher mobility of the microplastics suggests that particles will stay longer in suspension and might temporarily concentrate at the bottom of the lake in the water-substrate “fluffy” sediment layer sometimes called “flocculent layer”. The material in this layer is not yet buried to become part of the sediment record but is easily resuspended and transported throughout the bay. If the microplastics concentrate in the flocculent layer, even if seasonally, might affect the fauna.

Method development has been a key part of this project regarding plastic identification and quantification, since there is a lack of established or agreed protocols of sample pretreatment and analysis. Suspended microplastics in the water are relatively more challenging because of the need to isolate them from the predominant natural particles. We learned that nitric acid digestion seems to be more effective in removing natural organic matter before the Py-GC/MS analysis. The microscopic FTIR offers visualization as well as plastic identification based on the IR spectrum for a given piece of plastics on a filter. However, the IR analysis is based on reflectance, which greatly reduces the sensitivity or signal noise ratios, thus caution is needed when interpreting results from this technique. A much more sensitive technique, such as optical photothermal IR, may be necessary for such a purpose. For quantification purposes, Py-GC/MS seems to be a promising technique although the pretreatment is a critical component for reliable results. More work is clearly needed to standardized protocols for sample collection, pretreatment and analysis of microplastics in the environment.

Future research on the bay microplastics should focus on short events (floods, hurricanes) that might affect microplastics transport. And also, to understand the microplastics flux exchange between coastal bays and the Gulf of Mexico. The research findings suggest the bays do not represent ultimate sinks for microplastics.

REFERENCES

Anderson, J. B., Wallace, D. J., Rodriguez, A. B., & Simms, A. R. (2023). Unprecedented Historical Erosion of US Gulf Coast: A Consequence of Accelerated Sea-Level Rise?. Earth's Future, 11(9), e2023EF003676.

Bailey, W., Olariu, C., and Mohrig, D., (2025) Microplastics in Bays along the Central Texas Coast. Environmental Science & Technology, v. 59, p. 5249−5260.

Biltcliff-Ward, A.; Stead, J. L.; Hudson, M. D., 2022, The Estuarine Plastics Budget: A Conceptual Model and Meta-Analysis of Microplastic Abundance in Estuarine Systems. Estuarine, Coastal Shelf Sci., 275, 107963.

Bronikowski, J.L., 2004, Sedimentary Environments and Processes in a Shallow, Gulf Coast Estuary-Lavaca Bay, Texas. MS Thesis, Texas A&M University, 114 p.

Dellapenna, T., Allison, M.A., Gill, G.A., Lehman, R. D., and Warnken, K.W., 2006, The impact of shrimp trawling and associated sediment resuspension in mud dominated, shallow estuaries. Estuarine, Coastal and Shelf Science, V. 69, Issues 3–4, p. 519-530.

Feagin, R. A., Yeager, K. M., Brunner, C. A., & Paine, J. G. (2013). Active fault motion in a coastal wetland: Matagorda, Texas. Geomorphology, 199, 150-159.

Gibeaut, J. C., White, W. A., Hepner, T., Gutierrez, R., Tremblay, T. A., Smyth, R., & Andrews, J. L. (2000). Texas Shoreline Change Project. Gulf of Mexico Shoreline Change from Brazos to Pass Cavallo.

Larm, K., 1989, Study of Sediment Resuspension due to Hurricane Carla in Lavaca Bay. MS Thesis, Texas A&M University, 107 p.

Löder, M. G. J. et al. Methodology Used for the Detection and Identification of Microplastics—A Critical Appraisal. Marine Anthropogenic Litter 201–227 (2015) doi:10.1007/978-3-319-16510-3_8.

Mallinson, C., Jiang, X., and Liu, Z., 2022. Microplastics in the sediment of Matagorda & San Antonio Bays: separation and identification. Undergraduate Report/Thesis, UT MSI.

McGowen, J. H. (1979). Geochemistry of bottom sediments--Matagorda Bay system, Texas. Virtual Landscapes of Texas.

McGowen, J.H., Byrne, J.R., and Wilkinson, B.H., 1979, Geochemistry of Bottom Sediments Matagorda Bay System, Texas. Bureau of Economic Geology, 64 p.

Näkki, P., Setälä, O., and Lehtiniemi, M., 2017, Bioturbation transports secondary microplastics to deeper layers in soft marine sediments of the northern Baltic Sea, Marine Pollution Bulletin, V. 119, Issue 1, p. 255-261.

Paine, J.G., Caudle, T.L., and Andrews, J.R.., 2017, Shoreline and sand storage dynamics from annual airborne LIDAR surveys, Texas gulf coast. Journal of Coastal Research, v. 33, p. 487-506.

Palanques, A., Guillen, J., Puig, P., 2001. Impact of bottom trawling on water turbidity and muddy sediment of an unfished continental shelf. Limnology and Oceanography 46, 1100e1110.

Wright, K., Hariharan, J., Passalacqua, P., Salter, G., & Lamb, M. P. (2022). From grains to plastics: Modeling nourishment patterns and hydraulic sorting of fluvially transported materials in deltas. Journal of Geophysical Research: Earth Surface, 127(11), e2022JF006769.